Spring 1-1-2013

Characterization and Control of Microbially Induced Concrete Corrosion

Alison Leslie Ling
University of Colorado at Boulder, alison.ling@colorado.edu

Characterization and Control of Microbially Induced Concrete Corrosion

By Alison L. Ling
B.C.E. University of Minnesota, 2008
M.S. University of Colorado, 2012

A thesis submitted to the

Faculty of the Graduate School of the

University of Colorado in partial fulfillment

of the requirement for the degree of Doctor of Philosophy

Department of Civil, Environmental, and Architectural Engineering

2013

Signature Page:

This thesis entitled
Characterization and Control of Microbially Induced Concrete Corrosion,
written by Alison L. Ling,
has been approved for the Department of Civil, Environmental, and Architectural Engineering

_____

Mark Hernandez, Committee Chair

_____

Norman Pace, Committee Member

_____

JoAnn Silverstein, Committee Member

_____

Yunping Xi, Committee Member

_____

Alina Handorean, Committee Member

The final copy of this thesis has been examined by the signatories, and we find that both the content and the form meet acceptable presentation standards of scholarly work in the above mentioned discipline.

Abstract

Characterization and Control of Microbially Induced Concrete Corrosion

Alison Ling, Ph.D. Civil Engineering

Thesis directed by Professor Mark T. Hernandez.

Microbially induced corrosion of concrete wastewater infrastructure is associated with billions of dollars in rehabilitation costs each year. This phenomenon is caused by sulfur-oxidizing microbial communities that grow on hydrogen sulfide and reduced sulfur compounds in the headspace of wastewater conveyance and treatment structures. The occurrence of corrosion has increased markedly in the past 30 years as a result of industrial wastewater pre-treatment legislation, and will likely continue to increase due to ageing systems, climate change, and (sub)urbanization. Current prevention and treatment technologies are relatively expensive and do not target the causative microbiology.

In response to this widespread problem, the objectives of this thesis were to characterize the spatial and temporal trends in corrosion-associated microbial communities and to develop cost-effective engineering controls to prevent corrosion by inhibiting acidogenic biofilms *in situ*. Corroded concrete was collected from ten utilities in the United States and from specimens exposed in a manhole for between one and twelve months. Corrosion was found to be most severe in sites with high levels of gaseous hydrogen sulfide and carbon dioxide. These sites were characterized by concrete binder degradation, pore water pH values below 1, and low microbial diversity (less than 10 taxa). Severely corroded concrete was colonized primarily by acidophilic sulfur-oxidizer *Acidithiobacillus* spp. Early-stage corrosion communities were associated with neutral pore water pH and higher microbial diversity, including neutrophilic

sulfur-oxidizers and heterotrophs. Bacterial community succession on exposed concrete specimens was similar to that described by culture-based bacterial models. However, an acidophilic euryarchaeon, *Ferroplasma* spp., was observed in extreme corrosion communities.

A novel concrete formulation amended with activated carbon impregnated with heavy metals was designed to locally inhibit sulfur-oxidizing activity in response to local pH depression. Treated and untreated specimens were exposed in sanitary manholes for up to a year. Treated samples experienced significantly less corrosion than otherwise identical untreated samples, even though the bacterial community compositions of surface biofilms were similar. This formulation can be manufactured with reused metal from industrial wastes and is expected to be several orders of magnitude cheaper than competing products.

Acknowledgements:

Alison Ling was supported through the Department of Energy Office of Science Graduate Fellowship and a Departmental Fellowship from Civil, Environmental, and Architectural Engineering at the University of Colorado. Additional project funding was provided by an Alfred P. Sloan foundation grant to Norm Pace and various grants to Mark Hernandez.

Thanks to Mark Hernandez and Norm Pace for their most excellent mentorship and advice. Thanks to all the Hernandez and Pace labs personnel for their guidance and support.

Thanks to my committee members for guidance; to Ben Gallaher for his help in concrete fabrication; to Laura Baumgartner, Kristin Petersen, and Natalie Hull for Sanger Sequencing mentorship and support; to Kirk Harris, Dan Frank, Mark Stevens, and Cassie Kotter for MiSeq support; to Chuck Robertson for coding advice and sequence analysis; to Anna Campbell, Alejandro Caicedo-Ramirez, and Paige Pruisner for their contributions to testing the culture inhibition of the metals product; to Kim Ross for advice on figures and analysis; to Jeff Maier and Mark Hofmeister for help in the manhole study; to numerous wastewater engineers and operators for assistance in collecting corrosion samples; to John Spear, Shannon Ulrich, and Chase Williamson for the use of the Spear Lab's ESEM machine; to Lee Stanish for help with multivariate ordination; to Kevin McCabe for teaching me to build things; to Alina Handorean, Jane Turner, and Odessa Gomez for the sanity checks; to Erin Fletcher for teaching me statistics; to Tom Zearly for his edits; to Tim LaPara for his mentorship and writing advice; to Austa Marie Parker for support and office snacks.

Thanks to my parents and siblings for their love and support.

Above all, thanks to Matt Haggerty for his endless patience, support, and shenanigans.

Table of Contents

List of Figures

List of Tables

1. Introduction and Scope

1.1. Motivation and Impact

Microbially induced corrosion of concrete (MICC) in wastewater infrastructure is a widespread and costly problem. The maintenance and replacement of damaged sewer pipes carry significant financial and energy costs for metropolitan areas across the globe. In a 1989 survey of 89 wastewater utilities in the United States, 63% reported active corrosion prevention programs to rehabilitate concrete pipe corrosion, and 70% reported corrosion at various sites within their treatment plants (USEPA, 1991). Since this time, reports of corrosion occurrence have continued to increase. Wastewater collection systems in the United States consist of about 800,000 miles of sewers and 12 million wastewater manholes. About 25% of this infrastructure is over 40 years old, and over 80% is concrete (USEPA, 2009). Sewer pipes typically run below streets or developed property, so repair and replacement procedures disrupt community economic activity. In addition, hydrogen sulfide released from wastewater collection systems can and cause human health and aesthetic problems. The US Environmental Protection Agency (EPA) estimates that the rehabilitation and maintenance of about 8,000 miles of wastewater sewers annually costs about $4.5 billion (USEPA, 2009), $3.3 billion of which is spent on sewer rehabilitation (Carpenter, 2009). Concrete corrosion in wastewater infrastructure has been recognized as a serious problem for over a hundred years (Olmstead et al., 1900), and the biological etiology of MICC was first elucidated in 1945 (Parker, 1945). However, the spatial and temporal trends of these microbial communities remains poorly described.

1.2. Research Objectives

The research presented here was motivated by the research need to develop a better understanding of the microbial community that causes concrete corrosion in wastewater infrastructure and to practical need to develop a low cost metals-based antimicrobial cement coating for concrete structures that specifically inhibits the responsible microbes. Flow charts describing the generic approach to three aspects of this research effort are presented in Figure 1.1, Figure 1.2, and Figure 1.3.

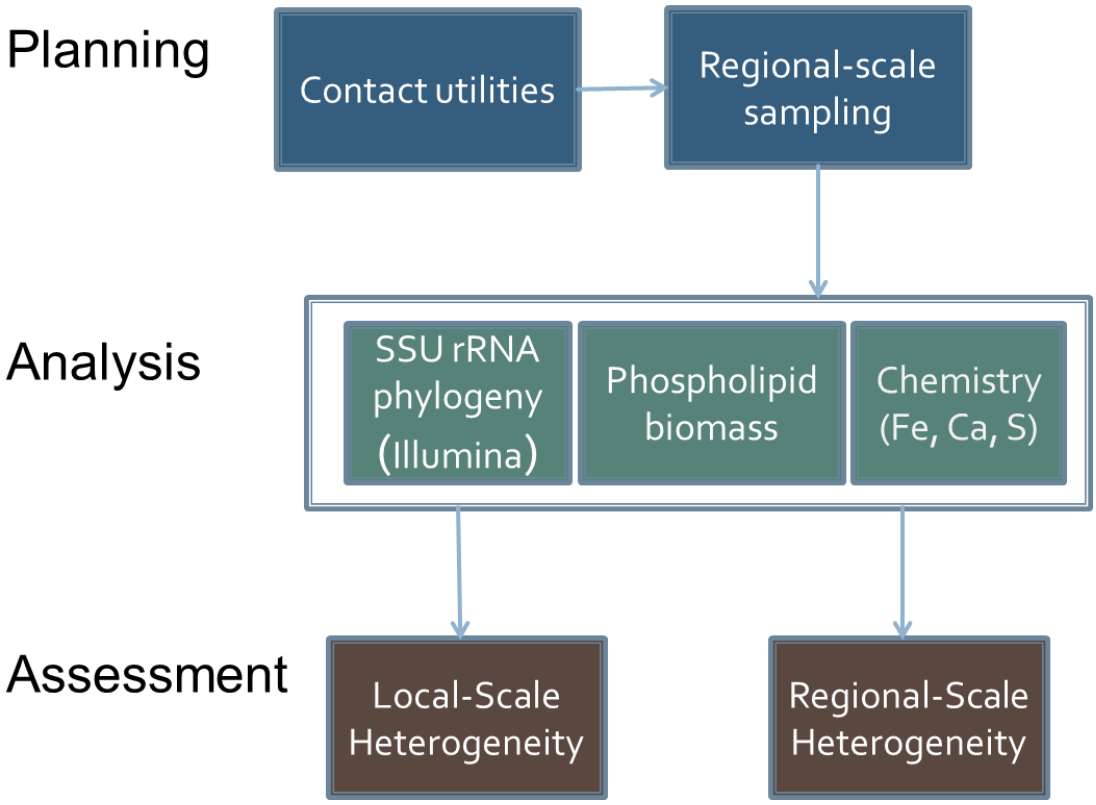

Figure 1.1: Flow chart of research aim 1 (spatial characterization)

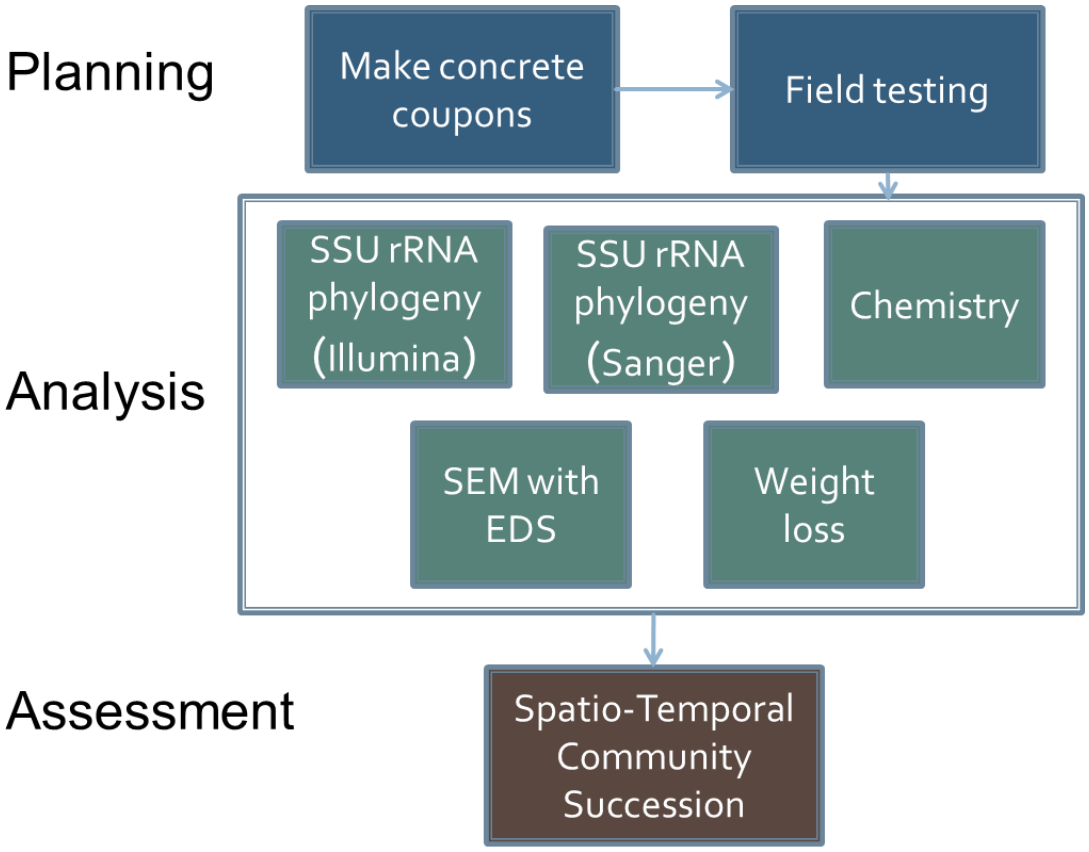

Figure 1.2: Flow chart of research aim 2 (temporal characterization)

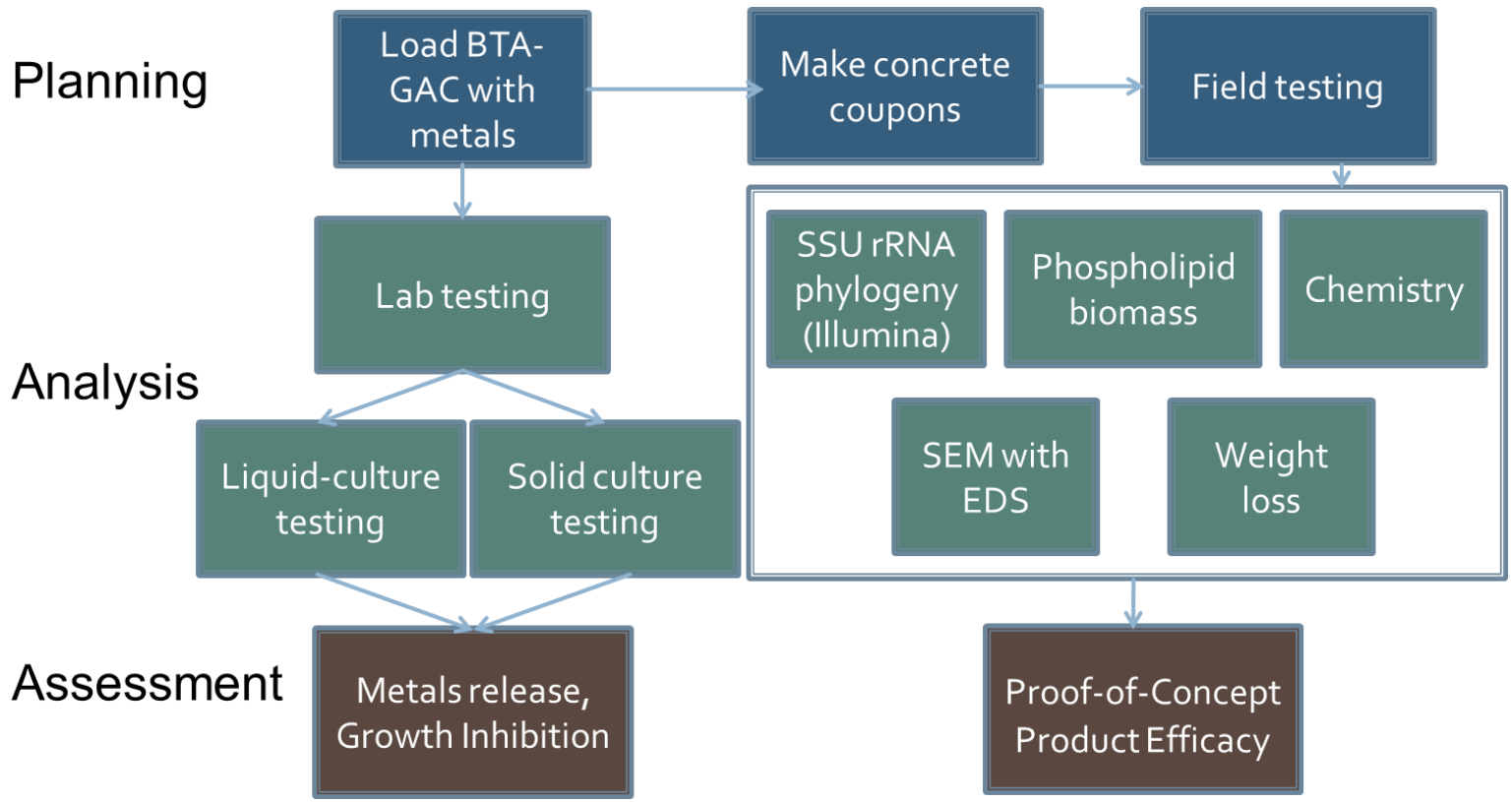

Figure 1.3: Flow chart of research aim 3 (formulation design and testing)

The first aim of this work was to use molecular biology and forensic chemistry methods to survey corroding concrete pipes and manholes in ten wastewater utilities across the United States. Utilities were selected based on location and availability. To date, only five peer-reviewed studies have published genetic sequence data from MICC biofilms (B. Cayford et al., 2012; Gomez-Alvarez et al., 2012; Okabe et al., 2007; Santo Domingo et al., 2011; Satoh et al., 2009); none have compared microbial communities between several wastewater systems on extended regional scales. Additionally, there has been no standard adopted for collecting and reporting environmental metadata associated with MICC. Although surface pH is likely the most important factor relating to corrosion rate, it is a difficult conglomerate parameter to acquire from corroding surfaces, and many studies do not report it. Headspace hydrogen sulfide is frequently measured, but other key redox- and metabolism-associated gasses, such as methane and carbon dioxide, are not usually observed or reported (Guisasola et al., 2008; Ismail et al., 1993). The effect of headspaces gases such as carbon dioxide, which serves as a carbon source for the autotrophic acidogenic microbes, or methane (Guisasola et al., 2008), which is a potential energy source for heterotrophic microbes, has not been elucidated. These research gaps preclude effective prevention measures, as designing systems to inhibit MICC requires fundamental knowledge of how corrosion mechanisms vary across geographical space and environmental gradients. To achieve this aim, 65 corrosion and biofilm samples were collected from 10 utilities in four distinct geographic regions. Analysis of the 16S rRNA gene was used to describe the associated bacterial communities. Correlations between community characteristics and metadata such as gas concentrations, location, pH, and sulfur content were investigated.

The second aim of this work was to develop a high-resolution sequence-based model of MICC microbial community succession. This is a key step in developing a unified

understanding of community structure, succession, and function in these novel and economically important environments. While culture-based models appear to successfully describe some of the microbes involved in the corrosion process, they fail to account for the presence of heterotrophic fungi and bacteria, especially in early stages of the corrosion process (Islander et al., 1991; Roberts et al., 2002). To track community succession with high resolution, concrete specimens were placed in two corrosive manholes in the Colorado Front Range in three independent longitudinal experiments for lasting between from three weeks to twelve months. Bacterial communities were described using phylogenetic methods based on sequences from V1V2 amplicons of 16S rRNA using an Illumina MiSeq platform and "universal" SSU rRNA clones using a Sanger sequencing platform. Pore water pH, percent of surface area corroded, and mass loss were used as indicators of corrosion extent; sulfur and calcium content were used to estimate the amounts of sulfur mineralized and calcium mobilized.

The third aim of this research was to develop a novel cement formulation that uses pH-dependent desorption of heavy metals to impair the growth of the sulfur-oxidizing organisms. Based on previous metal sorption studies (Kobya et al., 2005; Leyva-Ramos et al., 1997; Marzal et al., 1996; Reed et al., 1993), activated carbon formulations impregnated with heavy metals predictably release metal cations as their environment drops below pH 5. Based on these reports, metals can remain ionized at low pH conditions present on corroding concrete. The ions released are expected to cause acute metal toxicity to microbes present and thus inhibit corrosion progression. To test the efficacy of such a formulation, activated carbon of various sizes were loaded with cadmium and chromate ions at pH 8. Inhibition of neutrophilic and acidophilic sulfur-oxidizing bacterial growth by the formulation was tested in a laboratory setting. In addition, the metal-carbon formulations were surface-applied to concrete specimens. Treated

and untreated concrete samples were exposed to corrosive environments in working sanitary manholes and sampled periodically up to one year. The metal-carbon formulations tested here are potential alternatives to conventional concrete coatings, which are relatively expensive and typically do not target the microbes responsible for the corrosion process. Both components of the formulations tested can be produced from reused waste products for low-cost and sustainable production.

1.3. Hypotheses

Given the research goals stated above, the following hypotheses were formulated and tested to form a technical basis for this dissertation.

AIM 1: GEOGRAPHIC SURVEY OF CONCRETE CORROSION CHARACTERISTICS.

a. Chemical, environmental, and hydraulic conditions are more strongly associated with corrosion severity and community structure than geography. Differences in community composition are influenced by gaseous concentrations of hydrogen sulfide, carbon dioxide, and methane.

b. Highly corroded sites as measured by concrete loss are characterized by low α-diversity, high moisture, high estimated biomass, and extremely low pH. Associated microbial communities will be dominated by sulfur-oxidizing genus *Acidithiobacillus*.

AIM 2: MICROBIAL COMMUNITY SUCCESSION

c. Corrosion associated communities follow a distinct succession of neutrophiles to acidophiles and decreasing α-diversity in response to decreasing pore water pH.

AIM 3: REMEDIATION STRATEGY DESIGN AND TESTING

d. Microbially induced concrete corrosion can be inhibited in the field by surface application of a metal-carbon formulation designed to release metal ions in response to local-scale pH depression. Treated concrete coupons will experience less corrosion in the field than otherwise identical coupons as measured by mass loss, estimated biofilm biomass content, and pH drop.

e. The growth of both pure and enrichment sulfur-oxidizing cultures can be inhibited by selected metals liberated from activated carbon at low pH.

2. Literature Review

2.1. Financial Impacts of Microbially Induced Concrete Corrosion

As its occurrences and severity are exacerbated in the coming years, MICC is expected to exert significant financial pressure on wastewater utilities and associated government institutions. In their 2013 Report Card for Infrastructure, the American Society of Civil Engineers gave the nation's wastewater infrastructure a grade of D+. This report estimates a need for $298 billion in investments over the next 20 year, three-quarters of which will be needed to address pipe problems (ASCE, 2013). The Congressional Budget Office estimates that the cost of restoring wastewater infrastructure to proper function in the foreseeable future will be at least $12 billion per year (CBO, 2002; USEPA, 2010). As an example of this condition, the City and County of Los Angeles budgeted more than $2 million per year during the 1990's for chemical costs for corrosion prevention (USEPA, 1991). In another report, the United States Federal Highway Administration estimated replacement/rehabilitation costs of $36 billion per year to address corrosion of both drinking water and wastewater pipes (Koch et al., 2002).

2.2. Basic Mechanisms of Microbially Induced Concrete Corrosion

Microbially induced concrete corrosion is prevalent in structures with high headspace levels of hydrogen sulfide gas. This condition has been associated with concrete degradation rates of 1-5 mm per year (Monteny et al., 2000; Mori et al., 1992; USEPA, 1991). However, the levels of hydrogen sulfide (H_2S) exposure required to drive this process remains in question, and corrosion rates have been observed to vary by several orders of magnitude in different wastewater environments. Corrosion occurs as a result of microbially mediated sulfur cycling within wastewater collection systems. Sulfate present in wastewater is reduced to sulfide in

anoxic biofilms below the waterline. This sulfide can partition into the headspace of pipes and other wastewater structures (i.e. wet wells, manholes, and lift stations) as H_2S gas, which serves as a substrate for biofilms of acidogenic sulfur-oxidizing bacteria (SOBs) or sulfur-oxidizing microorganisms (SOMs) above the waterline. These biofilms produce sulfuric acid, which chemically dissolved the cement binder and weakens the concrete pipe or manhole.

Corrosion is most severe at the crown (top) and waterline of concrete wastewater collection pipes and manholes. Pipe walls are typically cooler than the wastewater flow, and resulting upward air flow in the center and downward air flow near pipe walls causes more condensation at the top of the pipe. This increased surface moisture facilitates the dissolution of hydrogen sulfide, which can then support acidogenic biofilms. Severe corrosion can also occur at the waterline, as wastewater flow continually erodes corroded material and exposes underlying concrete to headspace gasses, enabling further corrosion (Bowker et al., 1989). The corrosion process is diagrammed in Figure 2.1.

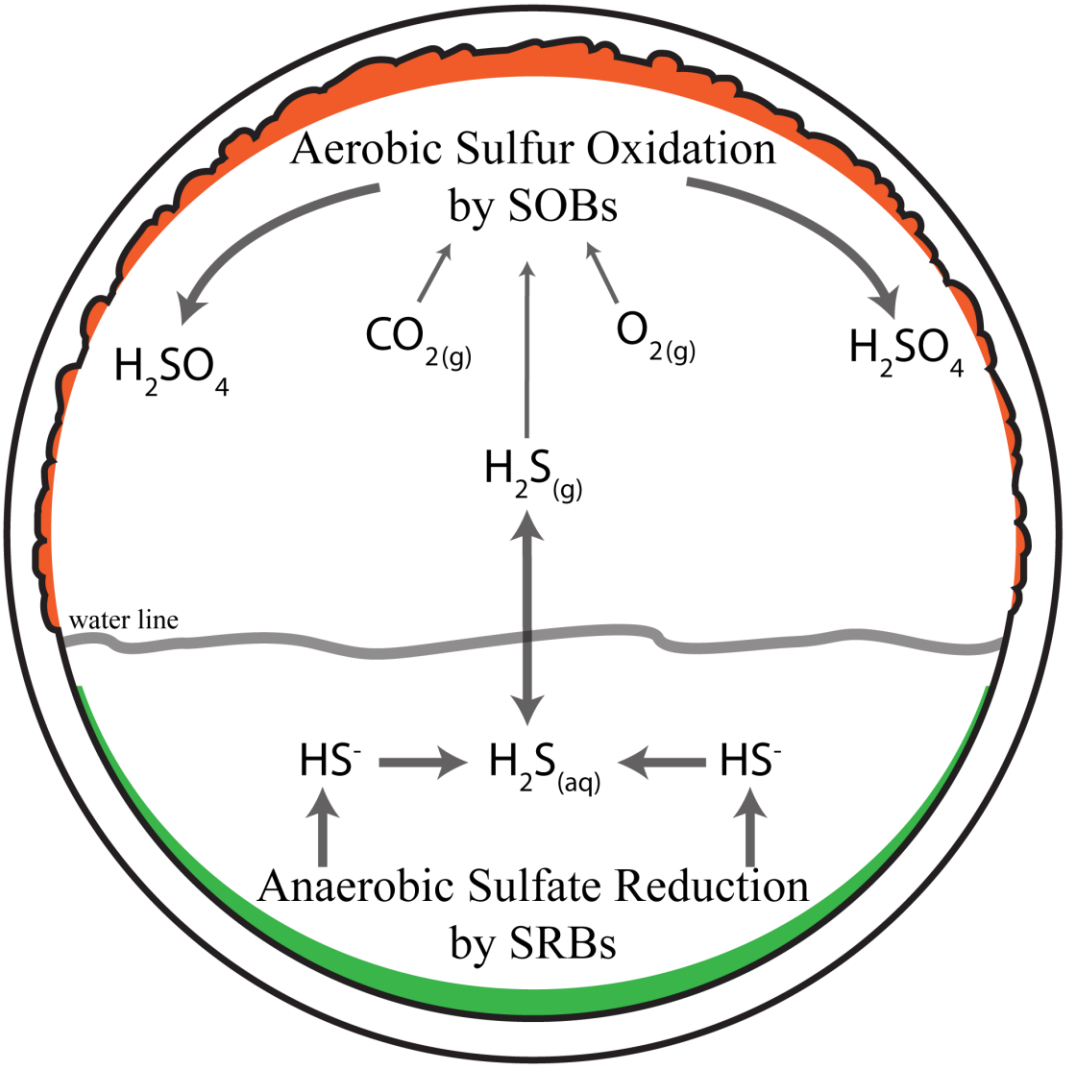

Figure 2.1: Cross-section of sewer pipe processes and sulfur cycling in microbially induced concrete corrosion, SOB stands for sulfur-oxidizing bacteria, SRB stands for sulfate-reducing bacteria. Green and orange shading represents sulfate-reducing and sulfur-oxidizing biofilms, respectively.

2.3. Sulfide in Sewers

2.3.1. Biological Sulfur Cycling

Corrosion in wastewater infrastructure is a self-sustaining biological sulfur cycle. Sulfur can exist at oxidation states between -2 to +6 (Table 2.1) and is a macronutrient used by all cells (Suzuki, 1999; Trudinger, 1979). Its speciation and redox state can be changed biologically by

microbes that use sulfur compounds as electron acceptors (dissimilatory or assimilatory sulfate reducers) or as energy sources (chemolithotrophs or photolithotrophs).

Table 2.1: Inorganic sulfur species and oxidation states, from Suzuki (1999)

Oxidation State				
-2	0	+2	+4	+6
H_2S hydrogen sulfide	S_8/S^0 elemental sulfur	(SO) sulfur monoxide	SO_2 sulfur dioxide	SO_3 sulfur trioxide
		H_2SO_2 sulfoxylic acid	H_2SO_3 sulfurous acid	H_2SO_4 sulfuric acid
HS^- bisulfide		$S_2O_3^{2-}$ thiosulfate	SO_3^{2-} sulfite	SO_4^{2-} sulfate
			$S_4O_6^{2-}$ tetrathionate	

2.3.2. **Sulfide Generation and Partitioning**

Sulfide production occurs in submerged anoxic biofilms, and is facilitated by high sulfate concentrations, low dissolved oxygen, low wastewater pH, low flows, and long residence times. As a result of the high organic content of wastewater, heterotrophic biofilms form along continuously wetted portions of the pipe circumference. If these biofilms become depleted of oxygen (anoxic), it becomes thermodynamically favorable for organisms to use sulfate as an electron acceptor to oxidize reduced organic matter substrates. These metabolic processes produce sulfide as a by-product, and are conducted by sulfate-reducing bacteria (SRBs) (Hvitved-Jacobsen, 2002; WERF, 2007). The thickness of these biofilms depends on pipe slope and substrate concentrations in wastewater. At flow velocities higher than 1 m/s, biofilm

thickness is typically less than 1 mm (Hvitved-Jacobsen, 2002). Biofilms typically need to be greater than 1 mm thick for the anoxic conditions required for sulfide production to develop (Zhang et al., 2008). However, concrete is very porous and may support anoxic conditions in pores even if the surface biofilm is less than 1 mm thick. See Figure 2.2 for a diagram of submerged biofilm processes.

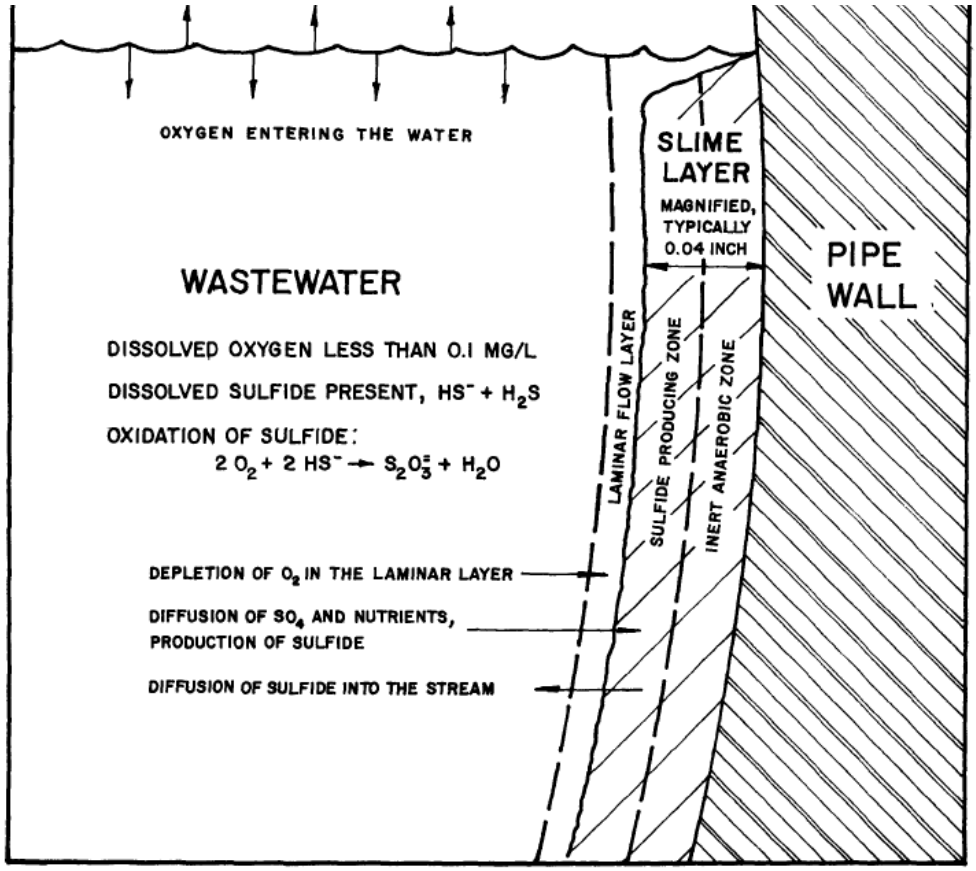

Figure 2.2: Submerged processes in sewers with sulfide production. Sulfide is produced in an intermediate biofilm layer where oxygen is depleted but sulfate is present, from USEPA (1974).

Sulfate-reducing bacteria (SRB) use organic matter as a substrate and sulfate as an electron acceptor. SRBs have commonly been observed to oxidize sulfate to sulfide through a dissimilatory sulfite reductase (*dsr*) gene cassette (Friedrich et al., 2005; Little et al., 2000; Santo Domingo et al., 2011). Dissolved sulfate is typically in wastewater at concentrations between

40-200 mg/L (Hvitved-Jacobsen, 2002; Tchobanoglous et al., 2002; Zhang et al., 2009). Higher sulfate concentrations support faster sulfide-production kinetics. Sulfide does not accumulate in systems where wastewater dissolved oxygen (DO) is maintained at concentrations above 0.5 mg oxygen/L, because it is chemically oxidized (Hvitved-Jacobsen, 2002). If dissolved oxygen is insufficient for complete sulfide oxidation, the sulfide persists in the wastewater. Hydraulic design characteristics that limit re-aeration of wastewater, such as low turbulence, long residence times, and full-flowing pipes, lead to low DO concentrations and high sulfide concentrations in wastewater (Bowker et al., 1989). Abundant dissolved sulfide kinetically favors the partitioning of H_2S gas into structure headspaces, but the process is pH dependent.

Of the three sulfide species—sulfide, bisulfide, and hydrogen sulfide—only hydrogen sulfide can partition into a gas phase. The pKa of hydrogen sulfide/bisulfide system is 7, so at pH values below 8, hydrogen sulfide will be present and can partition into the headspace (Nielsen et al., 2008; Stumm et al., 1996). At pH values below 7, most of the sulfide present will be in the hydrogen sulfide form. The typical pH of domestic wastewater is between 7-8 (Tchobanoglous et al., 2002; WERF, 2007), so even small changes in pH can drastically change hydrogen sulfide flux to the headspace. Because its partitioning is mediated by diffusion, H_2S gas and associated corrosion are more prevalent downstream of structures that increase the air-water interface through mixing, such as pump stations and force mains. As a result of the dependence of partitioning and biogenic rates on temperature, headspace sulfide concentrations are highly seasonal (USEPA, 1974).

2.3.3. **Strategies to Limit Sulfide Generation**

Engineers and scientists have investigated and implemented a variety of techniques to limit sulfide production and headspace partitioning. These fall into three categories: a.) methods

to inhibit the activity of sulfide-oxidizing bacteria, b.) methods to remove sulfides from the wastewater, and c.) methods to limit the partitioning of hydrogen sulfide from wastewater to headspace (USEPA, 1985; WERF, 2007).

One method to prevent the production of sulfide in sewers is to inhibit the activity of sulfate-reducing biofilms. This can be achieved by changing redox conditions through the addition of alternate electron acceptors such as nitrate (NO_3^-), which has been shown to prevent sulfide production at concentrations above 5 mg/L (Allen, 1949; Churchill et al., 1999; Rodríguez-Gómez et al., 2005). Periodic dosing of NaOH or $Mg(OH)_2$ can be used to pH-shock biofilm communities and has been shown to disrupt biofilm activity for up to two weeks (USEPA, 1991). SRB communities can also be inhibited by chemical biocides such as free nitrous acid (Jiang et al., 2011) or formaldehyde (Zhang et al., 2009).

Dissolved sulfide can be removed from wastewater by chemical or biological oxidation or through precipitation of metal sulfides. One method used to chemically oxidize sulfide is air or oxygen injection. Air or oxygen can be added to anoxic wastewater at appropriate dosing stations in order to maintain dissolved oxygen in the wastewater (Gutierrez et al., 2008; USEPA, 1991). However, use of air or oxygen addition has declined in recent years due to pumping costs, and chemical additions have become more common (Ganigue et al., 2011). Chemicals such as hydrogen peroxide (H_2O_2), chlorine (Cl_2 or HOCl), and potassium permanganate ($KMnO_4$) can also be used to chemically oxidize sulfide (Cadena et al., 1988; USEPA, 1985; Zhang et al., 2008). Alternately, biological oxidation of sulfide can be achieved by promoting the growth of nitrate-reducing sulfide-oxidizing bacteria. These bacteria are obligate nitrate-breathers, and can be active in the wastewater at less than 0.5 mg NO_3-N/mg HS-S (AEsoy et al., 2002; Zhang et al., 2008). Another widely used mechanism of removing sulfides from

wastewater streams is precipitation of metal sulfides, typically iron. Iron can be added as Fe(II) or Fe(III) salts or, in a waste reuse capacity, water treatment iron coagulation sludge (Edwards et al., 1997; Ganigue et al., 2011; Gustafsson, 2011; Nielsen et al., 2005; Zhang et al., 2008). Ferrous iron can quickly complex with sulfide to form FeS, which precipitates out of solution. Ferric iron can oxidize sulfide to elemental sulfur and is thus reduced to ferrous iron, which can then precipitate sulfide as FeS (Nielsen et al., 2005; Padival et al., 1995). Iron precipitation is most commonly used in large collection systems (Ganigue et al., 2011).

Diffusion of dissolved H_2S into the gas phase is facilitated by low pH and hydraulic conditions that increase the air-water interface. Wastewater pH can be raised to increase the ratio of bisulfide ion (HS^-) to H_2S and thus reduce the H_2S available to partition into the gas phase. $MgOH_2$ or NaOH are the most common chemicals used to raise wastewater pH (WERF, 2007). Alternately, new pipe systems can be designed to limit hydraulic mixing from sharp bends and lift stations. This approach can include using alternate designs for structures with hydraulic drops that minimize turbulence and designing force mains to discharge below manhole water levels (Bowker et al., 1989; WERF, 2007).

2.4. Sulfide Oxidation and Corrosion

Once in the headspace, the hydrogen sulfide (H_2S) dissolves into surface moisture on the crown or walls of pipes, manholes, and other structures. Sulfide can be oxidized biotically or abiotically to sulfuric acid (H_2SO_4) and intermediate sulfur species such as elemental sulfur (S^0) and thiosulfate ($S_2O_3^{2-}$) (Joseph et al., 2012). Environmental factors that affect sulfuric acid production rates and subsequent corrosion include hydrogen sulfide and carbon dioxide concentrations in the headspace, relative humidity, temperature, concrete mix design and admixtures used, and types of sulfur compounds present at the surface (Chang et al., 2005; De

Muynck et al., 2009; Hewayde et al., 2007b; Joseph et al., 2012; Mori et al., 1992; Roberts et al., 2002).

2.4.1. Concrete Composition and Chemistry

Over 70% of large (>20 inches) wastewater collection pipes in the United States are constructed from concrete, which is comprised of varying sizes of aggregate and cement binder (USEPA, 2009). Portland cement is the most common binder used in the United States. Concrete fabrication involves mixing the components with water, pouring the mix into molds, and curing the concrete at a specified temperature and humidity. Strength and corrosion resistance depend on the mix design, component characteristics, and curing conditions. Cured Portland cement is comprised primarily of calcium and silica oxide crystals, with some aluminum and iron and trace amounts of other elements. Calcium carbonates contribute alkalinity to the concrete, resulting in a pore water pH of 13-14 in fresh concrete (Lawrence, 1998).

2.4.2. Stages and Characteristics of MICC

The chemical degradation of concrete by oxidized sulfur and associated acids is collectively referred to as "sulfate attack," although it can involve other sulfur species. It can occur biotically or abiotically. Rates of corrosion are markedly higher under biological sulfate attack than under chemically-induced sulfate attack (Monteny et al., 2000). A biological model for the corrosion process proposed by Islander and colleagues (1991) outlines the stages of concrete corrosion. The pH of cured concrete is about 13 (Bowker et al., 1989; WERF, 2007). In stage 1 of MICC, the pH is abiotically reduced though carbonation and bisulfide dissolution, and a film of moisture forms on the concrete surface (Ismail et al., 1993; Joseph et al., 2012). Stage 2 begins once the surface pH reaches 9, and neutrophilic sulfide-oxidizing microbes

(SOMs) colonize the surface. These organisms oxidize reduced sulfur compounds to sulfuric acid, which further reduces the surface pH below 4. In stage 3, acidophilic sulfide-oxidizing microbes (SOMs) colonize the surface, corrosion rate increases, and pH decreases further (Islander et al., 1991). In this stage, the depressed pH and accelerated sulfuric acid production cause active surface corrosion. The stages of this process are illustrated in Figure 2.3.

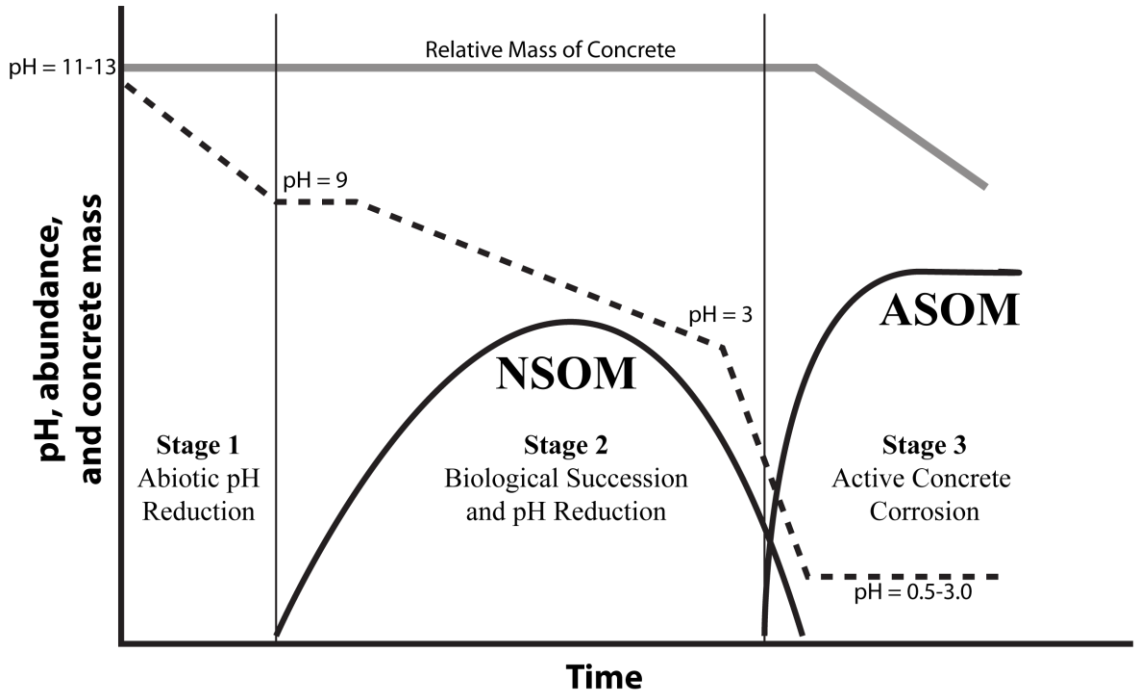

Figure 2.3: Temporal community succession and pH change in microbially induced concrete corrosion, adapted from Islander et al. (1991) and Roberts et al. (2002).

Portland cement contains about 64% calcium and 3% aluminum by mass, which are present primarily as carbonates and oxides (Lawrence, 1998). The sulfate produced by sulfur-oxidizing biofilms reacts with these calcium and aluminum oxides in the cured cement to produce corrosion products, dominated by gypsum, ettringite, and monosulfoaluminate. These collectively increase the volume of the matrix by 2-7 times (Monteny et al., 2000) and cause significant internal crystal pressure (Hewayde et al., 2007b; Hudon et al., 2011; Monteny et al., 2000; O'Connell et al., 2010; Roberts et al., 2002). A gypsum matrix can hold large quantities of

water, and is structurally much weaker than the calcium carbonates and oxides it replaces (Hewayde et al., 2007b; Islander et al., 1991; O'Connell et al., 2010). Ettringite is expansive, and can cause cracking (Hudon et al., 2011; Okabe et al., 2007). One study found that gypsum dominates the corrosion product at pH below 3, while ettringite dominates at higher pH values (Mori et al., 1992). These products can be washed away at high flows, resulting in decreased mass and reduced pipe thickness.

The corrosion surface is typically characterized by loss of cement binder, protruding aggregate, the presence of yellow elemental sulfur deposits, and occasionally grey, brown, or green staining from the biofilms that develop (Davis et al., 1998; Okabe et al., 2007; Parker, 1947). Scanning electron microscopy has shown the corroded surface to be comprised of numerous crystalline features (gypsum or other sulfur species) and microbial cells (Figure 2.4) (B. I. Cayford et al., 2010).

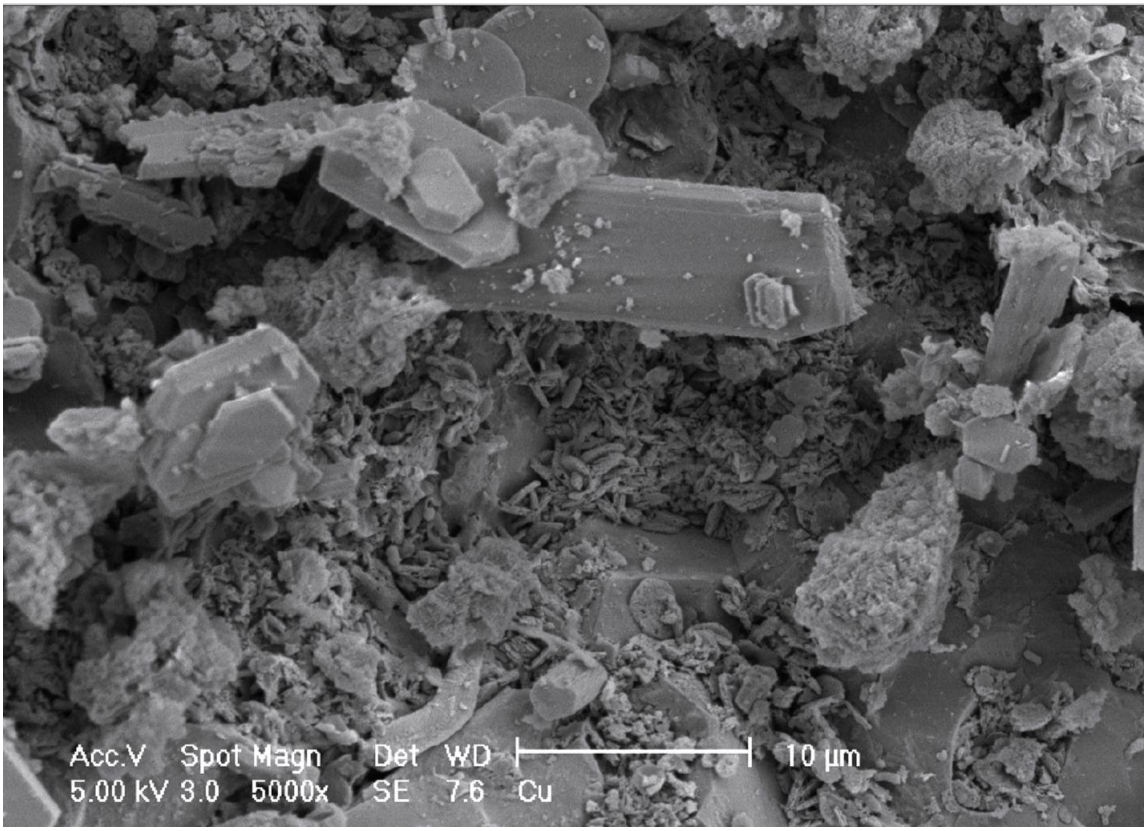

Figure 2.4: Scanning electron microscopy image of corroded concrete surface, from Cayford et al. (2012). Small elongated shapes are microbial cells, and angular crystal formations are sulfur-containing corrosion products.

One study found pH reduction rates of 0.025 pH units/day for initial corrosion stages based on a lab study of concrete coupons inoculated with SOMs and incubated at 99% relative humidity and 100 ppm H_2S (Roberts et al., 2002). However, pH reduction rates vary between corrosion environments. Although sulfuric acid has long been considered the main cause of corrosion, studies have shown that corrosive biofilms also produce organic acids, which can complex calcium ions and penetrate the concrete matrix to exacerbate corrosion severity (Gu et al., 1998; Valix et al., 2010b).

2.4.3. **Repair and Rehabilitation Methods to Limit Biological Sulfuric Acid Attack**

Depending on the degree of structural deterioration, corroded structures are typically repaired, rehabilitated, or replaced before corrosion causes structural failure scenarios. Concrete additives and coatings have been developed to impair corrosion in new concrete structures and to rehabilitate damaged structures (De Muynck et al., 2009). These methods fall into four general categories: a.) use of corrosion-resistant pipe materials, b.) surface coatings and linings, c.) concrete binder additives, and d.) antimicrobial additives. Methods are outlined in Table 2.2. There is still a need for standardized design and construction specifications for these methods (USEPA, 2009).

Table 2.2: Summary of treatment and rehabilitation techniques

treatment strategy	type of treatment	specific treatment examples
prevent sulfide production	Antimicrobials dosing oxidants oxygen injection	done with nitrous acid, nitrate dose with $KMnO_4$, Cl_2, H_2O_2 dose sewage flow with air or oxygen
prevent sulfide partitioning	pH elevation metal-sulfide precipitation	dose with NaOH, $Mg(OH)_2$ dose with iron salts dose with water treatment sludge
prevent acid production	antimicrobials crown spray	coat with metal zeolites, antimicrobial fibers
corrosion resistant material	alternate pipe materials alternate mix design	build with fiberglass, PVC, HDPE build with CAC, limestone aggregate
surface rehabilitation/repair	epoxy-based coatings spray-on linings cured in place linings	coat with polyurethane, coal tar coat with polymers, shotcrete coat with polyethylene, PVC

Polymer-based pipe materials such as polyvinyl chloride (PVC), fiberglass, and high-density polyethylene (HDPE) are not susceptible to acid attack and are thus resistant to corrosion. However, the cost of these materials is significantly higher than the cost of concrete,

and their structural load-bearing properties are often insufficient – particularly in large diameter pipes (Bowker et al., 1989; WERF, 2007).

Protective surface coatings aim to prevent corrosion by placing a physical barrier between biogenic sulfuric acid and the concrete surface. Application methods include spraying, painting, and slip-lining. Adequate surface preparation and effective application are important, as any leaks in the coating will allow corrosion to continue beneath the coating. This mitigation approach is especially difficult in sewer environments as a result of variable temperature, moisture, and the need to divert flow while work is conducted (Periasamy et al., 1994; Vadiya et al., 2007; WERF, 2007). Surfaces are prepared for coating by high-pressure washing, which removes corrosion product, biofilm growth, grease and dirt (Bowker et al., 1989), and sometimes by sand-blasting (Maier, 2013). Materials used for pipe surface coatings include epoxy, polyurethane, polyurea, and coal tar (USEPA, 2009). These polymer coatings are resistant to acid attack, and are more resistant to acid, abrasion, and moisture than untreated concrete surfaces (Berndt, 2011; De Muynck et al., 2009). Epoxy materials are cured with heat or through polymerization with amines or polyamides, and resistance is correlated with high solids content (Bowker et al., 1989). Spray-on cemetitious coatings (i.e. shotcrete) are another promising rehabilitation method, as they are easier to apply and cure. However, these coatings do not prevent further corrosion from occurring (USEPA, 2009). One common rehabilitation method is slip-lining degraded pipe with cure-in-place pipe (CIPP) plastic liners, which are both structurally supportive and resistant to corrosion. This method is documented under ASTM standard F-1216. After the corrosion products are removed, a lining is placed in the sewer pipe and cured by UV light or hot water. CIPP lining materials include reinforced polyethylene, polyvinyl chloride, and carbon/fiberglass (USEPA, 2009).

Changing concrete mix design through the addition of admixtures, alternate binders or alternate aggregate can also chemically improve corrosion resistance. Calcium aluminate cements have a higher aluminum content than Portland cement and have historically had better performance in sulfate rich environments (Scrivener et al., 1998). While low water to cement ratios generally result in stronger concrete, using a high water to cement (up to 50%) yielded less mass loss after immersion in sulfuric acid (Chang et al., 2005; Hewayde et al., 2007b). The addition of 5-10% silica fume or 40% blast furnace slag to the concrete mix design or the use of calcium aluminate mortars increased compressive strength and decreased permeability and etching by *Acidithiobacillus ferrooxidans* (Berndt, 2011). Concrete made with limestone aggregate in place of the more widely-utilized siliceous aggregate experienced lower mass loss and better load bearing characteristics after exposure to sulfuric acid due to the higher alkalinity/carbon content of limestone (Chang et al., 2005). Some polymer additives have also been shown to increase corrosion resistance (Chaussadent et al., 2012; Monteny et al., 2001)

Antimicrobial treatments for concrete inhibit the growth of sulfide-oxidizing microbes responsible for biogenic sulfuric acid production using metals or antimicrobial compounds (De Munyck et al., 2010; De Muynck et al., 2009). Antibiotic-loaded fibers (MicrobanB) inhibit bacterial growth using triclosan—an antibiotic that is also used in personal care products. These fibers can be added to concrete mixtures prior to curing to impart antibiotic properties to the surface, but this practice is not common in the field (De Munyck et al., 2010; De Muynck et al., 2009).

In the third aim of this thesis, a metal-carbon formulation is tested as a potential treatment to inhibit sulfur oxidation and resulting corrosion. Use of toxicity-based products for corrosion prevention remains uncommon the wastewater industry, and carbon sorbents have not been

previously used as a delivery mechanism. Several studies and one product (ZeoMighty, www.zeomic.co.jp) use zeolites to deliver metal ions. Zeolites are aluminosilicate adsorbent materials that are used in the corrosion industry to slowly deliver toxic heavy metal ions such as copper and silver to the concrete surface over the pipe's service life (De Muynck et al., 2009; T. Haile et al., 2008). Concrete mortars treated with either technology and inoculated with sulfide-oxidizing cultures had reduced levels of adenosine triphosphate (ATP) —an indicator of microbial activity—when compared to untreated cement mortar (De Muynck et al., 2009). Silver zeolites also inhibit the growth of *Acidithiobacillus thiooxidans* and other bacterial cultures (De Munyck et al., 2010; T. Haile et al., 2008). Heavy metal oxides (copper and silver) mixed with commercial epoxy coatings has been shown to inhibit sulfate-reducing cultures, but has not been tested with sulfide-oxidizing cultures (Hewayde et al., 2007a). These biofilm-targeting methods fare well in laboratory and small-scale tests, but are typically more expensive than polymer coatings (De Muynck et al., 2009; T Haile et al., 2010).

Another product (ConMicShield, www.conshield.com) uses silicone quaternary ammonium salts to kill bacteria electrostatically and has been widely applied in the field to inhibit corrosion-causing bacteria (ConMicShield, 2011; Holt, 2008; R. Kelly et al., 2011). However, the exact mechanism of inhibition remains proprietary. ConMicShield can be added to concrete mix prior to curing or applied retroactively using shotcrete.

2.5. Microbiology Associated with Concrete Corrosion

Temporal and spatial dynamics (on both small and large scales) of the microbiological agents responsible for sulfuric acid production in wastewater structures are still being elucidated. Previous studies have largely focused on biochemical kinetics using culture-based methods (Bielefeldt et al., 2009; Jensen et al., 2009; Roberts et al., 2002; Vollertsen et al., 2008). The

greater environmental microbiology literature contains only six reports which have used sequence-based phylogenetic analyses in microbially induced concrete corrosion (B. Cayford et al., 2012; Gomez-Alvarez et al., 2012; Okabe et al., 2007; Santo Domingo et al., 2011; Satoh et al., 2009; Vincke et al., 2001). However, each study in this cohort shares common spatial and temporal sampling limitations. None of the studies investigated the temporal succession of corrosion in one site over more than three time-points, and none compared microbial communities associated with corrosion across geographic regions.

2.5.1. **A Note on "Biofilms"**

Acidogenic, sulfur-oxidizing communities on the surface of corroding concrete are frequently referred to as "biofilms," which refers to bacterial cells embedded in a matrix of extra-polymeric substances (EPS). EPS compounds are adhesive organic compounds that enable sessile, or immobilized, bacterial lifestyles by facilitating surface adhesion, substrate access, sustained moisture, and intracellular communication (REF). The primary community member implicated, *Acidithiobacillus* spp., is known to produce hydrophobic lipopolysaccharide EPS compounds that facilitate sulfur access (Gehrke et al., 2001; Gehrke et al., 1998; González et al., 2012). However, not all sulfur-oxidizing organisms produce EPS. In the literature review and results discussion of this thesis, the term "biofilm" is used to refer to a microbial community existing on the surface or subsurface of a concrete or concrete coating. As EPS was not explicitly measured, the use of the word "biofilm" in this thesis does not refer to a scientifically validated EPS matrix.

2.5.2. **Traditional View of MICC Microbiology Based on Culture Studies**

The genera most typically associated in biogenic acid production at pH values below 3 is *Acidithiobacillus* spp., which can perform non-assimilatory oxidation of reduced sulfur

compounds at pH values below 1 (D. P. Kelly et al., 2000). *Acidithiobacillus ferrooxidans* can oxidize reduced sulfur or iron compounds for energy and are best known for their role in acid production and metal mobilization in acid mine drainage. *Acidithiobacillus thiooxidans*—formerly known as *Thiobacillus thiooxidans* and *Thiobacillus concretivorus*—is an obligate sulfur-oxidizer and was the first bacteria associated with MICC (D. P. Kelly et al., 2000; Parker, 1945). Many modules that test materials for resistance to biological sulfate attack use *At. thiooxidans* to form biogenic acid (Monteny et al., 2000). Neutrophilic sulfide-oxidizers *Thiobacillus thiomonas*, *Thiomonas intermedia*, *Halothiobacillus neapolitanus*, and *Starkya novella* have been associated with early stages of corrosion (Islander et al., 1991; Okabe et al., 2007; Roberts et al., 2002). These bacteria can use a variety of reduced sulfur compounds, including hydrogen sulfide (H_2S), elemental sulfur (S^0), thiosulfate ($S_2O_3^{2-}$), and tetrathionate ($S_4O_6^{2-}$) (Little et al., 2000). Some acidophilic sulfide-oxidizers have alternate metabolic pathways. For example, *Leptospirillum ferrooxidans* and *Acidithiobacillus ferrooxidans* can oxidize reduced iron for energy, and mixotroph *Acidiphilium acidophilium* can use reduced organics as an energy source (Little et al., 2000; Rohwerder et al., 2007). One study found that concrete corrosion could be caused by an fungi of genus *Fusarium* (Gu et al., 1998). The phylogenetic diversity of the species associated with concrete corrosion prior to data from phylogenetic studies is illustrated in Figure 2.5.

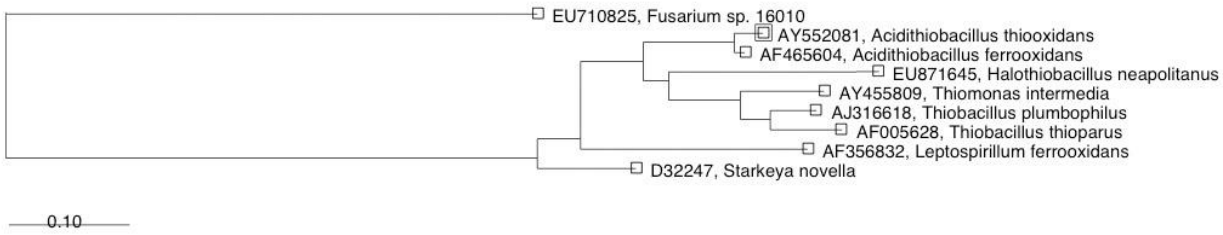

Figure 2.5: Maximum likelihood tree of species previously implicated in MICC, generated using the ARB software environment (Ludwig et al., 2004). The horizontal distance between species sequences represents the fraction of sequence that differs, with the legend bar representing 10% difference. Number codes indicate NCBI GenBank accession numbers.

2.5.3. Biochemistry of Acidophilic Sulfur Oxidation

Sulfur can be present in eight different oxidation states, ranging from -2 to +6 (Suzuki, 1999). Environmentally-stable sulfur compounds and their oxidation states are shown in Table 2.1. A range of reduced sulfur compounds are available as potential substrates for non-assimilatory oxidation in MICC biofilms. Full biological oxidation to sulfate occurs in several steps (Islander et al., 1991; Jensen et al., 2008; Rohwerder et al., 2007; Vollertsen et al., 2008). H_2S gas can dissolve in surface water to form bisulfide (HS^-) and sulfide (S^{2-}) ions. These species can be biotically or abiotically oxidized to elemental sulfur at the concrete surface. Biological mechanisms produce thiols (R-SH) and sulfite (SO_3^{2-}), which can be abiotically oxidized to thiosulfate ($S_2O_3^{2-}$) and tetrathionate ($S_4O_6^{2-}$). These compounds can all serve as electron donors for sulfur oxidation which can support different communities of microbes (Islander et al., 1991; Nica et al., 2000; Sand, 1987). Elemental sulfur (S^0) is the most thermodynamically stable species at acidic pH (Rohwerder et al., 2007). It is a metabolic intermediate that can act as an energy reservoir, enabling SOB communities to thrive after six months of hydrogen sulfide starvation (Jensen et al., 2008).

Early culture studies show that different reduced sulfur compounds select for different SOMs. While *Acidithiobacillus thiooxidans* were most present on concrete coupons with

hydrogen sulfide as a sulfur source, *Halothiobacillus neapolitanus* and *Thiobacillus intermedius* were more abundant on coupons with thiosulfate (Sand, 1987).

While bacterial sulfur oxidation in neutral pH ranges typically occurs via the well-characterized *sox* sulfur oxidation pathway, the biochemistry of inorganic sulfur oxidation in acidophiles is not fully understood, and mechanisms appear to differ between bacteria and archaea (Friedrich et al., 2005; Rohwerder et al., 2007). The key difference is that bacterial sulfur oxidation passes through an organic sulfur intermediate, while archaeal sulfur oxidation does not (Friedrich et al., 2005; Quatrini et al., 2009; Rohwerder et al., 2007).

In acidophilic proteobacteria, two sulfur oxidation mechanisms have been proposed. In the first (Figure 2.6), sulfide is transformed into organic thiol groups, which are oxidized to sulfite by sulfur diooxygenase (SDO). The sulfite is then oxidized to sulfate via a sulfite:acceptor oxidoreductase (SAR). In this system, abiotically produced thiosulfate can be oxidized to tetrathionate, which is oxidized by a tetrathionate hydrolase (TTH) to sulfate. TTH is the final enzyme leading to sulfuric acid production and has been observed in *Acidithiobacillus* spp. and *Acidiphilium* spp. (Rohwerder et al., 2007). The second proposed mechanism is a seven-gene heterodisulfide reductase complex observed in an *Acidithiobacillus ferrooxidans* strain. This complex was up-regulated in the presence of sulfur-containing media and catalyzes a reversible reduction of R-S-S-R organic sulfur groups (Quatrini et al., 2009). The inhibition of any of these enzyme systems through toxicity (i.e. heavy metals) could inhibit sulfur oxidation and subsequent concrete corrosion *in situ*.

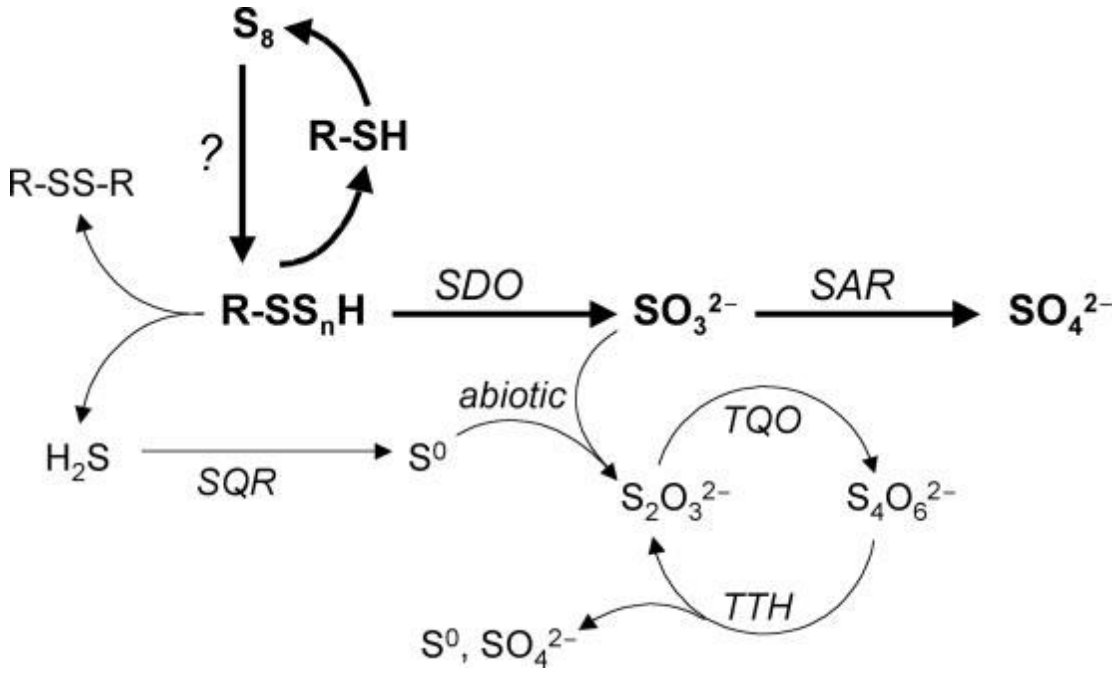

Figure 2.6: Inorganic sulfur oxidation by acidophilic proteobacteria. From Rohweder and Sand (2007). Enzymes listed are sulfide:quinone oxidoreductase (SQR), sulfur diooxygenase (SDO), sulfite:acceptor oxidoreductase (SAR), thiosulfate:quinone oxidoreductase (TQO), tetrathionate hydrolase (TTH).

Acidophilic archaea use a sulfur oxygenase reductase (SOR) to perform a disproportionation reaction, which forms both sulfite and hydrogen sulfide from elemental sulfur. This sulfite can be oxidized to sulfate using SAR or abiotically reduced to thiosulfate, which is oxidized to tetrathionate via a thiosulfate:quinone oxidoreductase (TQO) (Friedrich et al., 2005; Rohwerder et al., 2007).

2.5.4. Phylogenetic Studies of MICC Communities

Recent advances in molecular biology using the small subunit ribosomal RNA gene (SSU rRNA) as a phylogenetic marker have enabled an unprecedented view of the MICC community structure. DNA sequencing has become exponentially more affordable over the last few decades; millions of environmental genes can now be inexpensively sequenced and identified using public sequence databases (Hamady et al., 2008).

In accordance with previous culture-based work, phylogenetic studies suggest that pH is the primary environmental factor related to community composition. In longitudinal studies of up to one year, the microbial community observed became less diverse as the concrete surface becomes more acidic (Okabe et al., 2007; Satoh et al., 2009). The early community was dominated by heterotrophs and neutrophilic sulfur oxidizing gamma-proteobacteria, especially *Halothiobacillus* spp. As the surface pH drops, the community became dominated by acidophilic sulfide-oxidizing microbes, the most abundant of which was *Acidithiobacillus* spp. (Okabe et al., 2007; Satoh et al., 2009). The only heterotrophs that appeared to survive low pH surface conditions were *Mycobacterium* spp. (Okabe et al., 2007; Vincke et al., 2001); high levels of hydrophobic mycolic acid in their cell coat may protect the cells from extreme pH. The *Mycobacterium* genus includes pathogens such as *Mycobacterium tuberculosis* and *Mycobacterium avium*. Acidophilic mycobacteria have previously been observed in an endolithic geothermal environment in Yellowstone National Park (Walker et al., 2005). The decreased diversity observed in low pH MICC conditions is consistent with results of acid mine drainage studies; few species are adapted to maintain neutral cytoplasmic chemistry in an acidic environment (B. J. Baker et al., 2006; Bond et al., 2000).

The USEPA performed two studies investigating early stage corrosion microbiology on Cincinnati sewer pipes. In the first study, biofilm samples were collected from twenty-one sites, including manholes, pipe crowns, and pipe inverts (Santo Domingo et al., 2011). In crown communities, beta-Proteobacteria, including *Thiobacillus* spp. and *Thiomonas* spp., were the most dominant group. *Acidithiobacillus* spp., *Halothiobacillus* spp., and *Acidiphilium* spp. have all been previously implicated in MICC processes, but were not detected in this study of crown biofilms. Another study by the same group performed metagenomic analysis of a sample from

the crown and invert of a 65-year old pipe in Cincinnati (Gomez-Alvarez et al., 2012). The study found that bacteria dominate the MICC-associated community; archaeal, fungal, and phage sequences were also detected. The sulfur oxidizing bacteria detected were primarily *Thiobacillus* spp., *Thiomonas* spp., and *Acidiphilium* spp. No *Acidithiobacillus* spp. sequences were found. The majority of functional genes detected were affiliated with carbohydrate metabolism, indicating the activity of heterotrophs. Sulfur metabolism genes detected included those associated with thiosulfate and sulfate metabolism. An estimated 66% of sulfur-oxidizers contained the *soxB* gene, which is used for sulfur oxidation at neutral pH. Heavy metals resistance and antibiotic resistance genes were also detected (Gomez-Alvarez et al., 2012).

A recent PhD thesis investigated *in situ* MICC communities in six different municipalities in Australia and found *Acidithiobacillu*s spp., *Acidiphilium* spp., *Mycobacterium* spp., and Xanthomonadaceae to be the most abundant microbial groups across a range of environmental gradients (B. I. Cayford, 2013). Other previous phylogenetic studies have included at least three of these groups (Gomez-Alvarez et al., 2012; Okabe et al., 2007; Santo Domingo et al., 2011; Vincke et al., 2001), which indicates that these groups are likely to be major players in MICC communities, regardless of geographic region and local environment.

2.5.5. **Geography of MICC Microbiology**

Corrosion of wastewater infrastructure is a worldwide phenomenon that has been studied in many countries, including the United States (Gomez-Alvarez et al., 2012; Santo Domingo et al., 2011), Mexico (Wilczak et al., 1993), Germany (Sand et al., 1984), Belgium (Vincke et al., 2001), Denmark (Nielsen et al., 2008), Lebanon (Ayoub et al., 2004), Japan (Mori et al., 1992; Okabe et al., 2007), and Australia (B. Cayford et al., 2012; Valix et al., 2010b). In general, the microbial community observed appear correlated to the surface pH and extent of corrosion;

disparities between geographical areas have not been investigated. In a one-year Japanese study of corroding concrete in one location, the most abundant type of organism were gamma-proteobacteria such as *Halothiobacillus* spp. and *Acidithiobacillus* spp.; *Acidithiobacillus* spp. comprised over 50% of a late-stage corrosion community (Okabe et al., 2007). Conversely, a study of Cincinnati MICC biofilms found that beta-Proteobacteria such as *Thiomonas* spp. outnumber gamma-proteobacteria (Santo Domingo et al., 2011), and a study in Australia found that *Acidithiobacillus* spp. was frequently present but not always dominant (B. Cayford et al., 2012).

2.6. Risk Factors for MICC

The occurrence of MICC is strongly correlated to the hydraulic flow regimes and structure configuration in wastewater systems as well as the chemical characteristics of its wastewater (Table 2.3). H_2S concentration is generally assumed to be the most predictive factor for corrosion severity, though the correlation between these two factors has not been mathematically modeled (WERF, 2007). Pipes that are not designed to be self-cleaning (i.e. low pipe slopes) or have long hydraulic residence times (i.e. long, flat collection systems) promote increased sulfide generation in sewers. Hydraulic features that cause turbulence and mixing (i.e. force mains, lift stations) increase the air-water interface and speed the partitioning of hydrogen sulfide into the air phase, which also promotes corrosion (Bowker et al., 1989; USEPA, 2009). Lower wastewater pH is another risk factor, as pH-dependent sulfide speciation dictates how much hydrogen sulfide can partition into the headspace (Bowker et al., 1989; Nielsen et al., 2008). Additionally, high sulfate concentrations, low dissolved oxygen, and warm temperatures increase the kinetics of sulfide production in submerged biofilms (USEPA, 1974).

Table 2.3: Collection system risk factors for odor and corrosion

type of feature	system feature	type of risk
hydraulic	force mains lift stations turbulent pipe bends	H_2S partitioning
	long residence times low pipe slope	sulfide production
chemical	high SO_4 low DO	sulfide production
	low pH	H_2S partitioning
thermodynamic	high temperatures	sulfide production

MICC has increased substantially in the past few decades for several reasons (Bowker et al., 1989; Rootsey et al., 2010). First, industrial metal inputs to wastewater collection systems in the United States decreased in the 1970's due to National Pollutant Discharge Elimination System (NPDES) implemented as part of the Clean Water Act regulations (Congress, 1972). As a result, hydrogen sulfide concentrations in sewer gas were markedly lower before this time, and concrete corrosion was less prominent. This theory is supported by data from the Los Angeles County, where total sulfide in wastewater increased from 0.1 mg/L in 1971 to 1.4 mg/L in 1986 (CSDLAC, 1988; Morton et al., 1991; Stahl et al., 1989; USEPA, 1991). The reduction of iron, zinc, and chromium following pre-treatment legislation was projected to account for 95% of the increase in dissolved sulfide levels (Stahl et al., 1989). Some of these metals may also have inhibited the growth of sulfide-producing biofilm through toxicity. Laboratory testing indicates that sulfate-reducing bacteria and sulfide generation are inhibited by 5-50 mg/L of copper, nickel, cadmium, chromium, lead, or zinc (CSDLAC, 1988; Fang et al., 2002; USEPA, 1991; Utgikar et al., 2003). Secondly, urban growth has led to larger collections systems that require more pumping and have increased residence times. Pumping stations increase the area of the liquid-gas interface and allow for accelerated partitioning of H_2S to the gas phase, and long

residence times allow for more sulfide production in pipes. Thirdly, warming climates are expected to lead to higher wastewater temperatures and more microbial activity, which lead to lower dissolved oxygen in wastewater and more anoxic conditions in submerged biofilms. This in turn leads to increased sulfide production and higher biological acid production rates. In addition, corrosion is exacerbated by intrusion of sulfate-rich groundwater and seawater, which will become more serious if climate change leads to rising sea and groundwater levels (Rootsey et al., 2010).

2.7. Carbon and Metal Materials Aspects Relevant to Test Formulation

One component of this thesis research involves design and testing of a formulation comprised of activated carbon impregnated with metal that can confer toxicity to inhibit corrosion-causing biofilms. The following section summarizes relevant literature findings related to the design and feasibility of designing and implementing such a product

2.7.1. Activated Carbon

Activated carbon has been used widely in water treatment to remove taste and odor compounds, dissolved organic matter, and trace contaminants. It is characterized by very high surface areas, which enables contaminant sorption through ion- and electron-exchange (Snoeyink et al., 1967). To manufacture activated carbon, a variety of carbon materials (including coal, charcoal, nut shells, and fruit stones) can be carbonized to a char at temperatures below 600°C and activated through chemical oxidation at high temperatures (Kobya et al., 2005; Selvi et al., 2001; Snoeyink et al., 1967). Sorption capacity can be improved through the use of organic surface ligands, such as tetrabutyl ammonium and benzotriazole (Monser et al., 2002; Nevostrueva, 2009).

2.7.2. **Metal Sorption and Activated Carbon**

Sorption is the combination of adsorption to a surface and absorption into a surface. Heavy metal sorption to activated carbon has been well studied in the context of removing metal contaminants from waste streams. Both sorption of metals to activated carbon surface sites and desorption of metal from these sites is dependent on the solution pH, temperature, and activated carbon characteristics such as the point of zero charge, acid/base properties, and mesopore/micropore capacity (Hu et al., 2003; Kobya et al., 2005; Marzal et al., 1996; Reed et al., 1993; Selvi et al., 2001). Generally, cationic metal ions sorb more strongly at high pH, while anionic metal ions sorb more strongly at low pH. Additionally, metal ions sorption increases with increased temperatures (Leyva-Ramos et al., 1997; Marzal et al., 1996). While increased surface area is generally considered advantages to sorption processes, one study observed that the surface area of activated carbon granules did not significantly affect metal sorption (Reed et al., 1993). Metals loaded onto activated carbon in batch reactors have been observed to reach adsorption equilibrium after 48 hours (Kobya et al., 2005; Marzal et al., 1996).

Desorption of metal ions from activated carbon surfaces is less well documented. The amount of metal ions that can be recovered (desorbed) from activated carbon ultimately depends on how much has been sorbed to surface sites. However, sorption is not always fully reversible, and sorbed metals typically cannot be fully recovered as a result of irreversible binding of metals to surface sites (Fitzmorris et al., 2006; Hu et al., 2003; Jia et al., 1999; Ranganathan, 2000). The desorption process is typically slower than adsorption, and the flux and extent of desorption is dependent on temperature, solution pH, and metal type and speciation (Demiral et al., 2008; Fitzmorris et al., 2006; Hamdaoui et al., 2005; Hu et al., 2003; Periasamy et al., 1994; Rao et al., 2006; Wilczak et al., 1993). In addition, surface pore distribution affects desorption. Metals are

more easily removed from surface sites in mesoporous (2-50 nm pore diameter) than in microporous carbons (<2 nm pore diameter) (Hu et al., 2003). Desorption can additionally be facilitated by ultrasound (Hamdaoui et al., 2005). Aim 3 of this thesis leverages the pH-dependent sorption and desorption of heavy metal ions to deliver heavy metal toxicity to detrimental biofilms, an application which has not previously been patented or marketed.

Because of the potential for industrial recycling, the metals ions selected for the trial formulations developed in this work were cadmium (Cd^{2+}) and chromate (CrO_4^{2-}). Cadmium ions adsorb to activated carbon at pH values between 1 and 9. At higher pH values, the metal precipitates out of solution as $Cd(OH)_2$ salts. At lower pH, the activated carbon surface sites become increasingly protonated, decreasing the cadmium cation adsorption capacity (Kobya et al., 2005; Leyva-Ramos et al., 1997). One study found that cadmium sorption increased by a factor of ten between pH 1 and pH 6, and another found that cadmium sorption increased by a factor of five between pH 5 and pH 8 (Kobya et al., 2005; Marzal et al., 1996). Additional data relating the pH dependence of cadmium and chromate sorption are presented in Table 2.4. Cadmium sorption follows Langmuir isotherm model of adsorption, and appears to occur primarily through ion exchange (Leyva-Ramos et al., 1997; Periasamy et al., 1994).

Chromate sorption is a function of both solution pH and speciation (Table 2.4). At pH values below 3, the dominant form of the element is chromium (Cr^{3+}) which, like other metal cations, adsorbs poorly to activated carbon at low pH (Selvi et al., 2001). Chromate anions are more strongly sorbed to activated carbon at low pH values due to the positive charge of protonated surface sites (Kobya et al., 2005; Selvi et al., 2001). pE-pH diagrams for cadmium and chromium, as presented in Figure 2.7, outline speciation across a range of redox conditions and pH values.

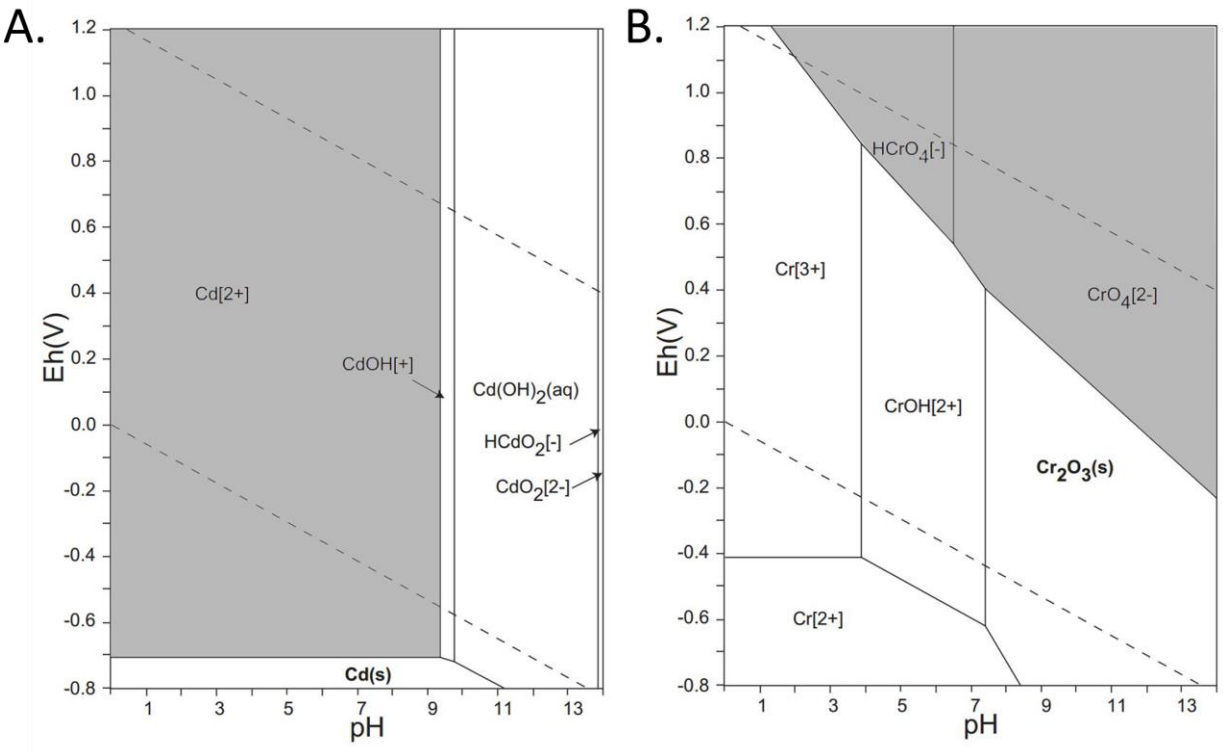

Figure 2.7: pe-pH diagrams for A.) cadmium and B.) chromium. Toxic, aqueous forms are highlighted in grey. Adapted from Takeno (2005).

Table 2.4: Sorption of cadmium and chromate ions to activated carbon at different pH values, from previous literature.

		% of Metal Removed from Solution				
Metal	Concentration (mg/L)	pH 2	pH 4	pH 6	pH 8	Reference
Cd(II)	67	53	89	99	-	Kobya et al. (2005)
Cd(II)	52	-	5	15	56	Marzal et al. (1996)
Cd(II)	6	-	13	47	91	Marzal et al. (1996)
Cd(II)	20	55	98	99	99	Kadirvelu and Namasivayam (2003)
Cd(II)	40	48	82	83	84	Kadirvelu and Namasivayam (2003)
Cd(II)	15	4	26	42	48	Teker et al. (1998)
Cr(VI)	70	97	54	10	-	Kobya et al. (2005)
Cr(VI)	100	100	33	28	20	Demiral et al. (2008)

2.7.3. **Mechanisms of Metal Toxicity and Resistance**

Transition metals act as micronutrients in biological systems and play a key role in enzyme cofactors and electron transporters. However, high levels of heavy metals can be toxic, as they impair microbial processes by replacing other micronutrient metals in enzymes or by denaturing protein molecules (Gadd et al., 1978). The degree of toxicity depends on many factors including cell age, nutrition, and location in a biofilm; metal speciation and concentration; the environmental pH, redox potential, and moisture content (Babich et al., 1980). Metals resistance mechanisms in bacteria can transfer between cells via horizontal gene transfer. These mechanisms include efflux pumps, sequestration, alteration, and exclusion (Dopson et al., 2003).

Cadmium is present in neutral and acidic aqueous solutions as Cd^{2+}. Its uptake into microbial cells is poorly understood, but is generally thought to occur through the manganese uptake system (Nies, 1999). Cadmium toxicity to microbes occurs through thiol binding, protein denaturation, or interference with zinc and calcium metabolism (Dopson et al., 2003). Cadmium can be removed from solution at high pH as $Cd(OH)_{2(s)}$, so increased ionization at low pH leads to increased toxicity. In wastewater environments, insoluble cadmium sulfide can form when Cd(II) reacts with H_2S (USEPA, 1991).

Chromium is not used beneficially by microbes. Of the two common oxidation states of chromium, chromium(III) has lower solubility and toxicity to microbes and is present in cationic form when dissolved. Conversely, chromium (VI) is toxic at low concentrations and soluble at environmental conditions as chromate (CrO_4^{2-}) or dichromate ($Cr_2O_7^{2-}$) anions (Kobya et al., 2005; Nies, 1999). Chromate (CrO_4^{-}) ions were selected for use, because they are in the Cr(VI) state. Chromate and other Group V and VI anions have previously been shown to inhibit thiosulfate oxidation in *Halothiobacillus neapolitanus* strains (D. P. Kelly et al., 1997). Previous work has found 25 mg/L chromium prevented sulfate oxidation (USEPA, 1991). Chromium resistance is based on a combination of reduction and efflux (Nies, 1999). Chromium sulfide (Cr_2S_3) can form from Cr(III) and H_2S, and is a potential fate of chromium added to the system.

2.7.4. **Metal-Sulfide Interactions**

Metal sulfides have extremely low solubility constants in aqueous solution, so they can act as removal sinks for dissolved sulfide in wastewater if metals are present. Studies suggest that prior to 1970's, when the National Pollutant Discharge Elimination System permits (enacted as part of the Clean Water Act legislation) limited industrial discharge of metals to municipal

sanitary sewers, metal complexation and precipitation removed sulfide from large stretches wastewater collection systems. Both complexation chemistry and cellular toxicity are strongly dependent on water quality parameters such as pH, hardness, and temperature (Babich et al., 1980; Gadd et al., 1978). Removal of metal ions from waste stream using sulfide precipitation has been successfully applied in both acid mine drainage and wastewater treatment (Benner et al., 2002; Bhattacharyya et al., 1979). In the context of this research, if metal ions released from carbon sorbents on treated concrete surfaces were to reach the wastewater flow, they would be removed from solution as metal sulfides. These compounds are nearly insoluble in water and would not induce toxicity in downstream biological processes.

3. Methods

3.1. Physical and Chemical Sampling and Analysis

3.1.1. Field Sampling Method

Corroded concrete samples were collected into two conical, sterile polycarbonate 15 mL tubes using sterilized, DNA-free metal spatulas. Samples for chemistry and phospholipids were collected in dry tubes. Samples for DNA analysis were collected in 3 mL of 1M Tris/0.01mM EDTA buffer to minimize DNA damage and to complex metal ions that could inhibit DNA amplification. All samples were kept at 4°C for a maximum of 48 hours before analysis and DNA extraction.

3.1.2. Headspace Gasses

Hydrogen sulfide (H_2S), carbon dioxide (CO_2), and methane (CH_4) were measured in structure headspaces in one of two ways. At sites E01-04, G01-05, and A31-45, CH_4 was measured using a MDU 420 dual-range methane monitor (Industrial Scientific Corp., Oakdale, PA) and CO_2 and H_2S were measured using a Draeger CMS analyzer (Draeger Safety Inc. Gas Monitors, Sugarland, TX). At all other sites and at manholes used for the longitudinal experiments, measurements for all three gasses were taken using a GasAlert Micro5 IR (BW Technologies, Lincolnshire, IL) equipped with H_2S, CO_2, CH_4, and oxygen sensors. Gas samplers were calibrated every 90 days.

3.1.3. Estimated Extent of Corrosion

The surface type at each regional site was rated on a subjective scale of 0 to 2 based on the descriptions in Table 3.1.

Table 3.1: Surface type characterization criteria

Corrosion Score	Surface Appearance	Typical pH	Typical % Moisture
0	Treated polymer surface, only biofilm sampled	0.5-7.0	0%
1	Mild corrosion, binder is fragile, aggregate exposed	2.0-7.0	0-15%
2	Significant concrete depth lost, binder is moist and expansive	< 2.0	> 20%

3.1.4. **Sample Moisture**

Corrosion product or biofilm samples were dried at 60°C in ceramic crucibles for at least 8 hours. Samples were massed before and after drying, and moisture content was calculated by dividing water mass lost by the original (wet) mass.

3.1.5. **Sample Chemistry**

All analytical chemistry analyses were conducted by the Laboratory for Environmental and Geologic Studies at the University of Colorado at Boulder. Oven-dried samples were sieved to remove silica-based aggregate particles larger than 300 μm. Samples were dissolved using a modified technique developed by Farrell et al. (1980). Five mL of a 7:3 mixture of hydrochloric acid and hydrofluoric acid were added to the digestion tubes containing samples followed by 2 mL of nitric acid, and the digests were heated to 95°C in a HotBlock digestion block (Environmental Express, Mount Pleasant, SC) for about two hours. Samples were then cooled and diluted to a volume of 50 mL with a 1.5%-by-weight boric acid solution. The samples were reheated to 95°C for about 15 minutes and cooled prior to analysis.

Eluents were analyzed for total iron, calcium, and sulfur using inductive coupled plasma/optical emission spectroscopy (ICP-OES 3140+) (Applied Research Laboratory). A blank and three standards were used for calibration. Most standards were made by accurately diluting certified standards. Sieved, dried samples from selected metal treated specimens were analyzed for total cadmium and chromium. Dissolved samples were analyzed using an Elan

DRC-e inductively coupled plasma mass spectrometer (ICP-MS), (Perkin Elmer SCIEX, Waltham, MA). Indium was used as an internal standard and four standards (blank, 100, 500 and 1000 ppb) were used for calibration. Standards were made by accurately diluting certified standards. Concentrations in pore water were estimated by dividing the amount of metal per dry gram by the amount of water per dry gram.

3.1.6. **Sample pH**

Pore water pH was estimated by adding a known amount of un-buffered double-distilled (ddi) water (pH 6-8) to sampled corrosion product. Hydrated samples were mixed and allowed to equilibrate for an hour, and pH was measured. Original pore water pH was estimated based on the volume of pore water in the sample (measured as described in Section 3.1.4), the volume of water added, and the original pH of the water using Equation 1. This calculation was developed for this thesis based on the assumption that pH is equal to the base-10 log of the hydronium ion concentration and the sum of pH and pOH is 14.

If $pH_m < pH_w$

$$pH = -log\left(\frac{(V_{sw}+V_w)*10^{-pHm}-V_w*10^{-pH_w}}{V_{sw}}\right) \quad \text{(Equation 1)}$$

If $pH_m > pH_w$

$$pH = 14 + log\left(\frac{(V_{sw}+V_w)*10^{-(14-pH_m)}-V_w*10^{-(14-pH_w)}}{V_{sw}}\right)$$

Where:

pH is calculated pH of sample water
pH_w is the pH of the added double distilled water
pH_m is the measured pH of equilibrated sample plus added water
V_{sw} is the volume of pore water in the original sample
V_w is the volume of double distilled water added

3.1.7. **Phospholipid Biomass Analysis**

Phospholipids are vital components of all cell membranes and enable cells to regulate their cytoplasmic chemistry (Madigan et al., 2009). In this work, phospholipids were measured

with the intent of using them as an index of microbial biomass. This method was adapted from a sediment application method reported by Findlay et al. (1989). Extractions were performed in triplicate, and three reagent blank extractions were analyzed with each set of samples. Bulk lipids were extracted from between 0.01 g and 0.6 g of corrosion product as previously described by adding 2 mL water, 5 mL methanol, and 2.5 mL chloroform. After 2-24 hours, 2.5 mL of 0.036N H_2SO_4 and 2.5 mL of chloroform was added (Bligh et al., 1959; Findlay et al., 1989; Wang et al., 1995). Phases were allowed to separate overnight. The organic phase was removed to a glass ampule and evaporated under nitrogen gas at 37°C. Dried lipids were digested with 900 µL of 5% potassium persulfate in 0.36N H_2SO_4 for 8-12 hours at 98°C to cleave phosphate groups from phospholipid molecules. Due to the presence of dark colored organic acids and/or yellow sulfur crystals in some samples, lipid digests were re-extracted in a 2 mL centrifuge tube with 500 µL of chloroform and 200 µL of potassium persulfide reagent to remove sulfur and discolorations. The mixture was centrifuged for 10 minutes at 10,000 g and the 900 µL of the supernatant was transferred to a UV/vis cuvette. The digestion reaction was stopped using 200 µL of 3.5M ammonium molybdate in 0.35N sulfuric acid. A 0.11% solution of malachite green dissolved in 1.11% polyvinyl alcohol was added to complex phosphate ions and absorbance at 610nm was measured using a Hach DR5000 UV-Visible Recording Spectrophotometer (Loveland, CO). Phosphate concentrations were calculated from standards using known concentrations of β-glycerophosphate disodium salt (Sigma Aldrich, St. Louis, MO). Signal from extraction reagent blanks was subtracted from the phosphate concentration for each sample.

3.1.8. **Environmental Scanning Electron Microscopy (ESEM)**

Selected sample surfaces were visualized using a Hitachi TM-1000 benchtop ESEM (Tokyo, Japan) with an Oxford Elemental Analysis (EDS) unit to obtain images of surface morphology from 1,000X to 10,000X magnification. These samples were stored at 4°C for a maximum of 72 hours prior to imaging. Samples were attached to the sample holder using carbon tape. Electron diffraction spectroscopy (EDS) was used in conjunction with ESEM images in order to compare the atomic composition and spatial arrangement of sulfur-based mineral crystals in the corrosion matrix (Huang et al., 2007).

3.2. Phylogeny Analysis

3.2.1. **DNA Extraction**

Buffered samples were vortexed and 800 µL of buffer removed from the top portion of the tube. This buffer was added to extraction tubes containing NaCl/TE buffer with SDS, equal parts phenol and chloroform, and 0.1 mm silica/zirconium beads. Tubes were then bead-beaten and centrifuged. DNA was precipitated from 500 µL of the supernatant using 10 µL of 10mg/mL glycogen, 200 µL of 7.5M ammonium acetate, and 700 µL of isopropanol (Dojka et al., 1998). The pellets were washed with 70% ethanol and re-suspended in sterile DNase/RNase-free water. Extracted DNA was stored at -80°C until further analysis. All extraction reagents were tested for contamination and inhibition by conducting negative control extractions with no sample added and positive control samples with a known DNA template. Only reagents with reliable quality control metrics were used.

3.2.2. **16S Clone Libraries and Amplicon Sequencing by Sanger Technology**

Extracted genomic DNA was amplified for cloning by PCR with (nominally) universal SSU rRNA gene primers 515F and 1391R (Table 3.2). PCRs were conducted at 94°C for 2 min,

followed by 30 cycles of 94°C for 20 s, 52°C for 20 s, and 65°C for 1.5 min, followed by a 65°C elongation step for 10 min. Each 50 μl reaction mixture contained 10 μl Eppendorf 2.5X Hot Master Mix (Eppendorf, New York, NY), 10 μl water, 0.05% bovine serum albumin (Sigma-Aldrich, St. Louis, MO), 100 ng of each oligonucleotide primer, and 1 to 5 ng of template DNA. Triplicate PCRs were conducted for each sample and pooled before purification with the Montage gel purification system (Millipore). PCR negative control reactions did not have visible template when separated by gel electrophoresis using ethidium bromide. PCR-amplified DNA genes were cloned into TOPO TA vectors and transformed into electrocompetent TOPO One-shot cells (Life Technologies, Carlsbad, CA) using an Transporator Plus electroporator (BTX, Holliston, MA). Transformed cells were grown overnight at 37°C on LB-agar with 1% ampicillin sodium-salt (Sigma-Aldrich, St. Louis, MO), and 96 colonies per sample were picked and prepared for sequencing. Cells were boiled to release DNA and the resulting supernatant was amplified using T3/T7 primers targeting the TOPO™ vector. T3/T7 PCR product was cleaned using ExoSAP-IT™ (Affymetrix, Santa Clara, CA). Plates were sequenced from both ends with capillary electrophoresis using an Amersham MegaBACE 1000 Sanger sequencer (GE Healthcare, Waukesha, WI) or an ABI PRISM 3730xl sequencer (Applied Biosystems, Carlsbad, CA) using BigDye™ Terminator Sequencing Kit v3.1 via Beckman Coulter Genomics (Danvers, MA).

Table 3.2: Summary of primers used for 16S rRNA phylogenetic analyses

Primer Name	Sequencing Platform	Primer Specificity	Primer Sequence
515F	Sanger	Universal	GTGCCAAGCAGCCGCGGTAA
1391R	Sanger	Universal	GACGGGCRGTGWGTRCA
27F	Illumina	Bacterial	AGAGTTTGATCCTGGCTCAG
338R	Illumina	Bacterial	GCTGCCTCCCGTAGGAGT

3.2.3. **Sanger Sequence Analysis**

MegaBACE chromatograms were converted to base-calls with phred (Ewing et al., 1998a; Ewing et al., 1998b); vendor base calls were used for Beckman-generated sequences. T3/T7 base-calls were assembled with phrap (Ewing et al., 1998a; Ewing et al., 1998b). Vector contamination and 16S primers were found by screening assembled sequences with crossmatch (Ewing et al., 1998a; Ewing et al., 1998b) against NCBI's Univec_core database (9/24/2012 version, ftp://ftp.ncbi.nih.gov/pub/UniVec/) and removed by trimming from point of discovery back to sequence ends. Nucleotides with mean quality scores less than 20 at over a 10-nucleotide window were trimmed from the ends until the requisite quality was met. Sequences containing more than one ambiguity or that were less than 500 nt were discarded. Potential chimeras identified with Uchime (usearch6.0.203_i86linux32) (Edgar et al., 2011) using the Schloss Silva reference sequences (Schloss et al., 2011b) were discarded.

Sequences were inserted into the guide tree of Silva 115NR99 (Quast et al., 2013) and taxonomy calls were generated via NDS export with ARB (Ludwig et al., 2004). Operational taxonomic units (OTUs) were produced by clustering sequences with identical taxonomic assignments and imported into Explicet (Robertson et al., 2013), which was used for display, analysis, and figure generation of results.

Selected Sanger sequences were further analyzed for phylogenetic placement. These sequences were inserted into the Silva 108 tree using parsimony insertion and the ARB Software Package (Ludwig et al., 2004), and their nearest neighbors were inspected to determine relatedness groups.

3.2.4. **16S Amplicon Sequencing by Illumina MiSeq Technology**

Bacterial community composition was analyzed using Illumina MiSeq personal sequencing platform to sequence V1V2 16S ribosomal RNA amplicons. This region of the rRNA gene is variable across bacteria and thus is useful for assessing bacterial community diversity to the genus level. MiSeq is a relatively new technology for low-cost high-throughput sequencing, which enables the recovery of millions of sequences and helps elucidate the rarer taxa present in the community. The technology uses 250 bp paired-end sequencing with a goal of producing 450 bp contigs (150 bp of primer, barcode, and sequencing adapters and 300 bp of sample DNA sequence). It produces large numbers of short sequences at low costs, but the V1V2 region only offer phylogenetic information for the bacterial domain of life. MiSeq sequencing was performed in collaboration with Professors J. Kirk Harris and Daniel Frank at the University of Colorado-Denver Medical School.

Amplicons of the 16S rRNA gene were generated via broad-range PCR using broad-range primers that amplify the ~300 bp V1V2 variable region using 27F and 338R primers (Table 3.2) following previously described methods (Hara et al., 2012; Markle et al., 2013). Primers were barcoded (Frank, 2009) and modified with sequences required for sequencing on the Illumina MiSeq personal sequencing platform.

PCR yields were normalized using a SequalPrep™ kit (Invitrogen, Carlsbad, CA), pooled, lyophilized, and gel purified, and concentrated using a DNA Clean and Concentrator Kit (Zymo, Irvine, CA) as previously described (Frank et al., 2010). Pooled amplicons were quantified using Qubit Fluorometer 2.0 (Invitrogen, Carlsbad, CA). The pool was diluted to 2nM and denatured with 0.2 N NaOH at room temperature. The denatured DNA was diluted to 15pM and spiked with 25% of the Illumina PhiX control DNA prior to loading the sequencer.

Illumina paired-end sequencing was performed on the Miseq platform with version 2.0 of the MiSeq Control Software, using a 500-cycle version 2 reagent kit. Raw paired-end Illumina MiSeq reads for the 86 samples sequenced were submitted to the NCBI Small Read Archive under accession number SRP022243.

3.2.5. **Illumina MiSeq Sequence Data Analysis**

Illumina MiSeq paired-end sequences were sorted by sample via barcodes in the paired reads with a python script. The sorted paired reads were assembled using phrap (Ewing et al., 1998a; Ewing et al., 1998b; Gordon et al., 1998). Assembled sequence ends were trimmed over a moving window of 5 nucleotides until average quality met or exceeded 20. Trimmed sequences with more than 1 ambiguity or shorter than 200 nt for Illumina or 500 nt for Sanger were discarded. Potential chimeras as identified with Uchime (usearch6.0.203_i86linux32) (Edgar et al., 2011) using the Schloss SILVA reference sequences (Schloss et al., 2011b) and were removed from subsequent analyses. Assembled sequences were aligned and classified with SINA 1.2.11 (Pruesse et al., 2012) using the 418,497 bacterial sequences in Silva 115NR99 (Quast et al., 2013). Operational taxonomic units (OTUs) were produced by clustering sequences with identical taxonomic assignments, and these taxa were used in future community analysis. The software package Explicet (Robertson et al., 2013) was used for display, analysis, and figure generation.

3.2.1. **Sequence Diversity Metrics**

Ecological indices of richness, diversity, and coverage (Magurran, 2004) were calculated with Explicet using the Illumina MiSeq data. In order to execute a fair comparison between sample libraries with different numbers of sequence recovered (between 4,478 and 53,291 in this data set), diversity statistics were calculated using only 4,478 (i.e. at the rarefaction point)

(Magurran, 2004). These indices were estimated through bootstrap resampling (1,000 replicates) and rarefaction of the taxa distributions obtained from each specimen. This means that for each library, 4,478 sequences were picked at random to be used in calculating diversity, and this process was repeated 1,000 times. Alpha- and beta-diversity metrics and associated statistical parameters were calculated based on these 1,000 replicates. The median Goods coverage score for libraries, a measure of completeness of sequencing, was ≥ 99%, indicating that the depth of sequencing was sufficient to fully describe the biodiversity of the samples (Lemos et al., 2012; Lemos et al., 2011).

Alpha Diversity Measurements

In traditional ecology, alpha diversity (α-diversity) is represented by species richness, or how many species are observed. Since any sequencing run cannot be guaranteed to recover every type present in a sample, richness is not a consistent way to measure alpha diversity (α-diversity). Instead, diversity metrics are used to estimate how many different taxa (sequence types) would be observed if all types were seen, i.e. if an infinite number of sequences could be recovered. In this thesis, Chao1 was used as an indicator of α-diversity (diversity within one sample). It takes into account both richness (number of OTUs observed) and evenness (equality of abundance between OTUs), and was calculated in Explicet using Equation 2 (Hughes et al., 2001).

$$S_{Chao1} = S_{obs} + \frac{n_1^2}{2n_2} \quad \text{(Equation 2)}$$

Where:

S_{chao1} = the estimated richness
S_{obs} = the observed number of species
n_1 = the number of OTUs with only one sequence (i.e. "singletons")
n_2 = the number of OTUs with only two sequences (i.e. "doubletons")

Beta Diversity Measurements

While alpha diversity relates the diversity within a single sample, beta diversity reflects the diversity observed between samples. Beta diversity (pairwise inter-sample diversity) was estimated using the Morisita-Horn metric function in Explicet (Magurran, 2004), which represents similarity between two libraries on a scale of 0 to 1 (where 0 represents no similarity, and 1 represents identical libraries). Morisita-Horn was used, because it is less biased by sample size and richness than other metrics (Wolda, 1981). This metric was calculated using Equation 3.

$$C_{MH} = \frac{2(a_i+b_i)}{(d_a+d_b)*(N_a \times N_b)} \quad \text{(Equation 3)}$$

Where:

C_{MH} = the Morisita-Horn similarity score between samples A and B
N_a = the total number of sequences in sample A
N_b = the total number of sequences in sample B
a_i = the number of sequences in the ith OTU from sample A
b_i = the number of sequences in the ith OTU from sample B
$d_a = \Sigma\ a_i^2/N_a^2$
$d_b = \Sigma\ b_i^2/N_b^2$

3.2.2. Statistical Tests

Two-Part Statistics

Individual microbial groups that differed in prevalence or abundance between treatment groups were identified through a two-part statistical test that accounts for zero-inflation and non-

normal distributions (Wagner et al., 2011). Because of the exploratory nature of this study, p-values were not corrected for multiple tests.

Multivariate Analysis Using Canonical Correspondence Analysis

Multivariate analysis was conducted using canonical correspondence analysis (CCA) from OTU tables and headspace gas metadata. CCA is a canonical, multivariate technique that uses weighted multiple linear regressions and chi-squared distances to calculate relationships between species/taxa data and environmental parameters. The method performs an eigenvalue decomposition of the input OUT and environmental matrices to compress data with many dimensions into a few dimensions based on environmental data. Resulting eigenvalues for the new axes can be used to estimate what proportion of community variation is explained by the environmental parameters given (Legendre et al., 1998).

Calculations were performed using the "vegan" package in R Statistics Program (Oksanen et al., 2013; RCoreTeam, 2013) using headspace gas data as environmental parameters. Data were transformed and scaled prior to analyses according to previous work (Braak, 1986; Legendre et al., 1998) as follows: taxa abundances were square-root transformed, H_2S concentrations were log-transformed, each headspace gas data point was scaled to number of standard deviations away from the mean. Samples without headspace gas concentrations were omitted from analysis.

Linear Regression

Linear regression models were developed using R Statistics Program (RCoreTeam, 2013) to relate environmental factors to community composition and corrosion severity. Pairwise comparisons of linear regression line slopes were compared using analysis of covariance (ANCOVA) (Chow, 1960; García-Berthou, 2001).

3.2.3. **Limitations of 16S rRNA Phylogenetic Methods**

While 16S rRNA methods have become the standard practice in the microbial ecology field, they are subject to a range of biases. DNA extraction efficiencies differ between different types of organisms as a result of varying rates of decay during sample storage, a range in the number of 16S rDNA copies in a cell, and specific extraction procedures (Feinstein et al., 2009; Martin-Laurent et al., 2001; Miller et al., 1999; Schloss et al., 2011a). Polymerase chain reaction (PCR) is used to make copies of the 16S rDNA gene prior to sequencing, but the process is subject to amplification biases that result from differing target sequence lengths and DNA chemistry between organisms (Polz et al., 1998), or from inhibiting compounds in the reaction mix such as calcium, iron, or organic acids (Kreader, 1996; Opel et al., 2010). As a result, the abundance of some taxa may be over- or under-estimated. Several procedure modifications were undertaken in this study to minimize these biases. Samples were collected into 1M Tris/0.01M EDTA buffer with the complimentary aims of complexing potential PCR inhibitors and minimizing pH-related DNA damage from acid hydrolysis. Samples were stored at 4°C immediately upon collection and were extracted within 48 hours to further deter DNA degradation. The DNA extraction procedure used involved bead-beating in a buffered phenol-chloroform solution, which has been shown to yield optimum DNA quantity and size when compared to other cell lysis methods (Miller et al., 1999). Bovine serum albumin was added to PCR reactions to facilitate amplification in the presence of inhibiting compounds (Kreader, 1996). For Sanger clone libraries, amplified DNA from three reaction mixtures were combined for cloning; this method of using multiple reactions has been shown to decrease amplification bias (Polz et al., 1998). Another shortcoming of rRNA based surveys involving amplification by PCR is the caveat that no primer set is truly "universal" (i.e. it amplifies rRNA sequence from all

known organisms) (G. C. Baker et al., 2003). In this study, "universal" bacterial (8F and 338R) and "universal" three-domain (515F and 1391R) primers were chosen based on the effective read length of the sequencing platforms (300 bp for Illumina MiSeq and 900 bp for Sanger) and the standards in the relevant literature.

In addition to biases introduced by DNA extraction and amplification, rRNA sequencing and subsequent analysis are also subject to a number of uncertainties (Ross et al., 2013). The Illumina MiSeq sequencing method uses small cameras to detect fluorescence on DNA clusters arranged in a two-dimensional space that indicate which base is being added to the DNA strand. The nature of the camera detector makes it difficult to distinguish between many clusters exhibiting the same color. This presents a problem when the sequencer is reading through the barcode and primer regions of the sequencing run and when the samples being sequenced are low diversity. To ameliorate this problem, a random number of Ns (nucleotides of any type) are added before the primer sequence to de-phase the sequences, and PhiX phage DNA and high diversity DNA samples were added to the sequencing reaction to provide more diversity.

Many sequence data analysis programs use naïve Bayesian methods to compare sequences to databases and assign a taxonomy call. This means that these methods do not use a full alignment of the sequences and do not consider secondary structure when assigning taxonomy; thus, the sequence data is treated as mathematical data rather than biological data. The method used to make taxonomy calls for this study uses rRNA secondary structure to align sequences to the 50,000 character alignment curated by SINA (Pruesse et al., 2012), which enables a more statistically robust and biologically sound phylogenetic classification system.

3.3. Metals Adsorption

3.3.1. Metals Chosen for this Study

The third aim of this thesis is to use heavy metal ions to inhibit the activity of sulfur-oxidizing biofilms responsible for corrosion. Cadmium and chromate ions from $CdSO_4$ and K_2CrO_4 salts were chosen for this study based on their recognized toxicity for microbes, their proven ability to adsorb to activated carbon, and their prevalence in industrial waste streams (Kobya et al., 2005; Trevors et al., 1985; USEPA, 1980, 1991). Acidophiles have been reported to develop resistance to high levels of these metals, but given their low concentrations in municipal wastewater environments, it is unlikely that the sustained selection pressure required for heavy metals resistance to persist will be present on the crowns of wastewater collection systems (see Section 6.4.1 for further discussion of resistance).

3.3.2. Metals Loading

Small-grained OL 20x50 granular activated carbon (GAC) and powdered F400 activated carbon (PAC) (Calgon Carbon Corp., Pittsburgh, PA) were used as carbon sorbent material in the metal-carbon formulation. The point of zero charge (pH_{PZC}) relates to the distribution of ions near surface sites (Snoeyink et al., 1967). pH_{PZC} values were determined for the two carbons using direct titration according to Nevostrueva (2009) and Milonjíc (1975). Briefly, carbons were soaked in 0.06M NaCl solutions at pH values from 1.8 to 10 (adjusted with HCl or NaOH), and final pH was compared to initial pH. The pH_{PZC} was determined as the pH where a plateau occurs. Activated carbon specifications are listed in Table 3.3. Carbons were loaded with metal ions by being shaken in a reactor containing 5 mM solutions of cadmium sulfate ($CdSO_4$) or potassium chromate (K_2CrO_4) for two days. Metal-loaded GAC and PAC were rinsed three times with double distilled water and dried at 60°C. Aliquots of the metal solution before and

after shaking were collected and measured for cadmium and chromium content using ICP/MS to determine metal loading rates. Loading rates were on the order of 1 mg metal/g carbon or one part per thousand.

Table 3.3: Activated carbon properties

Carbon	Calgon Type	Size Range	Point of Zero Charge (pH_{PZC})
GAC	OL 20x50	300-840 µm	7.5
PAC	F400	150-250 µm	8.0

3.3.3. Metals Leaching Curves

Leaching curves were conducted using phosphate- and citrate-buffered solutions at seven pH values between 2 and 8. 20 mL of buffer was added to 0.5 g of cadmium- or chromate-loaded GAC and allowed to equilibrate for one week. Final aqueous metal concentrations and solution pH were used to describe leaching characteristics. Leaching experiments were conducted in triplicate.

3.4. Culture Conditions

Pure stock cultures of *Acidithiobacillus thiooxidans* (ATCC #19377) and *Thiobacillus thioparus* (ATCC #23646) from the American Type Culture Collection (ATCC) (Mannassas, VA) were used to test the efficacy of the formulation in the laboratory. In addition, sulfur-oxidizing microbes from a field sample of late-stage corrosion product were enriched at pH 3. All enrichments and liquid culture experiments were conducted using modified ATCC thiosulfate media 290 consisting of 1.2g NaH_2PO_4, 1.8g KH_2PO_4, 0.025g $MgSO_4$, 0.1g $(NH_4)_2SO_4$, 0.03g $CaCl_2$, 0.02g $FeCl_2$, 0.03 $MnSO_4$, and 10.0g $Na_2S_2O_3$ per 1 L water (www.atcc.org). Other media tried for liquid-phase growth are ATCC medium 125, ATCC medium S6, and a *Thiobacillus thiooxidans* medium outlined by Waksman (1922). All media

were tested using either elemental sulfur (S^0) or dissolved thiosulfate ($S_2O_3^{2-}$) as a substrate. Media solutions were pH adjusted using HCl or NaOH and sterilized in an autoclave for 45 minutes.

3.4.1. **Liquid Media Culture Tests**

Liquid media tests were conducted on the three cultures (two pure strains and one enrichment culture) at four different target pH values (4.5, 6.0, 7.0 and 8.0 for neutrophile *T. thioparus* and 2.5, 3.5, 4.5, and 5.5 for acidophiles *At. thiooxidans* and the enrichment). Preliminary growth curves indicated that *T. thioparus* completed exponential growth after 48 hours at pH 6.6, and *At. thiooxidans* and the enrichment reached exponential growth after 7 days at pH 4.0. Consequently, experiments using neutrophiles were incubated for 48 hours, and experiments using acidophiles were incubated for 12 days to ensure that exponential growth had been achieved.

Each experiment included five different treatments at each pH: un-inoculated media (negative growth control), culture with no carbon added (positive growth control), culture with unloaded PAC, culture with cadmium-loaded PAC, and culture with chromate loaded PAC. Experiments were conducted in sterile 96-deep-well polystyrene plates with a liquid volume of 0.5 mL. Each well contained 0.5 mL of inoculated or un-inoculated ATCC 290 media at the appropriate pH. Wells treated with activated carbon contained 0.25µg of metal-loaded or unloaded activated carbon and were pH adjusted throughout the experiment due to the high buffering capacity of the activated carbon used.

Experiments were modeled at 5X scale using 5 mL volumes of media with 5 µg unloaded powdered activated carbon at each of the six target pH values. The pH of these solutions was

tested each day, and the amount of 1M HCl needed to return the solutions to the target pH was recorded. Acid additions to the growth inhibition assay were scaled based on these amounts.

Culture responses to metal-impregnated activated carbon were judged by direct microscopic counts. Sample volumes were chosen based on previous assay cell concentrations with a goal of 30 cells/field at 1000X. After incubation, wells were homogenized and sample volumes diluted to 1 mL with filtered double distilled water were fixed with 10 µL 37% formaldehyde and stained for 10 minutes with 100 µL of 4 mg/mL DAPI solution (Acros Organics, Geel, Belgium). DAPI is a DNA-intercalating agent which fluoresces blue when bound to double-stranded DNA. Stained samples were filtered onto 25 mm black polycarbonate filters with a pore size of 0.2 µm (GE Osmonics Inc., Minnetonka, MN). Filters were placed on microscope slides and kept in the dark at 4°C until counting. Bacterial cells were visualized and counted using 1000X magnification on a Nikon Eclipse E400 epifluorescent microscope with a Nikon HMX-4 lamphouse fitted with a 100W mercury bulb (Nikon Instruments, Inc. Melville, NY). At least ten fields of at least ten cells each were counted per slide, and counts were used to calculate bacterial cells per volume of culture. DAPI staining, formalin fixation, and filtering were adapted from the method of Porter and Feig (1980) and experimental design for statistical significance was conducted according to Kirchman et al. (1982). Each of the five experimental conditions for each pH values were conducted in six experimental replicates; two experimental replicates were combined to produce each of three filter replicates per condition (Figure 3.1).

	Positive Control	Unloaded PAC	Cadmium PAC	Chromate PAC
pH 6				
pH 4.5				
pH 3.5				
pH 2.5				

Figure 3.1: 96-well plate setup for liquid culture assays. Negative controls were conducted on parallel plate. Six replicates per treatment include triplicate filters and two experimental replicates per filter.

3.4.2. **Solid Media Culture Tests**

Enrichment cultures were grown on Thiobacillus agar with 2 mg/L bromcresol green (Sigma-Aldrich, St. Louis, MO). The agar medium contained 4g KH_2PO_4, 0.5g $MgSO_4*7H_2O$, 0.4g $(NH_4)_2SO_4$, 0.25g $CaCl_2$, 0.01g $FeSO_4$, 5.0g $Na_2S_2O_3$, and 12.5g agar per 1L water, and was autoclaved at 121°C for 45 minutes before being poured into 120 mm plastic plates (Starosvetsky et al., 2013). 300 uL (approximately 10^7 cells) of the enrichment stocks was plated using autoclaved glass beads. Known masses of metal-loaded and unloaded activated carbon were applied to 1 cm diameter circles of the inoculated plates. Plates were incubated at 30°C for 7 days and checked for inhibition zones.

3.5. Longitudinal Manhole Field Experiment

3.5.1. **Concrete Coupon Production for Field Experiment**

Concrete specimens for the time-series manhole exposures were cast in the laboratory. A concrete mix design was chosen based on the small size of the specimens. Concrete consisting of 9.9 lbs fine aggregate (fill sand), 11.3 lbs coarse aggregate (pea gravel), 4.0 lb Portland Type II cement, and 1.8 lbs water (for a water to cement ratio of 0.45) was mixed according to ASTM standard C192. Cubic specimens were casted in 1” by 10” rectangular racks with plastic cords

for hanging, and cured rectangles were cut into 1-inch cubes using a band saw. Eight 3x6 inch cylinders were casted with steel bolts to serve as one-year exposure samples in each manhole. Samples were cured at 90% RH for 24 hours before molds were removed.

Selected concrete specimens were treated with different formulations by application of a thin layer of hydrated cement (water to cement ratio of 0.35) about 5 mm thick and followed by application of GAC for an approximate loading of 1-3 g metal/m^2 concrete surface or 0.1 kg metal/cubic yard cement. Four treatments were used: untreated, carbon only, cadmium-carbon, and chromate-carbon.

3.5.2. **Field Experiment Design**

Field testing of treated and untreated samples was conducted from October 2011 to December 2012. Samples were hung from plastic steps in two manholes on the Front Range of Colorado (Figure 3.2 illustrates sample holder design). The two manholes are spaced about 100 yards apart on the same 72" fiberglass sewer interceptor. Previous studies with the manhole involving epoxy coatings recorded average H_2S concentrations of over 400 ppm in the MH1. Samples were installed on October 2, 2011 in a manhole designated MH1 and on December 12, 2011 in another designated MH2. Samples were removed for analysis at approximately 2-month intervals for 12 months. For each one-year field study, five 1-inch cubes and one 3x5 inch cylinder were exposed per treatment. An additional accelerated study was started on August 8, 2012 to perform a more detailed investigation of the early stages of corrosion. Six 1-inch cubes per treatment were installed in the severe manhole, and were sampled approximately every three weeks. The sampling schedule is summarized in Table 6.2.

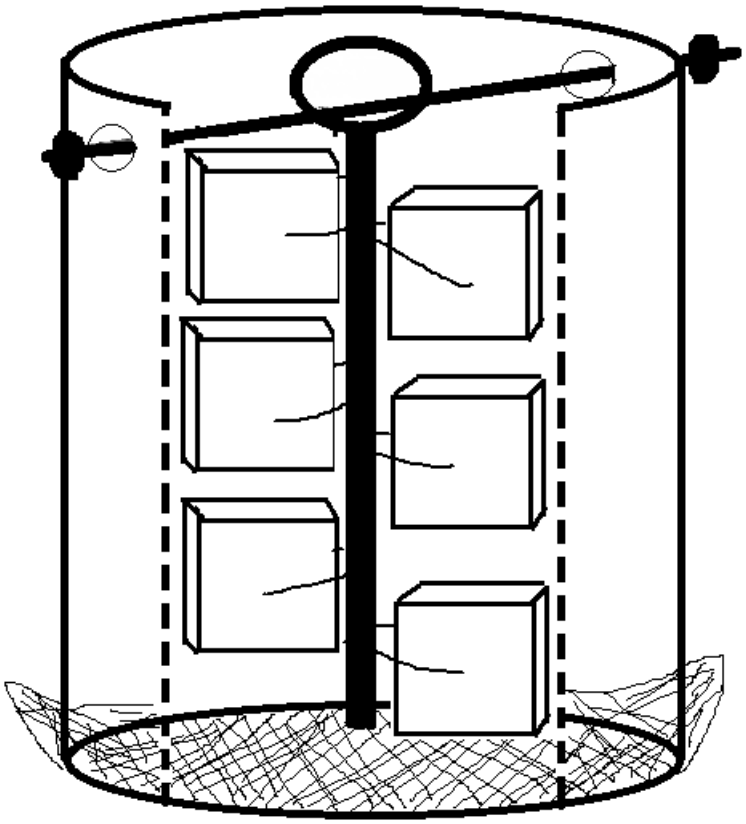

Figure 3.2: Diagram of manhole sample holder design. Holder consisted of a 6-inch diameter PVC tubing section capped at the lower end with polystyrene mesh. 1-inch cubic concrete specimens were hung from a stainless steel eyebolt by plastic cord.

3.5.3. **Field Experiment Sampling**

Gas readings for hydrogen sulfide, carbon dioxide, methane, and oxygen were taken at each sampling event prior to removal of the manhole lid using a GasAlert MicroIR gas meter (BW Technologies, Lincolnshire, IL). On sampling dates, one cube corresponding to each of the four treatments was removed and transported to the laboratory in sterile foil-covered beakers. Beakers were previously rendered sterile and DNA-free by burning them at 550°C for 3 hours. Samples were massed, and corroded material was scraped into burned ceramic crucibles. Scraped corrosion product was further analyzed for physical, chemical, and microbial

community parameters (i.e. relative abundance of taxa and α-diversity) as previously described in Sections 3.1 and 3.2.

3.5.4. **Experimental Setup Limitations**

The corroding specimen data were recovered from a time-series of observations using different specimens rather than recurring observations on one specimen. Each cube and each sampling point represents an independent observation, as limited space prevented the analysis of duplicate or triplicate specimens.

The polyvinyl chloride (PVC) casing was designed to protect the specimens from contact with the manhole wall or steps and from falling into the wastewater flow. For experiments 2 and 3, the PVC casing was four inches in diameter, which provided space for the specimens to hang freely when the cylindrical casing was upright. However, in the manhole, the casings were hung from manhole steps using carabiners and were tilted slightly off vertical. Biogenic acid formation was uninhibited on the PVC surface. As a result, some samples treated with the metal-carbon formulation were corroded only where they touched the side of the PVC casing, which may not be representative of corrosion caused by biofilms on the concrete. This experimental artifact affected data from experiments 2 and 3, especially in testing the metal-carbon formulation. For experiment 1, six-inch PVC was used for the casing and vertical orientation was maintained throughout the experiment.

4. Geographical Survey of Corrosion Biofilms (Aim 1)

4.1. Introduction and Background

The first aim of this research is to investigate how geographic location and environmental parameters may influence MICC communities and extent of corrosion. The types of microbial communities present in MICC biofilms likely depends on a large number of factors, but the limited amount of phylogenetic sequence data and associated metadata published thus far prevents a thorough understanding of how environmental factors and geography may correlate with or otherwise influence community characteristics. To date, only five peer-reviewed studies have published community DNA sequence data from MICC biofilms (B. Cayford et al., 2012; Gomez-Alvarez et al., 2012; Okabe et al., 2007; Santo Domingo et al., 2011; Satoh et al., 2009), and none have compared MICC communities recovered from distinctly different geographic regions. Furthermore, correlations of community composition with corrosion severity and environmental factors such as headspace gasses, iron content, and surface treatments have not been studied. There has been no standard for environmental metadata collected. Although surface pH is likely the most important factor in determining MICC communities and extent of corrosion, some studies do not report it. Headspace hydrogen sulfide is frequently measured, but methane and carbon dioxide, which can also affect the corrosion process, have not typically been reported (Guisasola et al., 2008; Ismail et al., 1993). Previous studies of microbial communities in concrete corrosion biofilms often have not included descriptions of the local environment or the severity of corrosion sampled, so comparisons between studies is difficult, as community composition is often dictated by environmental factors and corrosion extent. In addition, surface treatments are widely used to prevent or treat corrosion (Berndt, 2011; De Muynck et al., 2009;

Scrivener et al., 2013; USEPA, 2009), but the impact of these treatments on surface biofilm communities has not been investigated.

4.2. Experimental Design

To investigate this research aim, MICC biofilms were collected from sites in ten cities in the United States. In order to determine the microbial communities present, V1V2 region amplicons of the bacterial 16S rRNA gene were analyzed using Illumina MiSeq paired-end sequencing as described in Section 3.2.4. Associated environmental metadata such as pore water pH, corrosion matrix chemistry, and headspace gas concentrations were collected as described in Section 3.1. Linear regressions and multivariate analysis were used to determine which environmental and geographic factors are most correlated with corrosion and associated microbial groups. Multivariate statistical ordination techniques and linear regressions were used to determine which environmental and geographic factors are most correlated with corrosion and associated microbial groups (see Section 3.2.2 for description of methods). In addition, both bacterial (by Illumina MiSeq) and three-domain (by Sanger) communities were compared between treated and untreated samples exposed in the same environment for a year.

4.3. Sampling Strategy

Between three and twenty samples of corroded concrete or surface biofilm were collected from each of ten cities in four regions across the United States: 2 in the West, 2 in the Southeast, 2 in the Midwest, and 4 in the Rocky Mountain Region. Sampling within cities was planned with the aid of local sanitation district technicians with the goal of collecting biofilms from a variety of structures. If surface coloring or texture suggested acidogenic activity at a site,

samples were collected from areas representative of different surface appearances. The names and locations of the wastewater utilities sampled have been de-identified.

The naming convention for sampling sites was **Site X.N**, where **X** is the code for the utility, and **N** is the code for the site. This sampling campaign is broken down by region and summarized below.

4.3.1. Utility A, Rocky Mountain Region

This wastewater district has had numerous instances of corrosion at their primary 140 MGD treatment facility. Samples in this utility were collected from the wall and roof of a channel between primary and secondary treatment, the crown of a corroded interceptor, and walls of five corroded manholes.

A concrete channel leading into the plant's secondary treatment basins was replaced with fiberglass pipe in 2007 when the portions of the roof lost over six inches of concrete. A similar channel in a different treatment train was originally covered with a concrete slab that was highly corroded by 2010. Samples from the wall of this channel were collected by plant personnel on October 12th, 2010 (Site A.1). The corroded concrete roof was replaced on February 3rd, 2011. Samples were collected from the extricated roof approximately thirty minutes after removal (Site A.3) (Figure 4.1). Corrosion reached a depth of five centimeters in certain sites. The outermost corrosion layer was covered with either a light green or black biofilm or with yellow deposits (presumed to be sulfur). One set of layered samples (approximately 1cm for each layer) were taken at a location with a black surface appearance, and another set of layered samples was taken from a place with yellow deposits. Two samples were collected from sites near iron rebar or piping.

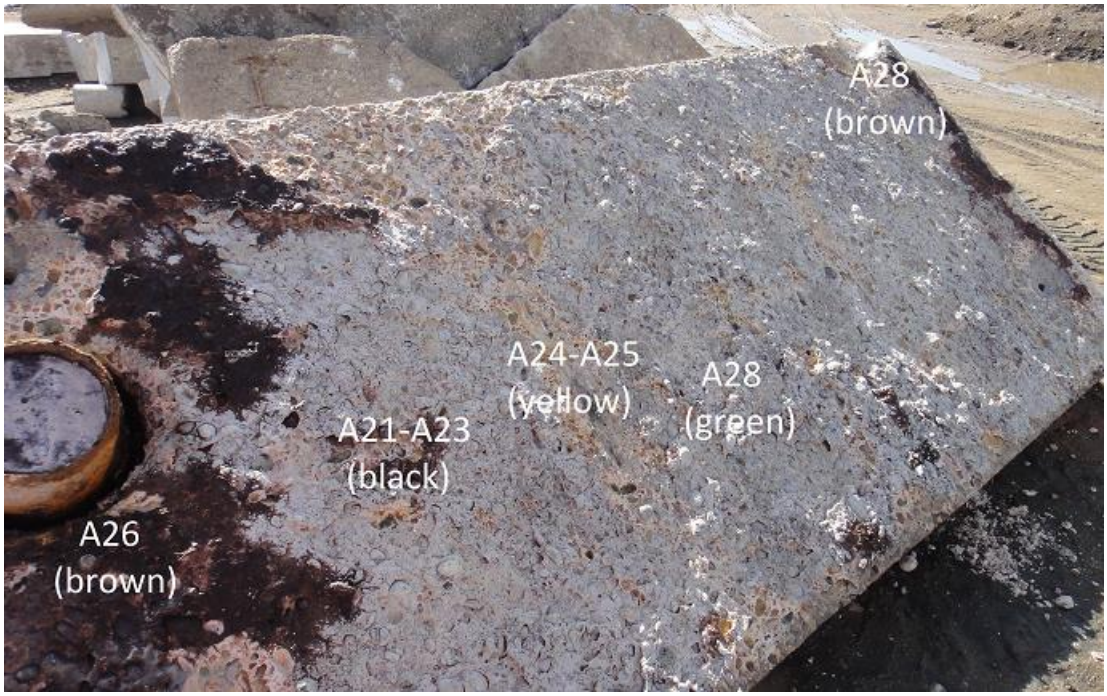

Figure 4.1: Surface appearance and sampling locations at site A.3 – corroded channel roof.

Utility A also experiences microbially induced corrosion in its collection system. Samples were collected on February 2nd, 2011 from a core removed from the top of a 72" reinforced concrete interceptor located one mile upstream of the wastewater treatment facility (Site A.2).

Additional samples were collected from manholes in two areas of the collection system. The first manhole area (Sites A.4 and A.5), served a 72" fiberglass pipe downstream of a lift station. This line collects flow from a large flat suburban region, and experienced long residence times. Hydrogen peroxide was dosed into the flow about 100 meters upstream of Site A.5, which was about 300 meters upstream of Site A.4. A surface coating company was concurrently performing product testing in these sites using 4x6 inch cylinders. Samples of corroded concrete cylinders and biofilms growing on treated surfaces were collected from the two manholes after 1 year of exposure on October 11, 2011 (Site A.4) and August 8, 2012 (Site A.5).

The second manhole area is several miles upstream of the wastewater treatment plant and received large wastewater flows. Samples were collected at one manhole with grey- and brown-stained corroded concrete (Site A.6), and at another manhole upstream of the first with grey-colored corrosion (Site A.7). Cement scrapings were also collected from a less corroded manhole in the same area but on a different interceptor (Site A.8). This manhole was less corroded, but still showed protruding aggregate. Samples were collected from this area on September 26, 2012.

4.3.2. Utility B, Rocky Mountain Region

The 12 MGD wastewater treatment plant for Utility B had experienced corrosion in several places. In a wet well where anaerobic digester effluent was mixed, both sulfide and methane exist in the headspace as a result of anaerobic microbial activity in the digesters. The corroded surface was characterized by yellow granules (presumed to be sulfur), and flow was about three meters below grade. Samples were collected from a surface layer and a subsurface layer of corrosion in the wet well (Site B.1). Samples were also collected in the headworks area from the wall of a covered channel downstream of the bar screen (Site B.2), the wall of an outside channel upstream of the bar screen (Site B.3), and from an enclosed area adjacent to the bar screen (Site B.4). Samples were collected September 20, 2010, January 30, 2012 and October 16, 2012.

4.3.3. Utility C, Rocky Mountain Region

Utility C experienced mild corrosion in the influent and digester areas of its 12 MGD treatment plant. In an anaerobic digester overflow well with intermittent flow treated with a light green epoxy coating, a sample was collected from a brown flaky biofilm growing on the surface (Site C.1). Corroded concrete was sampled near a gas leak at the top of a working digester (Site

C.2). The concrete near the seal was structurally deteriorated and exposed to the sun and rain. Digested sludge traveled to a metal-lidded still on top of the digester on the way to solids processing. A brown biofilm growing on the wall of a white epoxy coating in this still well was sampled (Site C.3).

The flow into the plant was measured by a metering station in a sunken open-air flow channel. A sample was collected from the wall of this channel about 15 cm above the outlet (Site C.4). In an epoxy treated manhole just upstream of the metering station, samples were collected from green biofilm growing on the epoxy coat and from the corroded concrete below the epoxy (Site C.5). The epoxy was degraded in spots, and the concrete below was severely corroded. Samples were collected on June 7, 2012.

4.3.4. Utility D, Rocky Mountain Region

The 54 MGD plant in Utility D experienced corrosion near the headworks. Gasses entering the plant from the collection system were piped into an above ground gas treatment station. White and yellow concrete corrosion products were collected near a gasket leak where the supporting concrete slab is very corroded (Site D.1). A metal-lidded channel between grit chamber and headworks experienced mild corrosion (Site D.2). Grey-colored corroded concrete was sampled. Corroded concrete from brown-stained area located beneath a corroded rebar piece was also sampled. Samples were collected October 5, 2012.

4.3.5. Utility E, Midwestern Region

Utility E has a combined sewer system, and the 120 MGD wastewater treatment plant experienced huge variations in flows depending on weather. Samples were taken from the wall of a moderately corroded wet well near the plant influent (Site E.1). Samples were also collected from a manhole on the plant site that carries flow from an interceptor to the plant headworks

(Site E.2). The concrete surface in this manhole showed protruding aggregate and yellow and brown staining. Samples were collected July 26, 2011.

4.3.6. Utility F, Midwestern Region

Utility F has experienced such extensive corrosion in its interceptor system that it has moved to fiberglass as a standard interceptor material. Samples were collected from a manhole that has been coated with a butyl rubber sealant to prevent corrosion (Site F.1). Samples were collected from a white biofilm growing on the coating and a brown and orange biofilm under the coating. Brown/orange biofilm was also sampled from another manhole about 400 meters upstream of the first (Site F.2). The interceptor passed through a siphon that carries it under a small stream just downstream of the manholes to a 250 MGD treatment plant about one kilometer downstream.

Subsequent manholes sampled were just upstream from a smaller 30 MGD plant in the same system. Concrete did not appear corroded, but rusty brown films near the tops of the manholes were collected. This brown coloration may have been caused by iron oxidation where water dripped from the manhole cover. Site F.3 was the manhole directly upstream from the plant, and Site F.4 was about 300 meters upstream of F.3. All samples were collected May 22, 2012.

4.3.7. Utility G, Southeastern Region

Utility G experienced corrosion problems in a lift station that carries wastewater from outlying communities to the central treatment facility. This lift station historically had low levels of hydrogen sulfide and high levels of carbon dioxide and methane (Site G.1). The lift station was built in 2005 and was coated with coal tar epoxy when corrosion became apparent several years later. The epoxy layer eroded away within three years of application. The station

experienced intermittent flow about ten feet below grade. Samples were collected from white and brown-stained corroded concrete, from the corroded coal tar epoxy material, from the corroded concrete below it, and from a red-stained area near iron features on August 27, 2011.

4.3.8. **Utility H, Southeastern Region**

Samples in Utility H were collected within and in the vicinity of the main treatment plant on April 21, 2012. Site H.1 was a wet well where the wastewater collected from plant premises mixes before feeding into plant influent, which included some sludge dewatering fluid. Water level was about 20 feet below grade. The walls were lined with bituminous coal tar epoxy, which is flaking away. White and puffy concrete covered in greenish biofilm was sampled.

In a wet well at the entrance to the plant (Site H.2), sample was collected from biofilm growing on the walls. The pipe that carries flow from the city to the plant was a force main, so this site contained high levels of H_2S gas. Concrete was not severely corroded, but grey-colored dry biofilm was present on the surface. Site H.3 was a disposal well for septic tank trucks, and sample was collected from a white biofilm growing on the metal lid. Concrete walls were coated with brown fecal biomass, and the flow was about 2 feet from grade.

Site H.4 was an intermittently-flooded pump station about 5 miles upstream from the plant. The basement near the bar screens had wastewater debris on the floor and walls. A corroded concrete sample was collected from wall of the bar screen wells, which may have been contaminated by fecal material or spider webs.

4.3.9. **Utility J, Pacific West Region**

Samples were collected at a wastewater treatment plant in Utility J where odor concerns previously necessitated covering plant processes and treating corroded areas with epoxy. Site J.1 was at the wall of a secondary clarifier, and only mild corrosion was observed. Site J.2 was a

wet well between primary and secondary treatment trains. Corrosion was minimal, but two distinct biofilm morphologies were sampled: a ridged grey biofilm near the surface and a green thin biofilm about 6 inches below the surface. Samples were collected on February 8, 2012.

4.3.10. **Utility K, Pacific West Region**

At Utility K's 80 MGD wastewater treatment facility, samples were collected from the headworks and anaerobic digester areas. In the wet weather flow headworks channels, there was negligible flow at the time of sampling, but mild corrosion had occurred previously. A wet-well upstream of the headworks had been lined with a white plastic material. Samples were collected from a brown biofilm growing on the coated well walls, and from a white nubby biofilm growing on the metal edging of the well (Site K.1). Site K.2 was a channel located just before the primary clarifiers, where there was no flow in June. Mildly corroded concrete binder was collected. Site K.3 was the cake press room downstream of the anaerobic digesters. A sample was collected from a moderately corroded ceiling beam. The beam was located five feet above the grated metal flooring. Concrete was very crumbly and slightly yellowed in areas. Samples were collected on June 26, 2012.

Table 4.1: Summary of regional sampling sites

Sample	Region	Site	WWTP Flow	Location	Description	Color	Material	Type	Sequenced?
A01	RM	A.1	140	secondary influent channel	white corrosion product on wall	white	concrete	mild	X
A02	RM	A.1	140	secondary influent channel	white corrosion product on wall	white	concrete	mild	
A11	RM	A.2	140	interceptor core	cement scrapings from top of pipe	white/grey	concrete	mild	
A12	RM	A.2	140	interceptor core	cement scrapings from top of pipe	white/grey	concrete	severe	
A21	RM	A.3	140	secondary influent channel	roof black surface 0-1 cm	black	concrete	severe	X
A22	RM	A.3	140	secondary influent channel	roof black surface 1-2 cm	grey	concrete	severe	
A23	RM	A.3	140	secondary influent channel	roof black surface 2-3 cm	white	concrete	severe	
A24	RM	A.3	140	secondary influent channel	roof yellow surface 0-1 cm	yellow	concrete	severe	X
A25	RM	A.3	140	secondary influent channel	roof yellow surface 1-2 cm	white	concrete	severe	
A26	RM	A.3	140	secondary influent channel	roof near iron pipe	orange	concrete	severe	X
A27	RM	A.3	140	secondary influent channel	roof near iron rebar	orange	concrete	severe	X
A28	RM	A.3	140	secondary influent channel	roof green surface	green	concrete	severe	X
A31	RM	A.4	140	test cylinder in manhole	concrete cylinder 0-1 cm	white	concrete	severe	
A32	RM	A.4	140	test cylinder in manhole	concrete cylinder 1-2 cm	white	concrete	severe	
A33	RM	A.4	140	test cylinder in manhole	concrete cylinder 2-3 cm	grey	concrete	severe	
A34	RM	A.4	140	test cylinder in manhole	concrete cylinder yellow crust	yellow	concrete	severe	
A35	RM	A.4	140	test cylinder in manhole	concrete cylinder mucky stuff drip	grey	concrete	severe	
A41	RM	A.4	140	test cylinder in manhole	biofilm on epoxy	brown/yellow	film	coated	X
A42	RM	A.4	140	test cylinder in manhole	biofilm on epoxy	brown/yellow	film	coated	
A43	RM	A.4	140	test cylinder in manhole	biofilm on epoxy	yellow	film	coated	X
A44	RM	A.4	140	test cylinder in manhole	biofilm on epoxy	green	film	coated	X
A45	RM	A.4	140	test cylinder in manhole	biofilm on epoxy	green	film	coated	X
A51	RM	A.5	140	test cylinder in manhole	concrete cylinder 0-1 cm	white	concrete	severe	

A52	RM	A.5	140	test cylinder in manhole	concrete cylinder 1-2 cm	white/grey	concrete	severe	
A53	RM	A.5	140	rod for hanging test cylinder in manhole	scrapings from iron rod	red	iron	coated	
A54	RM	A.5	140	test cylinder in manhole	biofilm on epoxy	brown/yellow	film	coated	
A55	RM	A.5	140	test cylinder in manhole	biofilm on epoxy	brown/yellow	film	coated	
A56	RM	A.5	140	test cylinder in manhole	biofilm on epoxy	brown/yellow	film	coated	
A57	RM	A.5	140	test cylinder in manhole	biofilm on epoxy	yellow	film	coated	
A61	RM	A.6	140	manhole upstream of plant	grey corrosion product near surface	grey	concrete	severe	X
A62	RM	A.6	140	manhole upstream of plant	brown corrosion product near surface	brown	concrete	severe	X
A63	RM	A.7	140	manhole upstream of plant	grey corrosion product near surface	grey	concrete	mild	X
A64	RM	A.8	140	manhole upstream of plant	grey corrosion product near surface	white	concrete	mild	X
B01	RM	B.1	12	digester effluent well	yellow/white corrosion 0-1 cm	white/yellow	concrete/film	severe	X
B02	RM	B.1	12	digester effluent well	yellow/white corrosion 1-2 cm	white/yellow	concrete/film	severe	X
B03	RM	B.1	12	digester effluent well	yellow/white corrosion 0-1 cm	white/yellow	concrete/film	mild	
B04	RM	B.1	12	digester effluent well	yellow/white corrosion 0-1 cm	white/yellow	concrete/film	mild	X
B05	RM	B.2	12	bar screen effluent channel	biofilm on side of covered channel	grey	ridged	mild	
B06	RM	B.3	12	bar screen influent channel	cement scraping on outdoor channel	white	concrete	severe	X
B07	RM	B.4	12	bar screen chamber	cement scraping near bar screen	brown	film	severe	X
C01	RM	C.1	12	digester overflow well	brown biofilm on coated walls	brown	film	coated	
C02	RM	C.2	12	digester gas leak	outdoor surface near gas leak	white	concrete	mild	X
C03	RM	C.3	12	digester effluent well	brown biofilm on coated walls	brown	film	coated	
C04	RM	C.4	12	meter station wall	cement scrapings from wall	white/brown	concrete	mild	
C05	RM	C.5	12	manhole upstream of plant	green biofilm on epoxy	green	film	coated	
C06	RM	C.5	12	manhole upstream of plant	white product under epoxy	white	concrete	severe	
D01	RM	D.1	54	gas treatment system leak	outdoor surface near gas leak	white	concrete	severe	

D02	RM	D.1	54	gas treatment system leak	outdoor surface near gas leak	yellow	concrete	severe	
D03	RM	D.2	54	grit chamber effluent channel	grey corrosion product	grey	concrete	mild	X
D04	RM	D.2	54	grit chamber effluent channel	brown corrosion product under iron feature	brown	concrete	mild	
E01	MW	E.1	120	influent channel	at edge of ledge (vertical)	white/brown	concrete	mild	X
E02	MW	E.1	120	test cylinder in wet well	concrete plus brown debris	brown	concrete/fecal	mild	
E03	MW	E.1	120	test cylinder in wet well	brown debris only	brown	fecal	mild	
E04	MW	E.2	120	manhole within plant	white corrosion product on wall	white/yellow	concrete	mild	X
F01	MW	F.1	250	manhole upstream of siphon	brown-orange biofilm	orange	film	mild	X
F02	MW	F.1	250	manhole upstream of siphon	white spiky biofilm on epoxy 1' down	orange	film	mild	X
F03	MW	F.2	250	manhole upstream of siphon	brown-orange biofilm near rim	white	nubbins	coated	X
F04	MW	F.3	30	manhole upstream of plant	brown-orange biofilm near rim	brown	film	mild	
F05	MW	F.4	30	manhole upstream of plant	brown-orange biofilm near rim	brown	film	mild	X
G01	SE	G.1	1	lift station	white corrosion product	white	concrete	mild	X
G02	SE	G.1	1	lift station	brown coal tar epoxy-stained	brown	concrete	mild	
G03	SE	G.1	1	lift station	flaking coal tar epoxy	black	epoxy	coated	
G04	SE	G.1	1	lift station	brown, below coal tar epoxy	brown	concrete	mild	X
G05	SE	G.1	1	lift station	red stained, near iron features	orange	concrete	coated	
H01	SE	H.1	143	influent mixing well	corrosion with flaking black epoxy	white/green	concrete/film	severe	X
H02	SE	H.2	143	influent wet well	grey biofilm on coated walls	grey	film	coated	
H03	SE	H.3	143	septic truck discharge	biofilm on bottom of steel lid	white	nubbins	coated	X
H04	SE	H.4	143	pump station bar screen well	cement scraping near bar screen	white/brown	concrete/fecal	mild	X
J01	PW	J.1	350	secondary clarifier wall	grey biofilm on clarifier wall	grey	film	coated	X
J02	PW	J.2	350	well between primary and secondary	green biofilm 6" below	green	film	coated	X

J03	PW	J.2	350	well between primary and secondary	ridged biofilm near surface	grey	film	coated	
K01	PW	K.1	80	headworks wet well off-season	brown biofilm on coated walls	brown	film	coated	
K02	PW	K.1	80	headworks wet well off-season	white spiky biofilm in metal edging	white	film	coated	
K03	PW	K.2	80	headworks wet well off-season	representative grey corrosion product	white	concrete	mild	
K04	PW	K.3	80	cake press room beam	grey and yellow corrosion product	white/yellow	concrete	severe	X

4.4. Results and Discussion

4.4.1. Microbial Diversity of Corrosion Biofilms

All biofilm samples were sequenced using Illumina MiSeq to a Good's coverage (Magurran, 2004) of over 99%, indicating that at least 99% of community diversity was accounted for. Selected samples were also sequenced using Sanger technology, which resulted in longer sequences; this larger amount of data per sequence makes Sanger more appropriate for determining specific microbial taxonomy using phylogenetic analyses. The corrosion-associated microbial communities studied here showed relatively limited microbial α-diversity (as judged by Chao1 (Hughes et al., 2001)) when compared to other microbial habitats (Ley et al., 2006a; Ley et al., 2006b; Walker et al., 2005). Late-stage corrosion communities observed here had less than 10 taxa (bacterial types), which is a rare condition in environmental samples. This low α-diversity is likely a result of extreme selection pressures exerted by pH values below 2 and high ionic strength present at the corrosion front.

Throughout the samples analyzed, communities are dominated by inorganic sulfur oxidizers that have been previously associated with this environment in both culture-based and rRNA phylogeny-based studies (Figure 4.2). The communities observed generally fall into three groups: communities dominated (>50%) by acidophilic sulfur oxidizer *Acidithiobacillus* spp. (eighteen), communities dominated (>50%) by acidophilic mixotroph *Acidiphilium* spp. (three), and diverse communities with more than two major taxa (thirteen). These two dominant genera are acidophilic, sulfur-oxidizing bacteria that have previously been associated with both concrete corrosion biofilms and with acid mine drainage biofilms (Okabe et al., 2007; Toril-Gonzalez et al., 2003). Communities dominated by *Acidithiobacillus* were only observed in surface-treated

sites and sites with severely corroded concrete, and *Acidiphilium*-dominated communities were observed in three severely corroded samples.

More diverse communities were observed in mildly corroded environments, which typically had pH values higher than two and low levels of headspace H_2S. Neutrophilic sulfur oxidizing genera observed may have contributed to corrosion in these less corroded sites, and include *Thiomonas*, *Thiobacillus*, *Sulfubacillus*, and *Thermothiobacillus*. These groups were not observed in sites dominated by acidophiles *Acidithiobacillus* and *Acidiphilium* sequences.

Mycobacterium spp. were also observed in corrosion communities, mostly in severely corroded biofilms dominated by acidophilic sulfur oxidizers. This heterotrophic genus is not typically seen in extreme environments, but has observed before in MICC (B. I. Cayford, 2013; Vincke et al., 2001) in acidic soils (Walker et al., 2005), and in acidic hot spring environments (Kusumi et al., 2011). The high lipid content and extreme hydrophobicity of mycobacterial cell walls confers heightened resistance to many antibiotics and may account for their resistance to acidic environments (Madigan et al., 2009). Mycobacteria are typically heterotrophs that require organic material as an energy source, but one study isolated a chemolithotrophic organism related to *Mycobacterium* spp. by 16S rRNA sequencing that oxidized sulfur compounds at pH 3.6 (Kusumi et al., 2011). While reduced sulfur is considered the primary food source in this environment, these heterotrophic organisms are likely using microbial by-products from autotrophic cells as a substrate and would not be present without an associated autotrophic, sulfur-oxidizing biofilm (Cho et al., 1995; Harrison, 1984; Okabe et al., 2007). Based on 16S rRNA sequence parsimony insertion of Sanger sequences into the Silva 108 database, sequences obtained in this study do not appear to be closely related to the *Mycobacterium* spp. sequences observed in the acidic soils. Instead, they are most closely related to *M. intermedium* and *M.*

parascrofulaceum based on parsimony insertion into the SILVA 108 tree. *M. parascrofulaceum* is an opportunistic respiratory pathogen related to *M. simiae* (Turenne et al., 2004).

Previous studies of corrosion communities have reported sequences belonging to the Xanthomonadaceae in mildly corroded biofilms; these observation did not coincide with the presence of acidophiles such as *Acidithiobacillus* spp. and *Acidiphilium* spp. (B. Cayford et al., 2012; Okabe et al., 2007; Satoh et al., 2009). In this study, the Xanthomonad *Metallibacterium* spp. was the fourth most abundant taxa observed and did co-occur with both *Acidithiobacillus* spp. and *Acidiphilium* spp. *Metallibacterium* spp. comprised over 5% of relative community abundance only in sites with greater than 10,000 ppm of CO_2 and less than 10 ppm of H_2S. A strain of this newly identified genus was isolated from an acidic mining environment and grew optimally in a moderately acidic environment (pH 5.5), where it conducted heterotrophic metabolism and raised solution pH by producing ammonium (Ziegler et al., 2012). Another study reported this genus in an acidic hydrothermal site (Coman et al., 2013). Researchers have previously hypothesized that heterotrophs in this environment can contribute to corrosion by producing organic acids and by metabolizing microbial by-products that would otherwise inhibit sulfur-oxidizing populations (Borichewski, 1967; Cho et al., 1995; Harrison, 1984; Okabe et al., 2007).

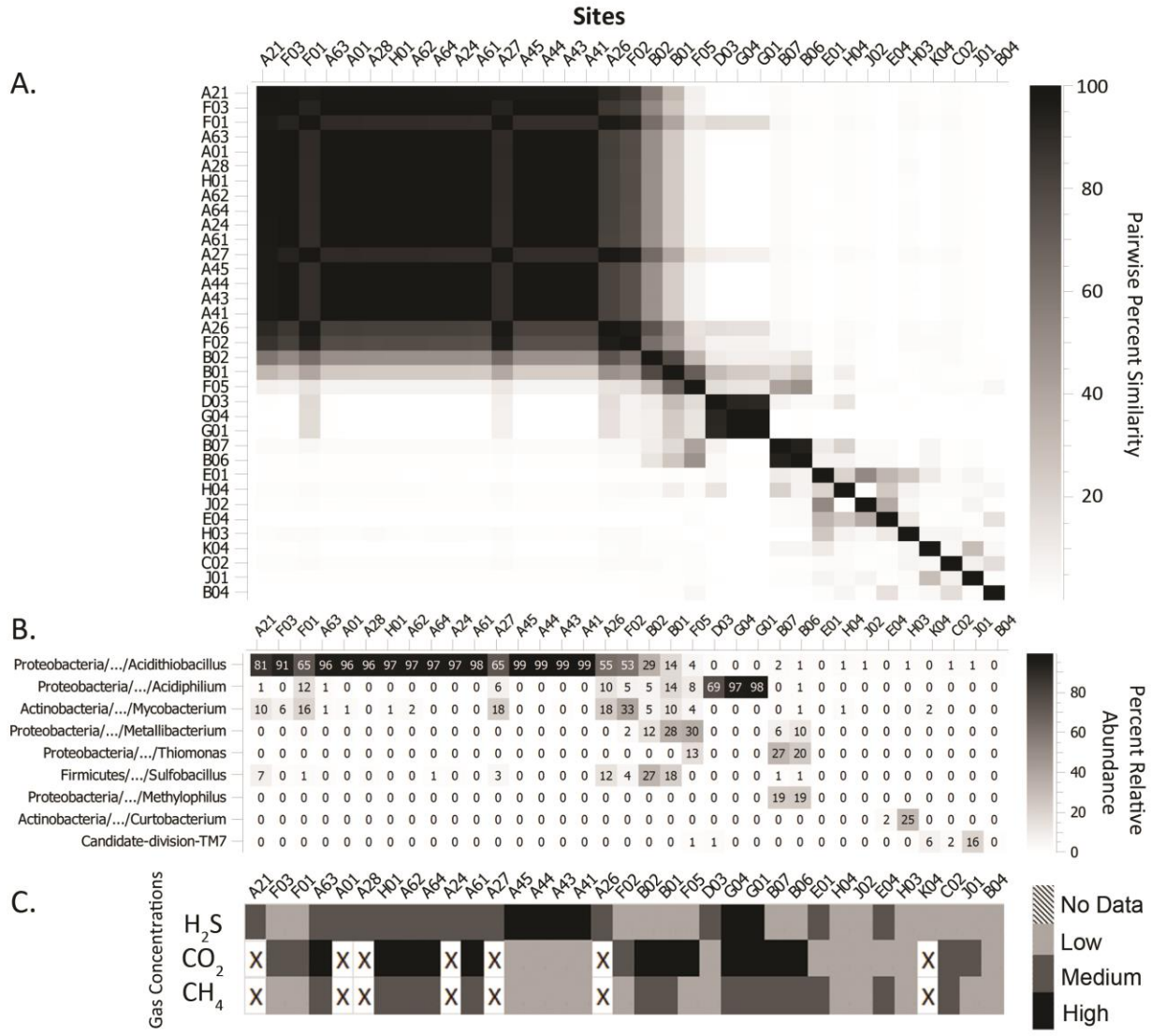

Figure 4.2: Geographical summary juxtaposing bacterial beta-diversity (A.), bacterial taxa relative abundance (B.), and the on-site concentrations of hydrogen sulfide, carbon dioxide, and methane gas (C.). In all cases, the black colors indicate higher levels of similarity, relative abundance, or gas concentrations. Site designations are presented on the horizontal axis and maintained throughout the three parts. For H_2S and CO_2, light grey (■), dark grey (■) and black (■) indicate concentrations in the range of 0-10, 10-100, and >100 ppm for H_2S and 0-5, 5-10, and >10 ppt for CO_2. For methane, light grey (■) indicates absence and dark grey (■) indicates presence. For all gasses, squares with "X" indicate no data.

4.4.2. **Effect of Environmental Parameters on Microbial Community and pH**

Each environmental metadata category was tested for potential correlation to community or environmental outcomes using pairwise linear regressions. H_2S concentration was the most significant environmental factor correlated to surface pH, percent relative abundance of *Acidithiobacillus* spp., and α-diversity. In the literature, these outcomes are all associated with severe corrosion (Islander et al., 1991; Okabe et al., 2007). The taxa with significantly different relative abundances between sites with H_2S concentrations below 20 ppm and those above as judged be two-part p-values below 0.05 are Commomonadaceae, Candidate Division TM7, *Legionella* spp., and *Sulfubacillus* spp. and *Acidithiobacillus* spp. All these groups except for *Acidithiobacillus* spp. were more abundant at sites with H_2S below 20 ppm.

High levels of CO_2 were also correlated to significantly lower microbial community α-diversity and increased relative abundance of *Acidithiobacillus* spp. (Table 4.2 and Figure 4.3). Elevated CO_2 concentrations were additionally associated with increased corrosion severity. The sulfur-oxidizing microbes that produce corrosion-causing acid are autotrophs that use CO_2 as a carbon source (Bielefeldt et al., 2009; D. P. Kelly, 1982). Environments with high CO_2 concentrations facilitate increased rates of diffusion into pore water and cell cytoplasmic fluid and are thus expected to be elevated with an associated increase in sulfur-oxidizing activity and corrosion. In addition, CO_2 causes carbonation and acidification of pore water, which has been observed to accelerate the corrosion process (Ismail et al., 1993).

While methane could potentially act as an alternate energy source to reduced sulfur compounds, elevated CH_4 levels generally did not appear to have a large effect on community composition. One environment (Samples B06 and B07) with CH_4 in the headspace supported bacteria related to C1 metabolizers *Methylophilus* spp. and *Methylomonas* spp., suggesting that

methane can serve as an alternate substrate for methylotrophs in these environments. However, samples collected from the same site fifteen months later had different communities without methylotrophs (B01 and B02). This indicates that corrosion communities are dynamic, and may change over time and in response to environmental changes. Methylotrophic bacteria have been previously reported just once in MICC communities (Vincke et al., 2001), but associated methane concentrations were not reported.

The extent of corrosion (mild or severe) was also correlated to α-diversity, moisture content, calcium content, and the sulfur to calcium ratio (Table 4.2). In the literature, late-stage corrosion is typified by high surface moisture and low pH—which is expected to cause decreased diversity and increased acidophile abundance (Islander et al., 1991; Okabe et al., 2007). Severe corrosion involves the oxidation of gaseous H_2S and the incorporation of sulfur into the cement matrix as gypsum or ettringite, which are expansive and wettable. These high-moisture severe corrosion products may explain the abundance of calcium and high calcium to sulfur ratios observed in the late-stage corrosion biofilms. Thirty-two taxa exhibited significantly different relative abundance in samples with less than 10% moisture and samples with more than 10% moisture. Only two of these, *Acidithiobacillus* spp. and *Mycobacterium* spp., were more abundant in higher moisture environments (two-part $p<0.05$).

Table 4.2: Significant pairwise linear regressions for regional data.

Outcome	Co-variate	p-value	Significance Threshold[†]
pH	log[H_2S]	0.009	***
Acidithiobacillus	log[H_2S]	0.0056	***
α-Diversity	log[H_2S]	0.014	**
Acidithiobacillus	pH	0.0405	**
α -Diversity	pH	0.023	**
Acidithiobacillus	CO_2	0.0521	*
α -Diversity	CO_2	0.012	**
Corrosion Stage	CO_2	0.046	**
α -Diversity	Corrosion Stage	0.052	*
Moisture	Corrosion Stage	0.023	**
Log[S:Ca]	Corrosion Stage	0.031	**
Free Calcium	Corrosion Stage	0.00016	***

[†] significance of 90%, 95%, and 99% confidence are indicated by *, **, and ***, respectively

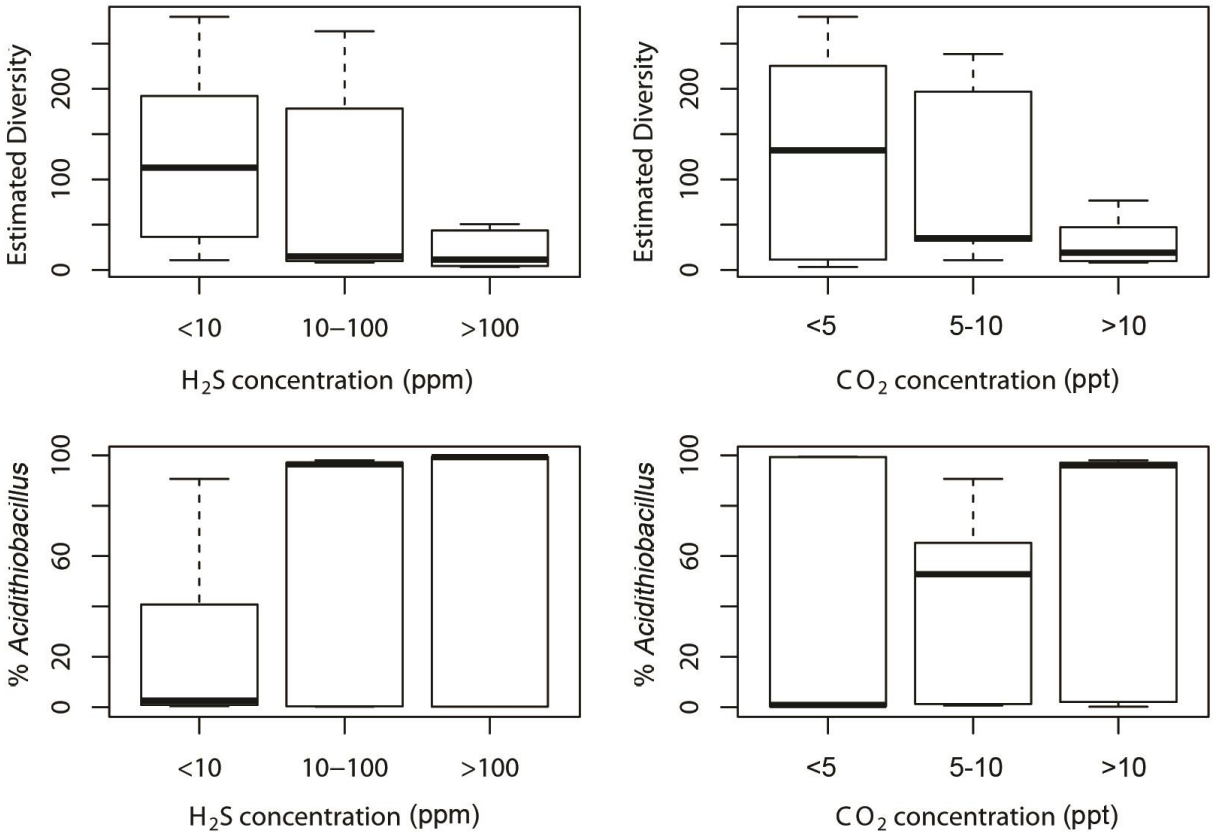

Figure 4.3: Comparison of *in situ* H_2S and CO_2 concentrations with descriptive community parameters. Top: Alpha Diversity (as predicted by Chao1 at rarefaction); Bottom: Percent of library comprised of *Acidithiobacillus*. Boxes represent 25th to 75th percentiles; bar terminus represents full observation range; dark bar represents median. n = 12, 8, and 6 for H_2S; n = 11, 5, and 7 for CO_2.

4.4.3. Effect of Geography on Corrosion Extent and Community

While based on pairwise linear regressions, the relative abundance of *Acidithiobacillus* spp. was significantly higher in the Rocky Mountain Region, and α-diversity was significantly higher in the Pacific West Region (Table 4.2), these findings are likely the result of sampling bias. Only three samples were sequenced from the Pacific West Region, and two of them had mild corrosion, so the α-diversity would be expected to be higher. In contrast, 21 samples from the Rocky Mountain Region were sequenced, and 15 were from severe corrosion environments

that would be expected to have high abundances of *Acidithiobacillus* spp. and low α-diversity. If more mildly corroded samples had been collected from Rocky Mountain locales, these correlations would likely not apply. Similarly, if more severely corroded samples had been sampled from Pacific West utilities, the α-diversity trend would probably not be upheld. Environmental and microbial community parameters were not observed to be significantly correlated to any other geographic regions. Additionally, the latitude and longitude of a site was not significantly correlated to the extent of corrosion or the microbial community composition, as measured by α-diversity and percent abundance of *Acidithiobacillus* spp. This finding is in agreement with a similar survey of acid mine drainage communities, which found that environmental conditions are better predictors of microbial community composition than geographical location (Kuang et al., 2013).

4.4.4. **Multivariate Analyses**

Based on canonical correspondence analysis (Legendre et al., 1998), the concentrations of the three headspace gases H_2S, CO_2, and CH_4 accounted for 29% of the community variation observed (Figure 4.4). The relatively small magnitude of the CH_4 vector indicates that methane is not as strongly correlated to community composition as either H_2S or CO_2. One unmeasured factor that likely affects community composition is the age of the concrete structure, as corrosion communities change over time with exposure to corrosive gasses. The three different types of communities emerge in Figure 4.4. The cluster at the right side of the diagram contains samples dominated by *Acidithiobacillus* spp., which is closely associated with the CCA1 axis. These samples coincide with high levels of both H_2S and CO_2, and were collected from manholes in two different areas within Utility A's collection system. In addition, one sample collected from a coated manhole in Utility F is included in the cluster. These nine samples and the other three

samples from Utility F comprise the only samples collected from collection system manholes that were successfully sequenced on the Illumina platform, and include both coated and uncoated concrete surfaces. This indicates that similar environments can harbor similar communities even if the type of surface is different. The small cluster in the center (G01, G04, and D03) contains samples dominated by *Acidiphilium* spp., and remaining samples have more diverse communities.

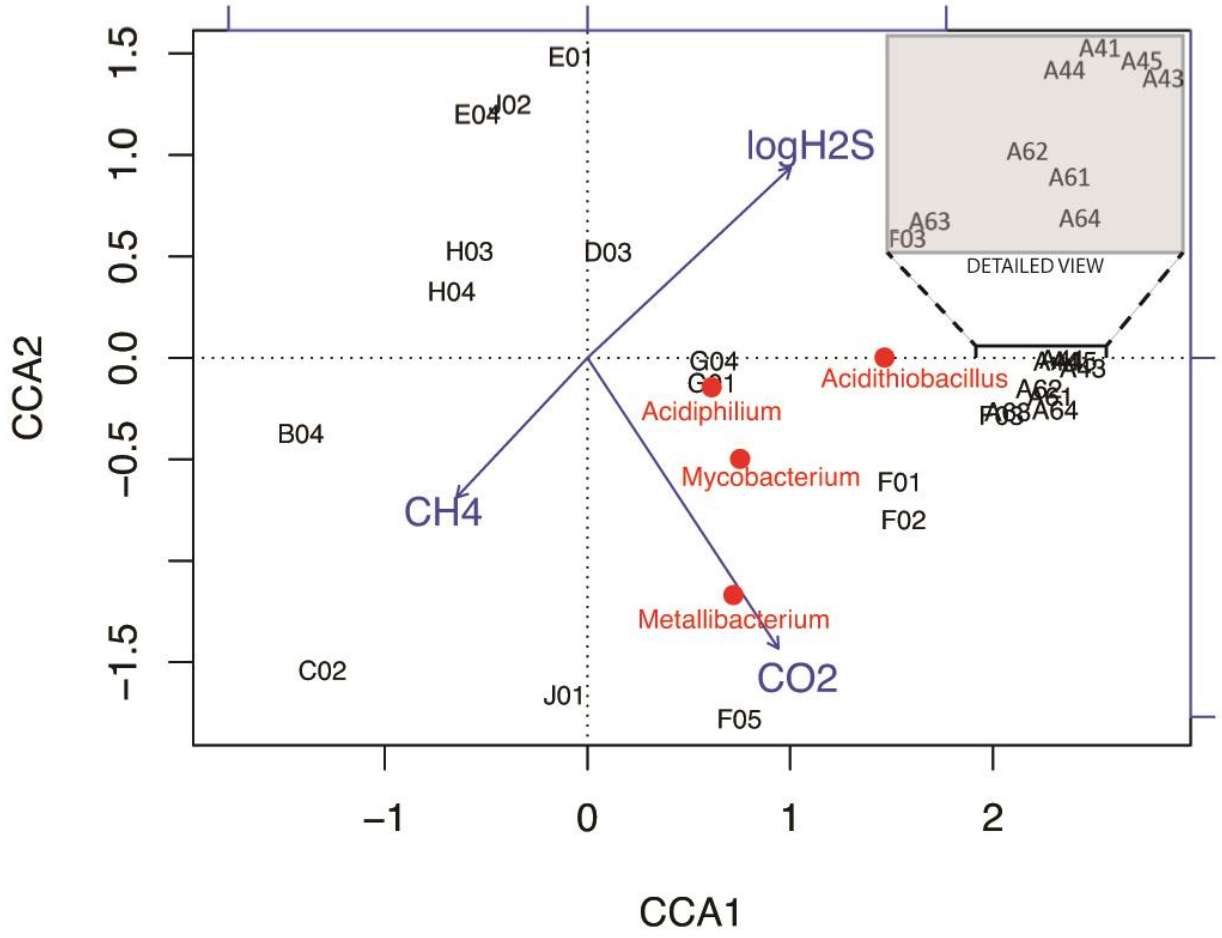

Figure 4.4: Canonical correspondence analysis of regional sample community composition using square-rooted value of relative OTU abundance. Samples are labeled in black. Blue vectors indicate the effect of scaled gas concentrations on sample community composition (as measured by relative abundance of bacterial taxa according to V1V2 Illumina sequencing). Red vectors indicate the contribution of four most abundant bacterial taxa.

4.4.5. Characteristics of Extreme Corrosion

Previous culture-based corrosion studies have long demonstrated that early stages of corrosion are characterized by higher diversity and more neutrophiles than acidophiles (Islander et al., 1991), trends which are confirmed by this study using modern phylogenetic analyses. Corroded concrete is an extreme environment typified by high moisture, low pH and high ionic

strength, which select for a less diverse, more acidophilic range of organisms than un-corroded or mildly corroded concrete.

The bacterial community associated with severe corrosion was similar to that associated with treated surfaces in high-sulfide headspaces. Both types of samples had low alpha diversity and high proportions of *Acidithiobacillus* spp. In contrast, mildly corroded concrete samples had higher alpha diversity (regression $p<0.1$) and lower relative abundance of *Acidithiobacillus* spp. than severely-corroded biofilms (regression $p<0.1$) (Figure 4.5). This resemblance between severely corroded sites and sites with surface coatings reflects the state of anti-corrosion measures taken by utilities. Because treatment is expensive, structures are usually coated only if they were previously corroded or are expected to be at risk. As a result, environmental parameters are often similar between severely corroded sites and surface-treated sites, and could be expected to select for similar bacterial communities.

Surface treatments protect the concrete from the acid produced by corrosion biofilms, but harbored the same types of microbial community as severely corroded concrete; this indicates that these coatings simply keep biogenic acids from reaching the concrete, but do net inhibit the growth of the causative microbes. Indeed, it appears that some coatings enhance the selection of *Acidithiobacillus* spp. (See Figure 4.7) These microbes utilize H_2S as their primary energy source and CO_2 as their carbon source, so corroding concrete and surface coatings in environments with high concentrations of these gasses are expected to select for similar microbial communities.

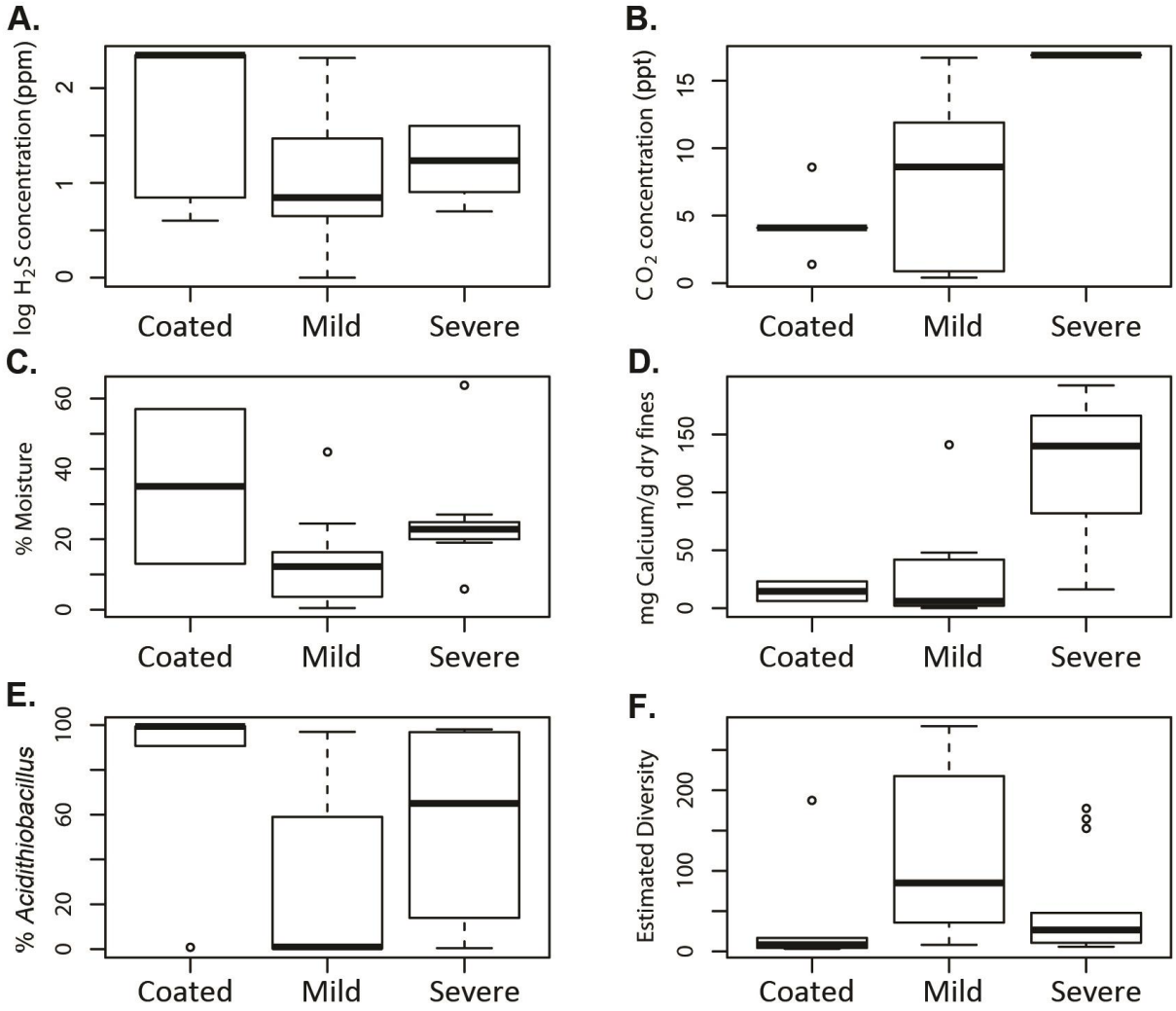

Figure 4.5: Chemical and microbiological characteristics of corrosive environments, as judged by utility personnel. A.) H_2S concentrations (n=6, 15, and 6), B.) CO_2 concentrations (n=6, 15, and 2), C.) Moisture content (n=2, 12, and 11), D.) Calcium content (n=2, 15, and 10), E.) Relative abundance of *Acidithiobacillus* spp. (n=6, 16, and 13), and F.) Estimated α-diversity by Chao1 (n=6, 16, and 13). Boxes represent 25th to 75th percentiles; bar terminus represents full observation range; dark bar represents median.

4.4.6. Communities Differences Between Samples Treated with Commercially Available Coatings and Untreated Samples

A coatings company performed field testing of uncoated concrete cylinders and otherwise identical cylinders treated with commercially available coatings in a severe manhole in Utility A. Corrosion product sample was collected from the uncoated cylinder (samples A31-A35), and

biofilm samples were collected from the coated cylinders (samples A41-A45). Table 4.3 outlines the types of treatments used, and Figure 4.6 shows images of treated and untreated cylinders after exposure. Treated cylinders all had similar appearances, with brown and yellow stains on the surface. Bacterial communities were determined using V1V2 amplicons on the Illumina MiSeq platform and three-domain communities were determined using "universal" primer clones and Sanger sequencing (see Section 3.2 for method details).

Table 4.3: Summary of treatments used on concrete cylinders

A34	Untreated Concrete
A41	100% Solids Reinforced Epoxy
A43	Calcium Aluminate Premix
A44	100% Solids Fiber-Reinforced Polyamine with Epoxy Glaze
A45	Aggregate Filled Epoxy

Figure 4.6: Cylinder treated with calcium aluminate premix (left) and untreated cylinder (right) after one year of exposure in a manhole with H_2S > 300 ppm.

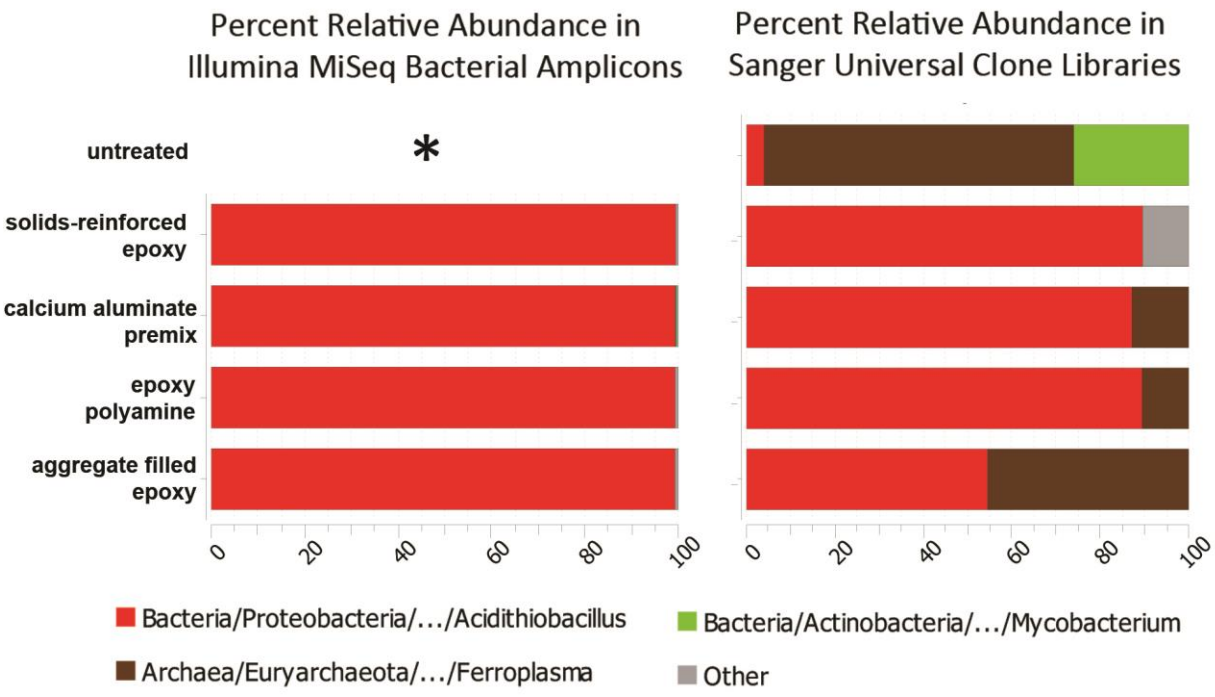

Figure 4.7: Bacterial communities recovered from the surface of treated and untreated concrete cylinders by Illumina and Sanger sequencing platforms. Bar widths indicate percent relative abundance of microbial taxa in sample libraries; bar colors indicate taxa identity. * indicates no data.

Based on Sanger sequencing using universal primers, treated concrete specimens exposed for one year were largely dominated by *Acidithiobacillus* spp. (Figure 4.7). In contrast, the archaeal genus *Ferroplasma* comprised 74% of the late-stage corrosion community on the uncoated concrete cylinder after the same one year duration of exposure in the same manhole. This sample was not successfully amplified for Illumina MiSeq sequencing, so this result could not be corroborated by a second sequencing platform. Sequences related to *Ferroplasma* spp. were also present in Sanger libraries from sample A01 (data not shown), which was collected from a very corroded covered channel in a wastewater treatment plant in the same utility system as the severe manhole. However, the reasons for *Ferroplasma* enrichment are unclear, because it was not observed in other samples with similarly low pH and high moisture content. This

community also had high (12%) abundance of *Mycobacterium* spp., which were not observed in Illumina or Sanger libraries for treated surface biofilm communities (Figure 4.7).

This difference in microbial community between treated and untreated surfaces may have been due to the difference in surface moisture between the treated and untreated cylinders, which could yield different selection pressures. While both types of cylinders had pore water pH values below 1, treated cylinders experienced no visible corrosion. As a result, moisture content was relatively low. In contrast, the corroded layer of the untreated sample contained over 30% water, and biofilms grew in a complex chemical matrix of corrosion products, sulfur compounds, and microbial cells. The high moisture content and specific chemistry of the corroded cement matrix may have facilitated *Ferroplasma* spp. selection.

Ferroplasma spp. has been observed in acid mine drainage environments, where it oxidizes iron (B. J. Baker et al., 2006; Schrenk et al., 1998). *Ferroplasma* is among the most acidophilic microbes known, and is capable of growing at pH 0 (Dopson et al., 2004; Ferrer et al., 2007). These organisms are also facultative anaerobes, which explains why they may be selected for the thick, high moisture environment found in this corrosion product (Dopson et al., 2004; Tyson et al., 2004) The *Ferroplasma acidarmanus* Fer1 genome, indicates that these organisms may be mixotrophic, i.e. capable of oxidizing iron, sulfur, or organics for energy. The genome has few genes related to extracellular polymer production (i.e. for biofilm formation) or motility (Tyson et al., 2004). Archaeal sequences have been previously reported in MICC communities (B. I. Cayford, 2013; Santo Domingo et al., 2011), but not as a dominant community member.

4.5. Conclusions

This work represents the largest regional sampling campaign of microbially induced concrete corrosion biofilms to date. Hydrogen sulfide and carbon dioxide gas concentrations in structure headspace correlated with bacterial community composition, particularly α-diversity the abundance of *Acidithiobacillus* spp. Relatively higher concentrations of H_2S and CO_2 gas present in structure headspaces was linked to decreased community α-diversity and increased relative abundance of acidophilic sulfur-oxidizer *Acidithiobacillus* spp., the genus most commonly associated with microbially induced concrete corrosion. CO_2 concentrations are not typically reported in environmental metadata associated with MICC, but appear to be as strongly correlated with corrosion outcomes as H_2S concentrations.

In concordance with previous molecular ecology studies in this environment (B. Cayford et al., 2012; Gomez-Alvarez et al., 2012; Santo Domingo et al., 2011; Satoh et al., 2009), acidophiles such as *Acidithiobacillus* spp. did not dominate mildly-corroded biofilm communities. Instead, mildly corroded samples hosted a diversity of bacterial genera, including heterotrophs, such as *Metallibacterium* spp., and nitrogen metabolizers.

In accordance with previous studies, extremely corroded sites frequently harbored bacterial genera *Acidithiobacillus*, *Acidiphilium*, and *Mycobacterium*. Both extremely corroded sites and treated surfaces were characterized by high levels of H_2S and CO_2 and the corrosion product had high moisture and calcium content, low microbial diversity, and high proportions of acidophilic sulfur oxidizers. The bacterial richness (observed α-diversity) in environmental samples can range from several hundred to several hundred thousand taxa (Fierer et al., 2011; Keller et al., 2004; Ley et al., 2006a; Ley et al., 2006b; Walker et al., 2005). The microbial α-diversity observed in severely corrosion communities (<10 taxa for some sites) in this study is

among the lowest ever observed in environmental samples. High α-diversity is typically associated with robust microbial communities that are resistant to changes in environmental conditions (Briones et al., 2003; Girvan et al., 2005). This low α-diversity indicates that these biofilms may be susceptible to disruption by toxicity or changing environmental parameters.

Sanger sequencing of treated and untreated concrete cylinders exposed to a corrosive environment indicate that different microbial communities are selected for on treated and untreated samples, despite similar bacterial communities and pH levels. This difference was only observed through three-domain sequencing, which revealed the presence of *Ferroplasma* spp. in severely corroded concrete biofilms. This is the first reported instance of archaeal sequences as a dominant member of this type of environment. This may be explained by the fact that previous studies have investigated MICC biofilms on working wastewater conveyance structures; these functional structures would be replaced or rehabilitated before the severe corrosion conditions that select for *Ferroplasma* spp. could occur.

In conclusion, headspace H_2S and CO_2 gas concentrations were significantly correlated to low α-diversity and increased abundance of acidophilic sulfur-oxidizing bacteria. These gasses can serve as an indication of concrete corrosion potential, and can be used in a practical sense by wastewater utilities attempting to predict corrosion. While most research in this field is primarily concerned with H_2S gas, this study indicates that CO_2 should also be considered a risk factor for corrosion. This work contributes to a better understanding of what factors influence communities involved in concrete corrosion. Such knowledge enables engineers to make more informed predictions about corrosion risks and conduct more efficient allocation of resources for rehabilitation of wastewater infrastructure.

5. Temporal Patterns in Concrete Corrosion Communities (Aim 2)

5.1. Introduction and Background

The second aim of this thesis is use high-resolution field experiments to develop a model of microbial community succession in MICC biofilms. While the succession of microbial communities involved in concrete corrosion has been hypothesized for over 20 years, only one study to date has performed a longitudinal phylogenetic study of corrosion communities starting with initial colonization, and only three sampling dates were analyzed for community composition (Okabe et al., 2007). Previous models of corrosion community succession have been culture-based and focused on sulfide-oxidizing bacteria, and these are still the accepted models in the wastewater industry today. However, recent studies using phylogenetic rRNA techniques have revealed a diversity of metabolic types, including heterotrophs (B. Cayford et al., 2012; Gomez-Alvarez et al., 2012; Okabe et al., 2005; Okabe et al., 2007; Santo Domingo et al., 2011; Satoh et al., 2009). The prevalence of these organisms, especially at early stages of corrosion where pH selection is less severe, is still poorly characterized.

5.2. Experimental Design

In this study, concrete specimens were placed in manholes on the Colorado Front Range for up to a year in three longitudinal experiments. All specimens were suspended in one of two manholes on the front range of Colorado with high headspace concentrations of hydrogen sulfide (>300 ppm), which provided an accelerated corrosion environment. In addition to the three longitudinal experiments, one additional sample was exposed from October 2010 to October 2011 and was analyzed by Sanger sequencing (Experiment 4). Community succession was analyzed using sequencing and phylogenetic analysis of 16S rRNA gene V1V2 region amplicons

and universal SSU rRNA clones according to Section 3.2. Surface pH, mass loss, and percent of surface area corroded were used as indicators of corrosion extent.

Table 5.1: Installation and sampling schedule for four longitudinal exposure field tests (I indicates sample installation, X indicates specimen removal event)

		'10	2011			2012											
Experiment	Manhole	O	O	N	D	J	F	M	A	M	J	J	A	S	O	N	D
1	MH2 (Moderate)				I		X		X		X		X		X		X
2	MH1 (Severe)												I	X X	X	X X	X
3	MH1 (Severe)		I		X		X		X		X		X		X		
4	MH1 (Severe)	I	X														

5.3. Results and Discussion

5.3.1. Severity of Corrosion over Time

The more severe MH1 experienced higher levels of hydrogen sulfide gas than its moderate counterpart, MH2 (Figure 5.2). This difference is likely a result of a hydrogen peroxide added at a dosing station upstream of the area, which chemically oxidizes dissolved sulfide in the wastewater. The interceptor pipe acts as a plug-flow reactor, so the sulfide concentrations are expected to decrease steadily downstream of the dosing station until the peroxide is quenched (Figure 5.1). This could explain the decreased levels of sulfide in MH2.

Figure 5.1: Map of manholes and peroxide dosing station. Red line indicates the path of 72" fiberglass wastewater interceptor, and red circles represent test manholes.

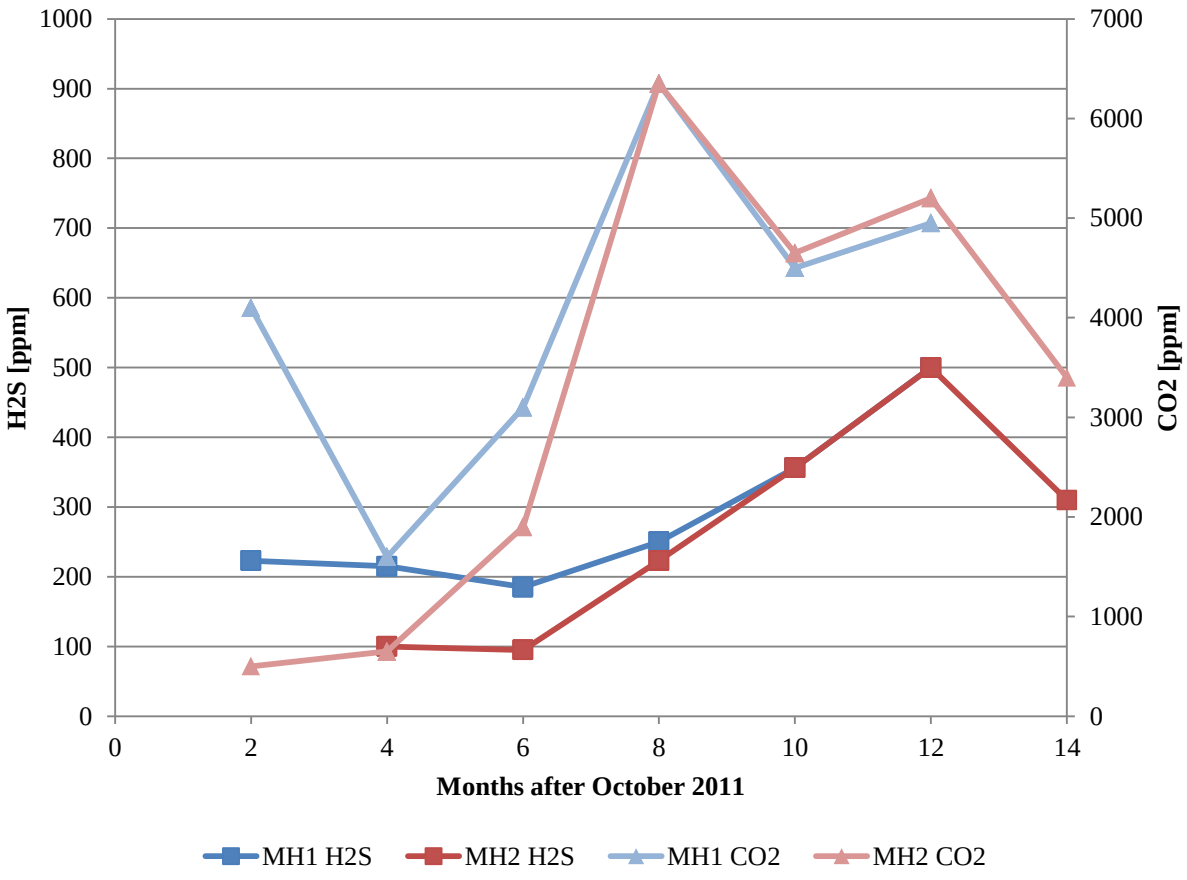

Figure 5.2: Hydrogen sulfide (dark lines) and carbon dioxide (light lines) concentrations in test manholes MH1 (blue) and MH2 (red).

Both surface area corrosion and mass loss increased over the course of all three experiments (Figure 5.3 and Figure 5.4) (regression $p<0.005$). Specimens exposed in MH1 (Experiments 2 and 3) experienced more mass loss and surface corrosion than those exposed in MH2 (ANCOVA $p<0.01$ for both) (Figure 5.3). This is likely because lower hydrogen sulfide gas concentrations in MH2 facilitated slower diffusion of hydrogen sulfide to the concrete surface moisture, resulting in reduced amounts of substrate for acidogenic bacteria. In MH2, the extent of corrosion as measured by mass loss and surface corrosion increased markedly between ten and twelve months. This may have resulted from the increase in hydrogen sulfide concentrations from 350 ppm to 500 ppm, or may be an artifact of using 3x5 inch cylinders for 12-months observations and 1-inch cubes for all other observations. The data also have some temporal inconsistencies, such that in some cases, certain samples are more corroded than at a later time point in the same series. This is a result of the lack of direct replication and the observation of a series of specimens rather than recurrent observations of one specimen.

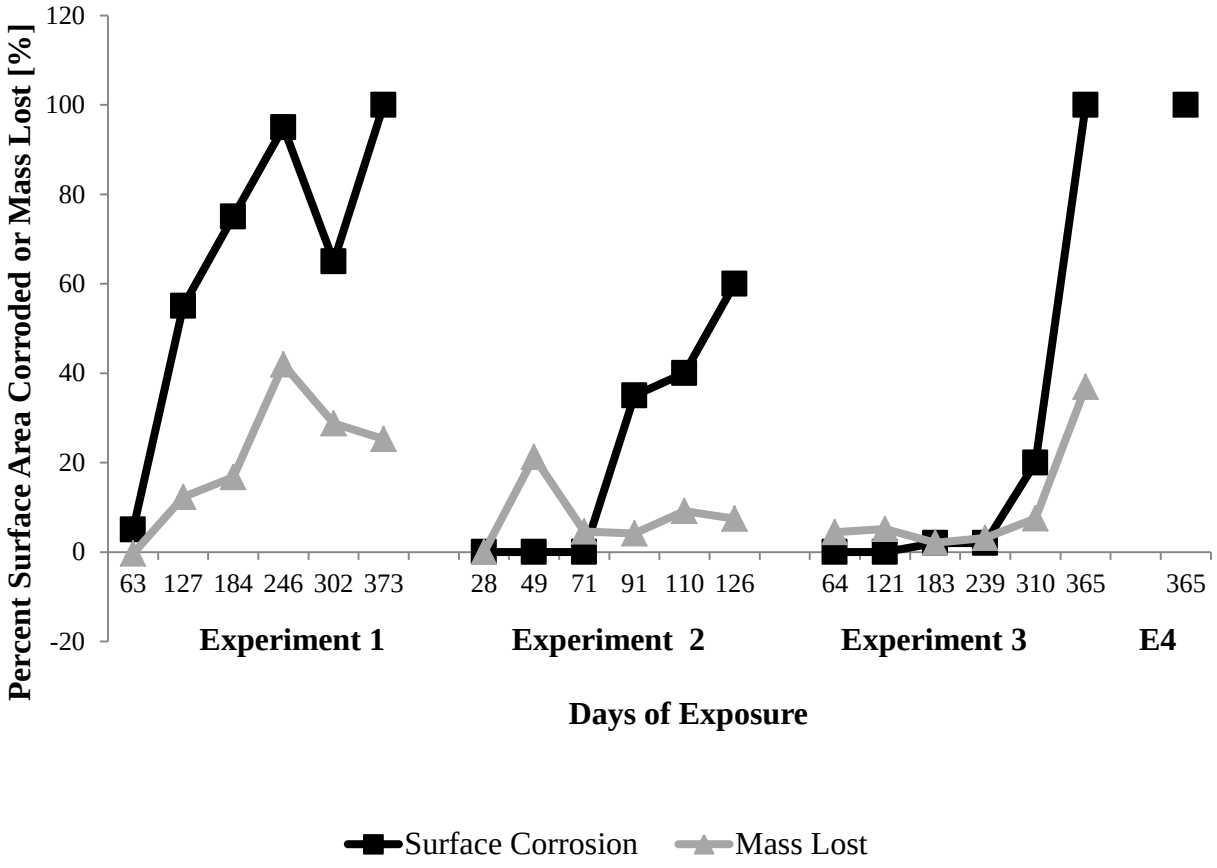

Figure 5.3: Percent of surface corroded (■) and dry concrete mass loss (◆) of concrete specimens exposed to corrosive manhole environments for one to twelve months.

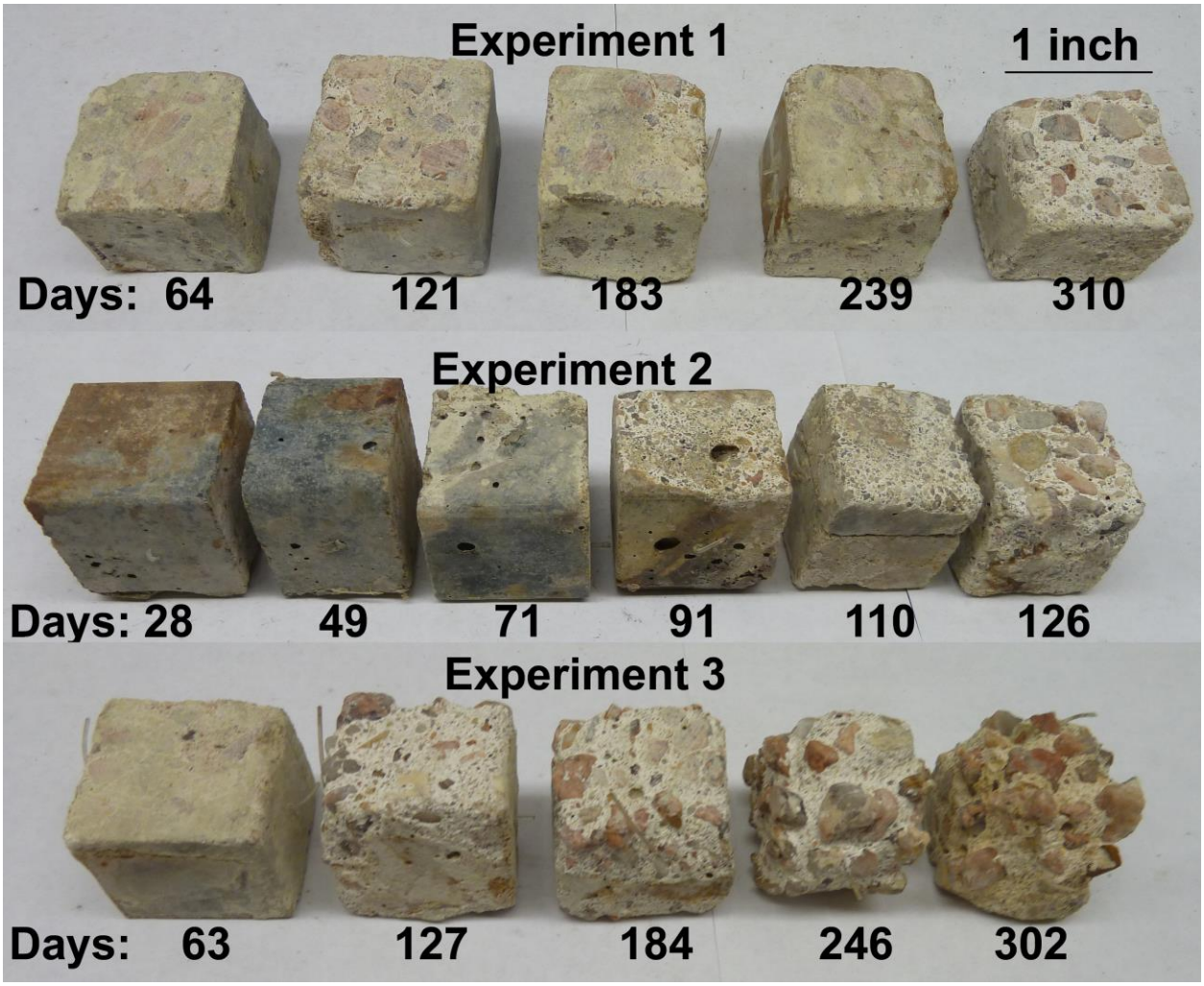

Figure 5.4: Cubic concrete specimens after exposure to corrosive environments. Specimens were exposed in one of two corrosive manholes for between 28 and 302 days, then scraped, rinsed, and dried prior to imaging.

5.3.2. Alpha Diversity and pH over Time

Biofilm bacterial α-diversity on samples in MH1 decreased over the course of each experiment (regression $p<0.1$). This trend coincides with a drop in pore water pH (Figure 5.5). In Experiment 1 in MH2, pore water pH dropped at a slower rate, and biofilm diversity increased for six months before decreasing. This sustained neutral pore water pH likely allowed for the development of a more complex neutrophilic microbial community before low pH selection pressure forced a less diverse acidophilic community. Estimated α-diversity after three months

in MH1 or six months in MH2 was less than 20 taxa. This was atypically low for environmental microbial communities (Ley et al., 2006a; Ley et al., 2006b; Walker et al., 2005). Extreme selection and subsequently low α-diversity was likely a result of only one primary food source, very acidic conditions, and high salt content.

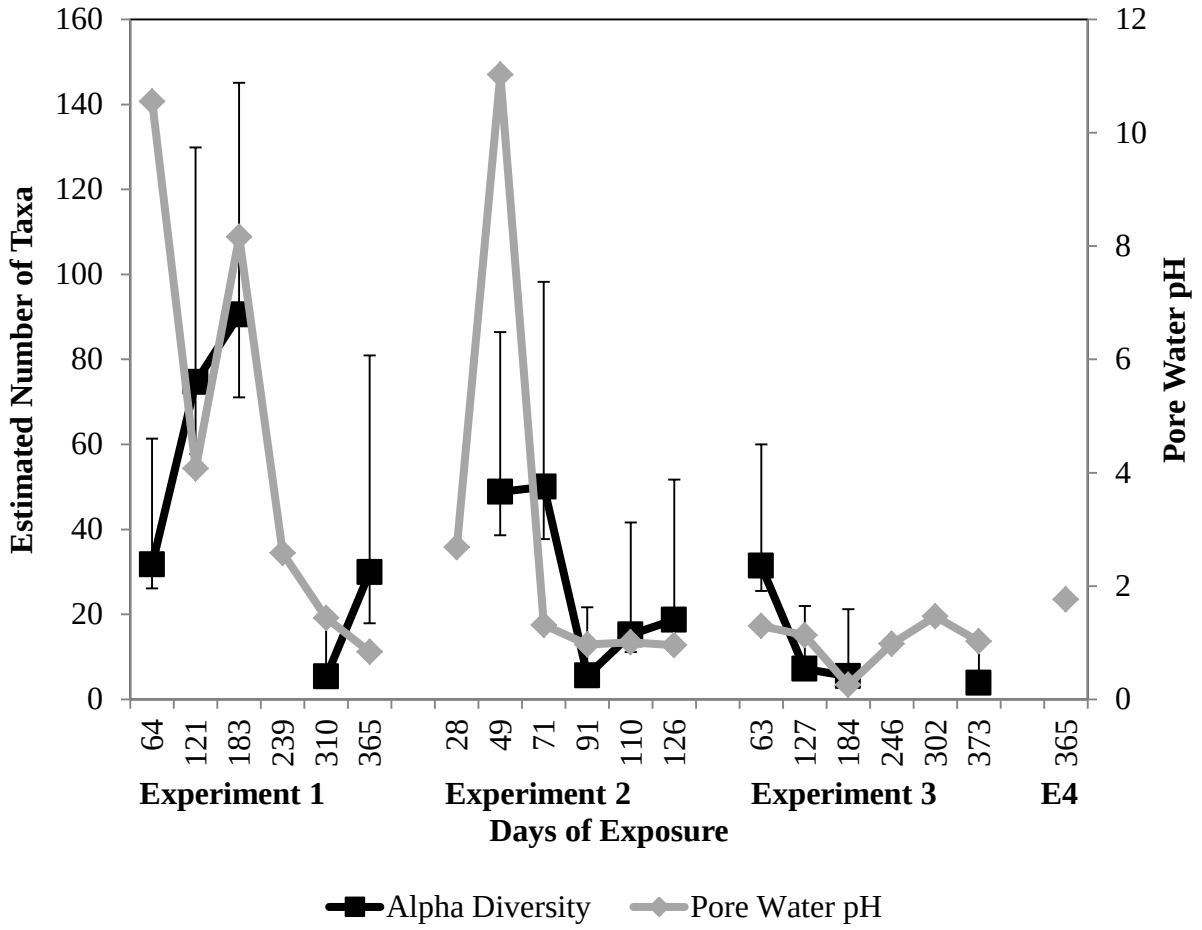

Figure 5.5: Estimated surface biofilm bacterial community α-diversity as judged by Chao1 using Illumina MiSeq V1V2 16S amplicon sequencing (■) and estimated pore water pH (◆) after one to twelve months of exposure in a manhole environment. Error bars indicate 95% confidence intervals for Chao1.

5.3.3. Abundance of Sulfur

Hydrogen sulfide gas serves as the source of sulfur, which reaches the biofilm through chemical diffusion. The sulfide in the biofilm matrix can then be oxidized by sulfur-oxidizing

bacteria, which allows for favorable kinetics for continued diffusion of hydrogen sulfide gas. Thus, sulfur content in the surface biofilms may serve as an indicator for both sulfur-oxidizing activity and extent of corrosion. Exposed samples generally experienced increasing amounts of total sulfur per cube over the exposure periods (Figure 5.6), indicating increased rates of sulfide oxidation.

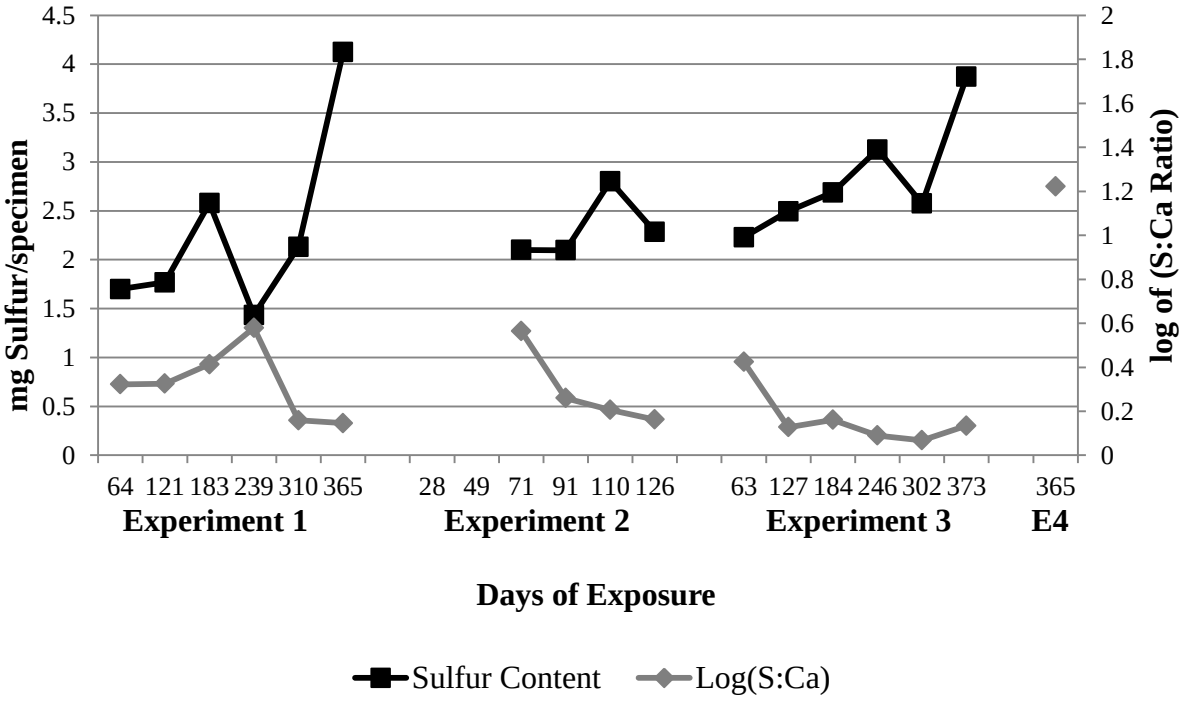

Figure 5.6: Total sulfur content per concrete specimen (■) and sulfur to calcium ratios (◆) after one to twelve months of exposure to corrosion environment, as measured by inductively coupled plasma optical emission spectroscopy (ICP-OES) of acid extracted samples.

Once biogenic acids begin to degrade the cement binder, the corroded concrete contains calcium-rich corrosion products (Hudon et al., 2011; O'Connell et al., 2010; Roberts et al., 2002), so the of calcium yield is expected to increase as corrosion progresses. Thus, the ratio of sulfur to calcium (S:Ca) in the scraping samples can be an indicator how much sulfur has been oxidized per unit of cement binder corroded. Over time, the S:Ca ratio generally decreases in biofilm scrapings (Figure 5.6) as a result of increasing quantities of unstable calcium-based corrosion

product. This means that binder degradation occurs more rapidly than sulfur mineralization at late stages of corrosion.

Experiment 1 is in MH2, a less corrosive manhole than MH1 used in Experiments 2, 3, and 4. Experiment 1 specimens experience a slight increase in the sulfur to calcium ratio during the first eight months of exposure, which correlates to an increase in observed taxa on these samples. This is likely due to the presence of a diversity of neutrophilic sulfide-oxidizing microbes that produce sulfur, but do not reduce pore water pH enough to corrode the binder and release calcium. This is corroborated by less than 5% surface corrosion for these specimens (Figure 5.3).

5.3.4. Microbial Succession by Illumina Bacterial V1V2 Amplicon Sequencing

Bacterial community succession was analyzed using Illumina sequencing of 16S rRNA genes. In each experiment, neutrophilic genera are replaced by acidophilic genera as pore water pH decreases with extended exposure (Figure 5.7). Early communities (less than 2 months in the severe manhole and less than 6 months in the moderate manhole) exhibit high relative abundances of *Halothiobacillus* spp., a neutrophilic sulfur-oxidizing bacteria. Later communities are strongly dominated (>95%) by acidophilic sulfur-oxidizer, *Acidithiobacillus* spp.

Early stage communities have higher diversity and larger abundances of taxa related to heterotrophic genera such as *Pseudomonas*, *Serratia*, and *Stenotropomonas*. Twenty-four genera, mostly related to heterotrophs, were significantly more abundant before 100 days of exposure than after (two-part $p<0.05$). Previous work indicates that heterotrophs in this environment may contribute to corrosion by metabolizing microbial by-products that would otherwise inhibit the sulfide-oxidizing populations and by producing organic acids that

contribute to surface acidification (Harrison, 1984; Okabe et al., 2007). While reduced sulfur is considered the primary food source in this environment, organic material could accumulate at the concrete surface as a result of decomposing cellular debris and/or wastewater splash. Also detected in this study are taxa related to denitrifying bacteria (*Rhodanobacter* spp.) and nitrogen fixers (*Rhizobium* spp.), indicating that the metabolic diversity of MICC biofilms may be higher than previously hypothesized.

Of the four phylogenetic groups previously hypothesized to be the major players in MICC communities (*Acidithiobacillus, Acidiphilium, Mycobacterium,* and Xanthomonadaceae) (B. I. Cayford, 2013), only *Acidithiobacillus* spp. were present at more than 1% relative abundance in more than one community library. *Stenotropomonas*, a member of the Xanthomonadaceae family, comprised 9% of the community in one Experiment 1 sample.

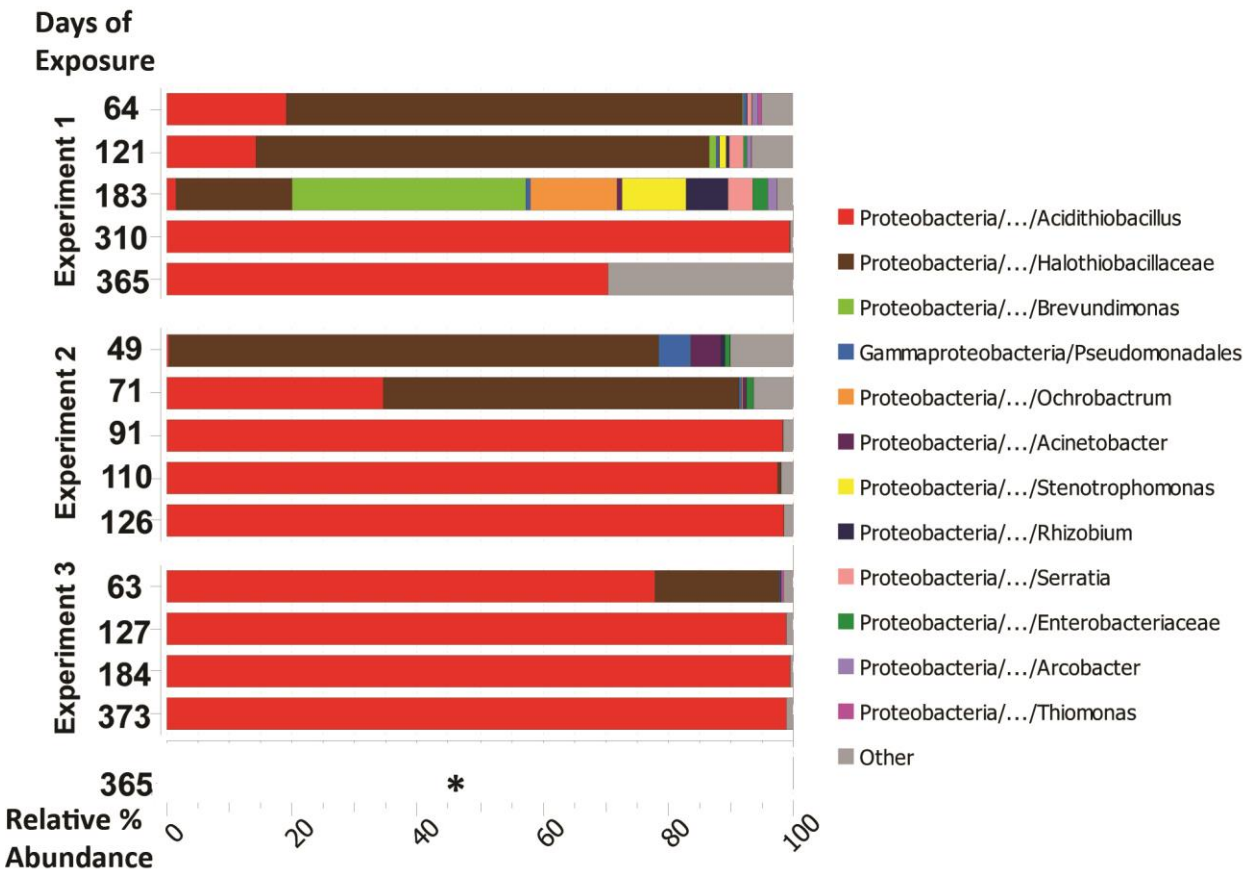

Figure 5.7: Bacterial taxa observed in concrete surface biofilms three longitudinal experiments in high H_2S manholes (Illumina MiSeq). Taxa with greater than 1% representation in total data set are shown. Bar widths indicate percent relative abundance of microbial taxa in sample libraries; bar colors indicate taxa identity.

5.3.5. Microbial Succession by Sanger Universal Clone Libraries

Despite the high yields of Illumina sequencing, there are as yet no universal primers optimized for the platform, so it can only be reliably used to help describe bacterial diversity. In order to account for archaeal and eukaryal community members, "universal" 16S clones were also analyzed. The bacterial component of universal library communities composition closely matched that observed in Illumina sequencing of bacterial amplicons. Communities were originally dominated by *Halothiobacillus* spp., which were replaced over time with *Acidithiobacillus* spp. (Figure 5.8). Eukarya sequences were observed in some communities

sampled between 100 and 200 days in a severely corrosive manhole (MH1) and in one community sampled after 310 days in a moderately corrosive manhole (MH2). Sequence data were insufficient to enable classification of these sequences to a more specific group, but previous studies have implicated acidophilic fungus in abetting the structural deterioration of corroding concrete by means of expanding hyphae (Cho et al., 1995). In addition, the sample exposed in the severe manhole for one year in Experiment 4 was dominated (88%) by *Ferroplasma* archaeal sequences (discussed in Section 4.4.6). The prevalence of this genus in the late-stage community may result from the biochemical difference between bacterial and archaeal acidophilic sulfur oxidation (Section 2.5.3). The archaeal pathway involves the disproportionation of elemental sulfur, and thus requires a buildup of elemental sulfur (i.e. advanced corrosion) to be thermodynamically favorable. The remainder of this library was comprised of *Mycobacterium* spp. sequences. This sample was not successfully amplified for Illumina MiSeq sequencing, so this result could not be corroborated by a second sequencing platform. This community was not similar to the community observed on the 373 day exposed specimen in Experiment 3, despite the fact that these two samples were exposed for a similar amount of time in the same manhole, albeit one year apart. The reason for this difference may have several potential causes. The two samples were poured by different facilities with different mix designs, which could have resulted in different corrosion product chemistry at the process, progressed. In addition, the Experiment 4 specimen was placed lower in the manhole than the Experiment 3 samples, which may have exposed it to higher relative humidity (closer to the wastewater flow) and higher H_2S concentrations (because H_2S is heavier than air).

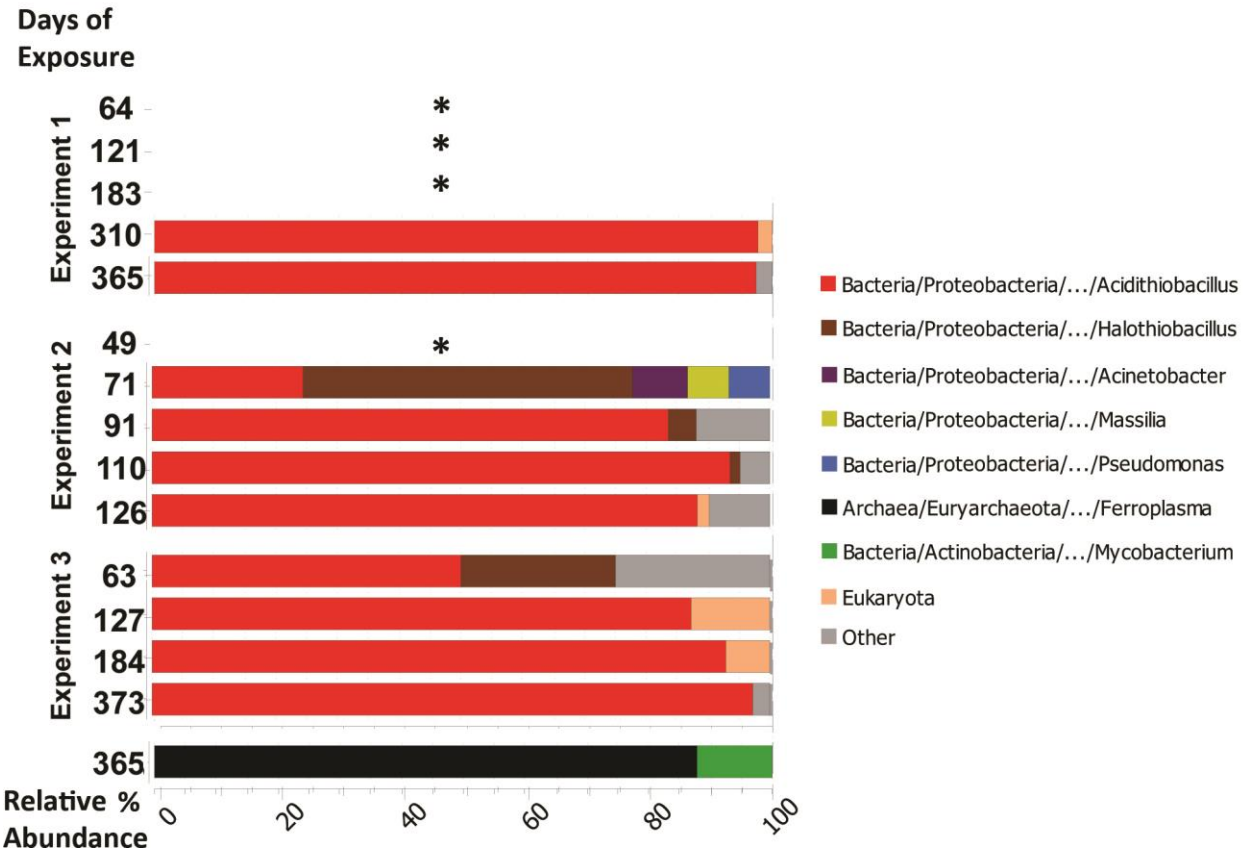

Figure 5.8: Taxa observed by time-course experiments in the severe manhole (Sanger). Bar widths indicate percent relative abundance of microbial taxa in sample libraries; bar colors indicate taxa identity.

5.3.6. Comparison of Results from Illumina and Sanger Sequencing Platforms

The extremely low α-diversity in corrosion-associated microbial communities suggests that the Sanger sequencing method used here (about one-hundred 600 bp universal sequences per sample) may be as or more informative than the Illumina MiSeq sequencing method used (~5000 300bp bacterial sequences per sample); 100 sequences may be informative enough when there are less than ten taxa present, and non-bacterial players can be observed. While the examination of universal clones sequenced by Sanger technology illustrated a bacterial community similar to that observed from Illumina sequencing V1V2 amplicons, it also revealed archaeal and eukaryal community members.

5.4. Conclusions

This study comprises the largest cohort of longitudinal bacterial community observations reported in this type of environment to date. Significant decreases in bacterial community diversity were observed over time as community members shifted from neutrophilic to acidophilic sulfur oxidizing microbes. This trend is coincident with a drop in pore water pH, indicating that pH has a significant influence on microbial diversity.

The culture-based model hypothesized by Islander in 1991 included a succession from neutrophile *Halothiobacillus neapolitanus* to acidophile *Acidithiobacillus thiooxidans* (Islander et al., 1991). The results observed here differ only in the presence of diverse metabolic types at early stages and the emergence of *Ferroplasma* spp. in very late stage corrosion. This congruency is rare when comparing culture-based observations to those from molecular phylogeny-based, because the majority of environmental microorganisms have not been cultured (Amann et al., 1990; Hu et al., 2003). Molecular phylogeny-based studies in other engineering systems, including drinking water distribution systems and activated sludge, have recovered higher phylogenetic and metabolic diversity than was previously accounted for in culture-based studies (Jia et al., 1999; Rao et al., 2006; Reed et al., 1994). In addition, the diversity observed by 16S rRNA phylogeny in this study—less than ten taxa per sample—is among the lowest observed. This low diversity may explain why the microbial community could be relatively well described with culture-based observations.

The use of "next generation" sequencing technology enables the production of millions of base pairs sequence of data. However, the relatively short read lengths attainable (currently about 400 bp) limit the phylogenetic resolution that can be recovered from these data. In addition, there is not currently a vetted "universal" primer set that can be used to sequence all

three domains of life on Illumina platforms. As seen in this study, this bias toward "bacterial diversity" instead of "microbial diversity" can miss key community players. Culture-based studies and direct microscopy also suggest that fungi coexist in these sulfur-oxidizing biofilms at low pH (Cho et al., 1995; Gu et al., 1998).

Corrosion of wastewater infrastructure poses an imminent problem for our society. This study reports the largest number of longitudinal bacterial community observations reported in this type of environment and uses high-resolution and multi-domain sequencing technology to elucidate community composition. Generally, our findings support previous culture-based community succession models in concrete corrosion biofilms, with several notable exceptions, including the dominance of archaeon *Ferroplasma* spp. in late stage corrosion environments with high moisture. This contribution to the understanding of how these communities develop can help engineers assess risk factors and help scientists elucidate community dynamics in this extreme, low-diversity ecosystem.

6. Assessment of Remediation Strategies (Aim 3)

6.1. Introduction and Background

The third aim of this thesis is to develop and test a novel cement admixture formulation designed to inhibit the activity of sulfur-oxidizing biofilms and subsequent corrosion through pH-dependent release of metal ions on the micro-scales relevant to *in situ* bacterial activity. This formulation is expected to be competitive both functionally and economically with commercially available concrete coating treatments. While current coating technology can often protect concrete surfaces from biogenic acids, they do not inhibit microbial activity or associated acid production *in situ*. In some cases, corrosion can continue under the coatings when hydrogen sulfide diffuses through them, or acid leaks through gaps or perforations (Periasamy et al., 1994; Valix et al., 2010a; WERF, 2007). In addition, coating efficacy is highly dependent on the skills of the operators applying a coating. Several companies sell antimicrobial coatings or metal-based additives that can inhibit of corrosion-causing biofilms, but production remains relatively expensive in this market sector. This work aims to develop and test the efficacy of a low-cost, pH-responsive concrete formulation to inhibit corrosion-causing biofilms. This concept was then forwarded to field trials in the most corrosive locations identified in the regional survey. The use of carbon-based sorbent for pH-dependent release of metals to inhibit detrimental biofilms has not previously been applied.

In the context of treating waste streams with high metal loads, heavy metal sorption to activated carbon has been well studied and applied to practice (Kobya et al., 2005; Leyva-Ramos et al., 1997; Marzal et al., 1996; Selvi et al., 2001). The formulation tested here intentionally reverses this removal process in a controlled and targeted manner for the express purpose of inhibiting microbially induced corrosion. It can be manufactured sustainably using waste

materials and is expected to be several orders of magnitude less expensive than current rehabilitation products.

6.2. Experimental Design

In this research, powdered activated carbon (PAC) loaded with cadmium (Cd^{2+}) or chromate (CrO_4^{2-}) ions was tested for its ability to impair the growth of sulfur-oxidizing cultures in the laboratory. Additionally, granular activated carbon (GAC) loaded with the same metals was surface-applied to concrete and tested for corrosion prevention efficacy in two working sanitary manholes on the front range of Colorado. Treated specimens were compared to untreated specimens on the basis of mass loss, pH depression, and bacterial community characteristics as measured by V1V2 16S rRNA amplicon sequencing.

6.3. Results and Discussion

6.3.1. Metal Desorption Characteristics

The metal leaching behavior of the GAC impregnated with Cd^{2+} or CrO_4^{2-} ions was determined using phosphate or citrate buffer solutions according to Section 3.3.3. Cadmium desorption showed a strong pH dependency, with increasing desorption at pH values below 6 (Figure 6.1). This is consistent with previous studies that found cadmium and other metal cations sorbed to activated carbon most strongly at high pH (Kobya et al., 2005; Marzal et al., 1996; Reed et al., 1993). On the other hand, chromate anion appears to sorb strongly at pH above 7 and pH below 5. Previous studies have found that chromate anions have increased sorption to activated carbon at low pH (Kobya et al., 2005; Selvi et al., 2001).

The window from pH 5 to pH 7 is the ideal range for metal ion desorption to inhibit corrosion biofilms for several reasons: a.) at these pH values, corrosion is initiated but does not

progress at a rate which causes serious deterioration and b.) this is the range where diverse neutrophilic sulfur-oxidizing communities are replaced by low-diversity acidophilic communities. By delivering toxicity in the pH range where this transition between community types occurs, the metal-carbon formulations could prevent acidophile colonization. These results indicate that both cadmium cations and chromate anions desorb from pre-loaded granular activated carbon in a pH range that is germane to biofilm activity in corroding sewer infrastructure. Cadmium cation sorption is more ideal for this corrosion prevention application because metal remains in solution as corrosion progresses to pH values below 6. While chromate ions may resorb onto the carbon below pH 4 (Figure 6.1), this will not dampen their effectiveness in the target pH range of pH 5 to pH 7.

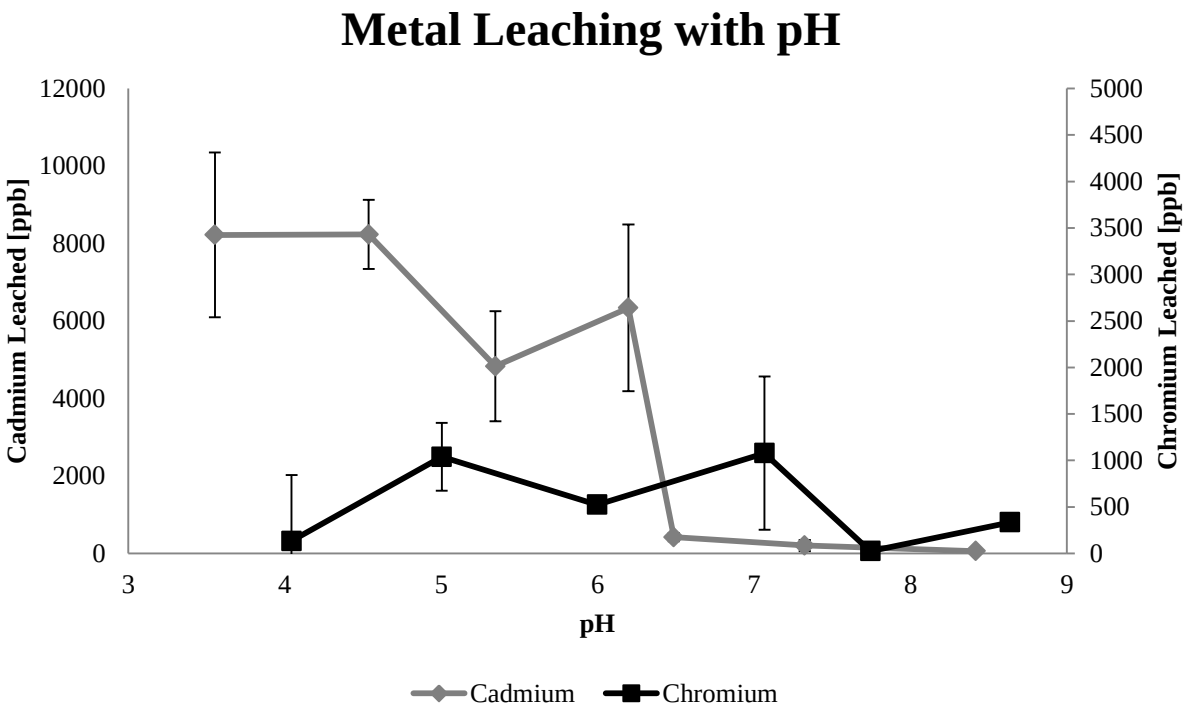

Figure 6.1: Metal leached from GAC pre-loaded with cadmium (♦) or chromate (■) ions in buffered solutions at various pH values. Phosphate or citrate buffering was used to stabilize pH. Points represent the mean of three observations. Error bars indicate standard deviation.

6.3.2. **Laboratory Testing of Growth Inhibition in Liquid Media**

Both liquid and solid media inhibition experiments were attempted with the goal of testing inhibition of sulfur-oxidizing bacterial growth in the presence of the metal-carbon formulations through a range of pH values relevant to the corrosion process. Cultures used in liquid testing are ATCC pure cultures of *Acidithiobacillus thiooxidans* (ATCC #19377) and *Thiobacillus thioparus* (ATCC #23646) and an enrichment culture from severely corroded concrete comprised of over 99% *Acidithiobacillus* spp. as judged by Illumina MiSeq bacterial V1V2 16S amplicon sequencing (methods in Section 3.2). Both of these genera have been previously implicated in the corrosion process and were observed at multiple sites in the regional corrosion survey discussed in Chapter 4 of this thesis.

Ultimately, liquid culture testing was not successful despite the application of a variety of growth media and experimental procedures. The liquid media tests may have been complicated by the following factors: a.) quantitation of growth by chemical assays could not be achieved, b.) released metals may have been complexed by salts in the growth media, and c.) solution pH was confounded by activated carbon buffering—which increased the pH over a span of weeks—and sulfur-oxidizing metabolic activity—which decreased the pH at varying rates.

Several methods for quantifying bacterial growth were tested. Optical density was not directly correlated to cell concentrations, because precipitates in the media were abundant and depended on pH. Redox-based growth indicators resazurin, CTC tetrazolium salt (5-cyano-2,3-ditolyl tetrazolium chloride), and INT tetrazolium salt (2-p-iodophenyl-3-p-nitrophenyl-5-phenyl tetrazolium chloride) were tested, but all these compounds were found to be inappropriately reactive to acidic pH as well as redox conditions, so they could not be used throughout the experimental targeted pH range. The phospholipid biomass assay described in Section 3.1.7 was

also tested for growth quantitation, but biomass differences in the range of growth examined could not be resolved. In addition, the phosphate concentration included in growth media for its buffering capacity caused interfering backgrounds in phospholipid assay blanks. Sulfur oxidizer growth was not directly related to optical density, so cell counting by epifluorescence microscopy was required to quantitate growth responses.

Water chemistry modeling with Visual MINTEQ suggested that salt concentrations in the sulfur-oxidizing ATCC 290 medium used likely complexed over 90% of cadmium and chromium (Gustafsson, 2011). To address this issue, the amount of metal-carbon formulation added to treated wells was increased by a factor of 10 in order to ensure toxic concentrations of free metal ions could be liberated into test-solutions under acidic conditions. However, this increase in activated carbon further exacerbated the pH instability of the cultures.

Table 6.1: Expected cadmium and chromium speciation in liquid media at pH 3 and pH 5. Total metal concentrations based on leaching experiments in media, metal speciation modeled with Visual MINTEQ software.

	pH3		pH5	
Cadmium Species	Concentration [mM]	Percent of Total Cd	Concentration [mM]	Percent of Total Cd
Cd^{+2}	**9.27E-06**	**0.0%**	**5.66E-06**	**0.0%**
$Cd(NH_3)_2^{+2}$	8.20E-13	0.0%	4.92E-09	0.0%
$Cd(NH_3)_3^{+2}$	2.84E-17	0.0%	1.68E-11	0.0%
$Cd(NH_3)_4^{+2}$	2.89E-22	0.0%	1.70E-14	0.0%
$Cd(OH)_{2\ (aq)}$	2.31E-19	0.0%	1.41E-15	0.0%
$Cd(OH)_3^-$	3.05E-29	0.0%	1.86E-23	0.0%
$Cd(OH)_4^{-2}$	4.78E-41	0.0%	2.91E-33	0.0%
$Cd(S_2O_3)_2^{-2}$	8.11E-01	91.1%	8.27E-01	93.0%
$Cd(S_2O_3)_3^{-4}$	1.15E-04	0.0%	1.52E-04	0.0%
$Cd(SO_4)_2^{-2}$	2.76E-07	0.0%	2.78E-07	0.0%
Cd_2OH^{+3}	1.84E-17	0.0%	6.85E-16	0.0%
$CdCl^+$	1.29E-04	0.0%	1.02E-04	0.0%
$CdCl_{2\ (aq)}$	8.84E-06	0.0%	9.09E-06	0.0%
$CdHPO_{4\ (aq)}$	3.41E-06	0.0%	8.62E-05	0.0%
$CdNH_3^{+2}$	5.19E-09	0.0%	3.14E-07	0.0%
$CdOH^+$	4.87E-12	0.0%	2.97E-10	0.0%
$CdS_2O_{3\ (aq)}$	7.90E-02	8.9%	6.24E-02	7.0%
$CdSO_{4\ (aq)}$	3.26E-05	0.0%	2.56E-05	0.0%
Total Cadmium	8.90E-01		8.90E-01	

	pH3		pH5	
Chromium Species	Concentration [mM]	Percent of Total Cr	Concentration [mM]	Percent of Total Cr
$Cr_2O_7^{-2}$	**4.56E-04**	**10.0%**	**3.91E-04**	**47.6%**
CrO_4^{-2}	**3.20E-07**	**0.0%**	**2.96E-05**	**3.6%**
CrO_3Cl^-	9.72E-07	0.0%	1.18E-08	0.0%
$CrO_3H_2PO_4^-$	3.12E-03	68.3%	1.23E-05	1.5%
$CrO_3HPO_4^{-2}$	9.85E-04	21.6%	3.89E-04	47.3%
$CrO_3SO_4^{-2}$	9.96E-07	0.0%	1.19E-08	0.0%
Total Chromium	4.56E-03		8.22E-04	

Controlling the pH of experimental cultures in the presence of metal-laden PAC was important to maintain a relatively stable environment for bacterial growth and to assess the potential effect of the toxicity of these formulations at different pH values. The powdered activated carbon used for this proof-of-concept study had a high buffering capacity, neutralizing

up to 3 moles of acid per kilogram carbon over the course of two weeks. While this characteristic is advantageous for treating corroding concrete, it impedes rigorous laboratory testing. As a result, culture solutions in wells treated with carbon experienced significant increases in pH that were rapidly initiated. To address this issue and help stabilize pH, acid was added every day during the course of 12-day enrichment experiments to maintain pH in targeted ranges. However, the resulting magnitude of daily pH fluctuations appeared to inhibit bacteria in experimental replicates both with and without metals, and reliable control conditions could not be established. In a series of parallel experiments, the carbon's expected acid adsorption capacity (3 moles acid/kg carbon) was added to un-innoculated wells and allowed to equilibrate for two weeks before starting the growth assay. This experiment was also unsuccessful.

The sulfur-oxidizing bacterial cultures used were selected as models for their role in concrete corrosion as a result of their biogenic acid production. These cultures produced acid both in liquid culture experiments, which further confounded pH stabilization. In some cases, the pH of treated cultures remained close to original values, while positive control cultures had a final pH values below 1 due to biogenic acid production. This pH change could not be accurately accounted for, because the degree of pH change directly depended on the amount of bacterial growth. Determining bacterial growth was the aim of this experiment, so the rate of growth and the associated rate of pH change were unknown.

6.3.3. **Laboratory Testing of Growth Inhibition in Solid Media**

Growth inhibition testing on solid culture media was also executed with an experimental design analogous to classical antibiotic resistance screening. These experiments were complicated by the difficulty of growing autotrophs on solid media and by the high sorption capacity of the carbon. Only one sulfur oxidizing culture (the *Acidithiobacillus* enrichment) was

successfully grown on solid media. Solid agar media is a relatively dry and oxidizing environment, and is less amenable to hosting these types of microbes than liquid media. Once this culture was successfully grown on solid agar media, experiments were further complicated by the propensity for activated carbon to sorb nutrients from the media. Inhibition zones were observed around both unloaded and metal-loaded carbon, indicating that the carbon sorption was inhibiting cell growth. Crystalline structures about 100 µm in length were observed on and around the carbon grains, and likely originated from salts removed from the growth medium (Figure 6.2). Further testing was subsequently abandoned.

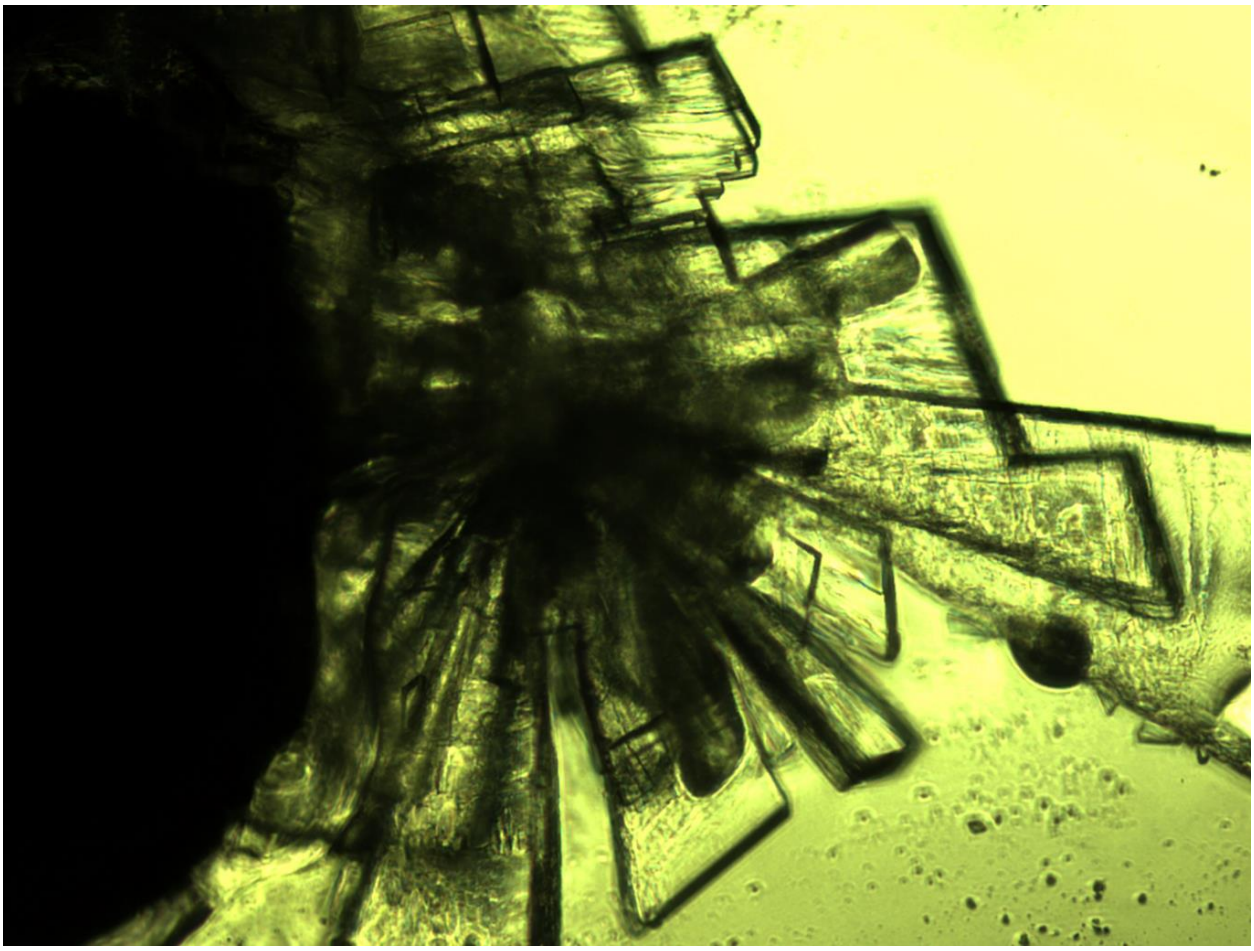

Figure 6.2: Crystalline structures observed on surface of granular activated carbon following contact with solid culture media, 1000X magnification

Table 6.2: Installation and sampling schedule for three field tests using treated and untreated samples (I indicates sample installation, X indicates specimen removal)

		2011			2012											
Experiment	Manhole	O	N	D	J	F	M	A	M	J	J	A	S	O	N	D
A	MH2 (Moderate)			I		X		X		X		X		X		X
B	MH1 (Severe)											I	X X	X	X X	X
C	MH1 (Severe)	I		X		X		X		X		X		X		

6.3.4. **Field Testing: Physical and Chemical Characteristics**

Under the most corrosive field conditions used in this study (MH1) (Experiments B and C), specimens treated with a surficial cement coating containing cadmium- or chromate-loaded granular activated carbon experienced significantly less corrosion as judged by surface area corrosion and dry mass loss when compared to untreated samples (ANCOVA $p < 0.005$) (Figure 6.4 and Figure 6.5). In MH2 (Experiment A), corrosion was less severe (<10% mass lost and <20% surface corrosion). When considering all data points, no significant differences in surface area corrosion or mass loss were observed between treated and untreated specimens in either manhole. However, treated specimens exposed for eight to twelve months in MH1 experienced less mass loss and surface corrosion than otherwise identical control specimens (Figure 6.4). After four months, treated specimens were characterized by red and black surface coloring (Figure 6.5). Some treated specimens experienced corrosion only where they touched the plastic sample holder casing (as in Figure 6.5, top right corner), which introduced and unfortunate experimental artifact. This corrosion was likely caused by sulfuric acid produced by bacteria growing on the casing surface that inadvertently dripped onto the specimen (see Section 3.5.4 for detailed discussion) (Figure 6.3). For this reason, it is expected that the corrosion prevention capacity of the treatment is underestimated by these results.

Some mildly-corroded specimens gained dry mass over the experiment. This is likely a result of biologically-produced sulfate being incorporated into minerals such as gypsum. The source of the sulfate is gaseous hydrogen sulfide and oxygen, which would not be part of the original specimen mass.

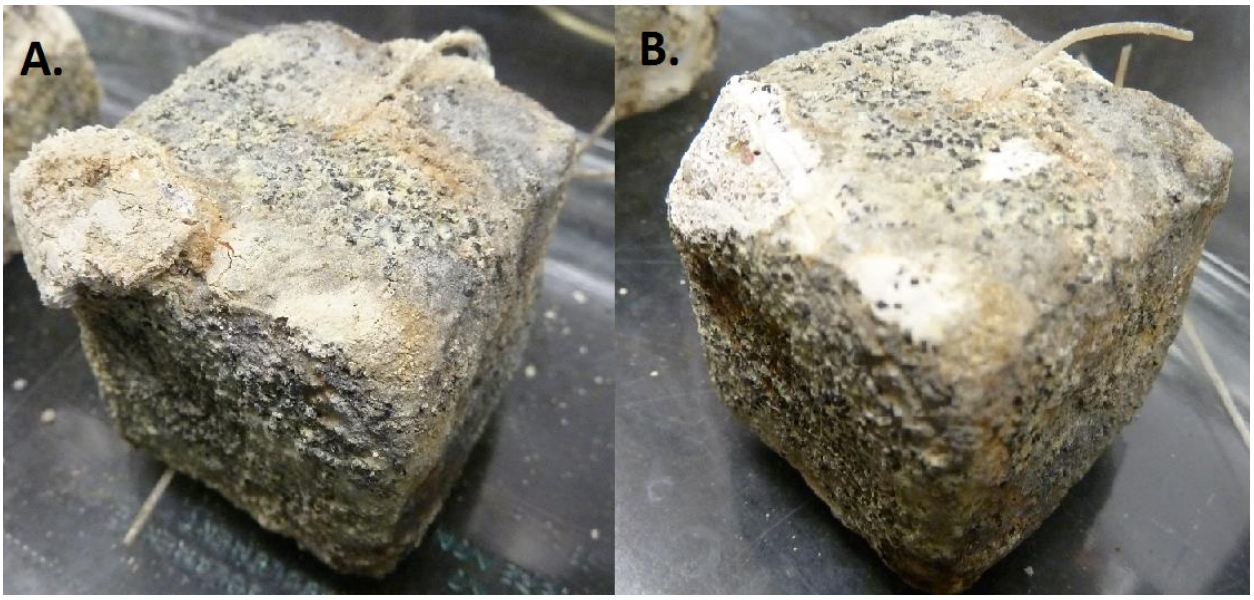

Figure 6.3: Example specimens treated with metal-GAC formulation that experienced corrosion only where surface directly contacted PVC casing (upper-left of cube). This cadmium-GAC treated specimen was exposed for ten months in MH1, and is shown before (A.) and after (B.) removal of corroded layer.

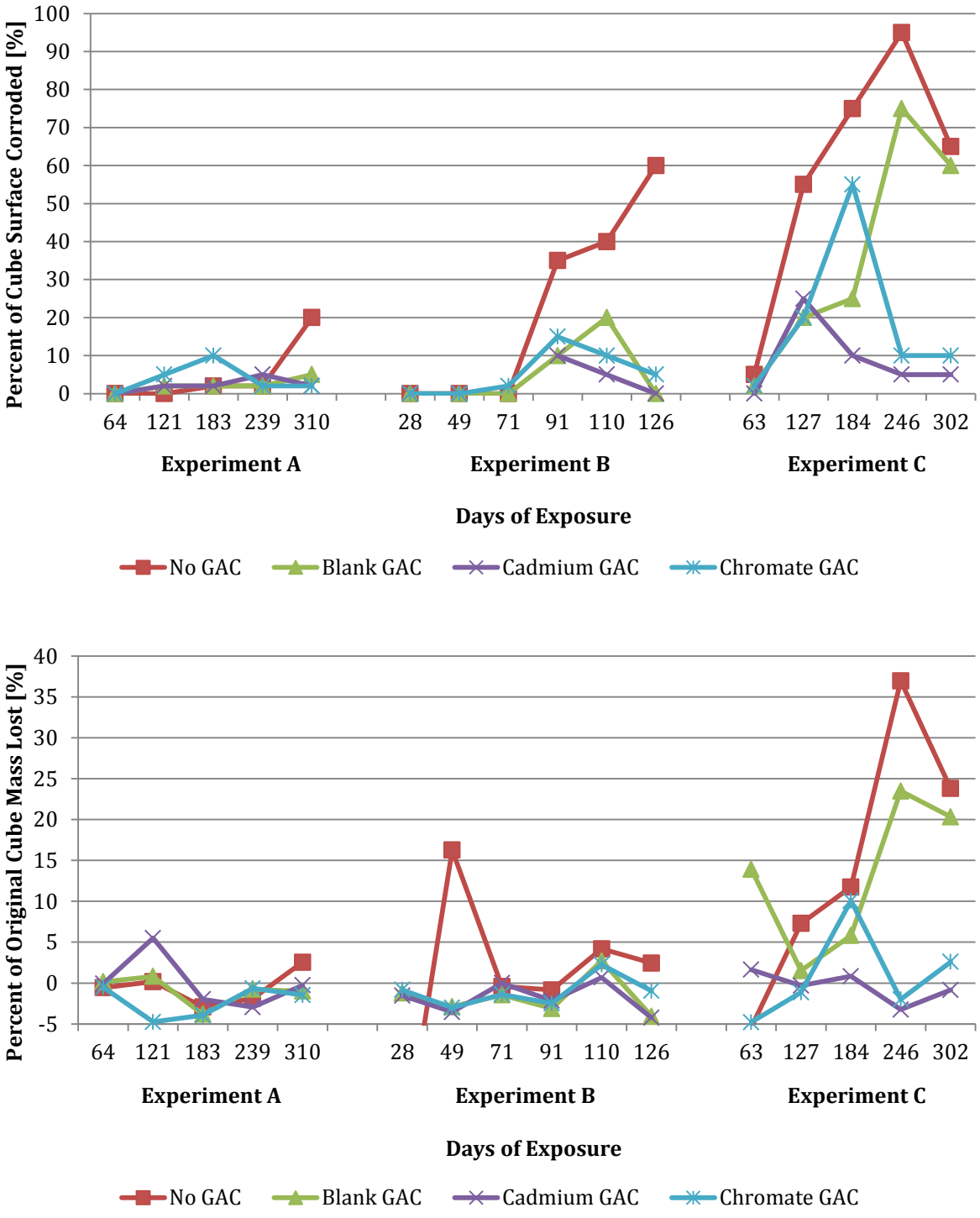

Figure 6.4: Comparison of percent of surface corroded and percent of original mass lost for untreated concrete specimens (red and green) and for specimens treated with a surficial application of a metal-carbon formulation (purple and blue). (■) No GAC control; (Δ) GAC without metal; (×) GAC impregnated with cadmium cations; (*) GAC impregnated with chromate anions.

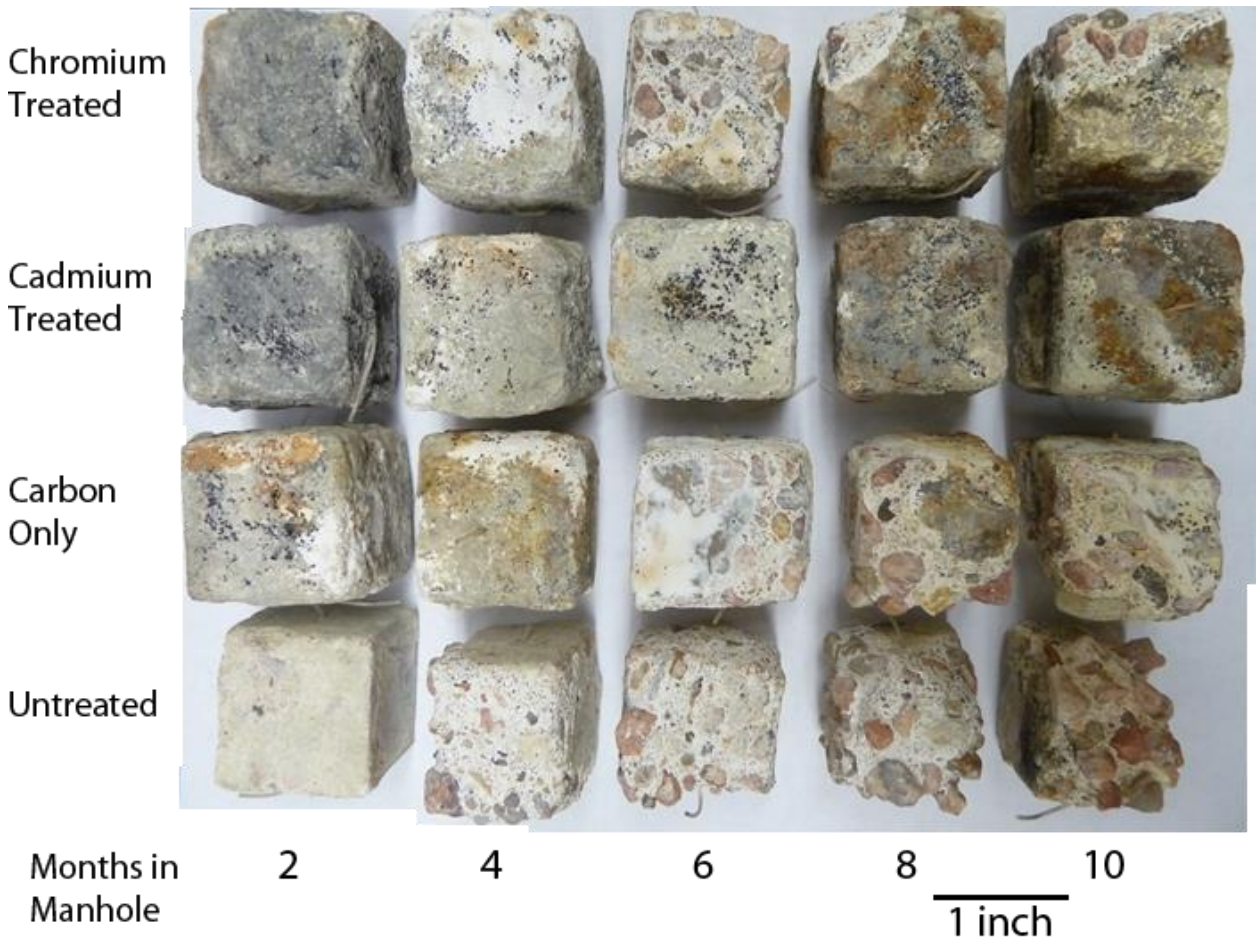

Figure 6.5: Concrete cubes following exposure in the MH1 (Experiment 3, H_2S concentrations >300 ppm) for two to ten months. Specimens were removed from the manhole and taken to the lab for analysis. Photograph shows specimens after corrosion product was removed and specimens were dried.

6.3.5. Field Testing: Cadmium and Chromium in Treated Samples

Cadmium and chromium were measured in dry sieved corrosion products for the treated samples in Experiment B, and are presented both as ng/g dry sieved fines as well as µM in pore water (Figure 6.6). These metals are typically present in Portland Cement at average concentrations of 0.34 ng/g Cd and 76 ng/g Cr (Lawrence, 1998). Generally, metals concentration observed in treated corroded concrete in this study were significantly higher than

expected background concentrations, indicating that the metal-carbon formulation successfully released metal ions at the corrosion front. Aside from one chromium outlier at 71 days, metal concentrations in the dry fine material after 50 days stayed relatively constant between 400 and 800 ng/g. This timing of metals release corresponds to a concomitant decrease in pore water pH for both cadmium- and chromate-treated specimens from pH 12 to pH 2 occuring between 49 and 71 days of field exposure.

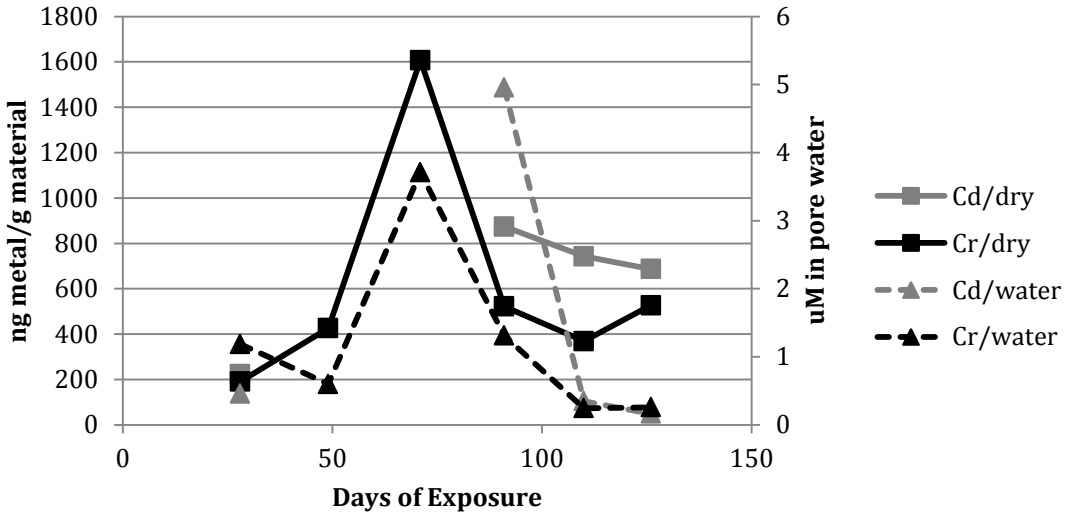

Figure 6.6: Cadmium (grey) and chromium (black) levels at concrete surface in dried, sieved corrosion product as ng metal/g (solid lines) and in pore water as µM (dashed lines) for 26-126 days of exposure in high H_2S atmosphere (Experiment 2). (■) Cadmium in dry fines; (■) chromium in dry fines; (◆) cadmium in pore water; (◆) chromium in pore water. Metal concentrations measured by inductively coupled plasma mass spectrometry (ICP-MS) of acid extracted samples.

Metal concentrations—micromolar levels of both cadmium and chomium—in pore water are also shown; these levels represent the concentrations which drive metal diffusion into bacterial cells on the corrosion front. Pore water concentrations increased to several µM after 70 days, and subsequently receded to less than 0.2 µM by the end of the experiment at 126 days

(Figure 6.6). This decrease in pore water concentrations is likely due to a marked increase in surface moisture as the experiment progressed (up to 23% moisture), which diluted the released metal ions. Cadmium and chromium at μM concentrations have been shown to inhibit bacteria involved in wastewater treatement under certain conditions (Bonnet et al., 1999; Mazierski, 1995; Tsai et al., 2005), and are about an order of magnitude higher than typical concentrations observed in municipal wastewater (Choubert et al., 2011; Jenkins et al., 1994). While many studies have shown acidiphilic sulfur oxidizing bacteria can be resistant to mM concentrations of metals in mining environments (Cabrera et al., 2005; Tyson et al., 2004; Watkin et al., 2009), the lack of selection pressure in wastewater systems and the location of corrosion on the sewer crown (away from wastewater flow) suggests that corrosion biofilms are unlikely to harbor or acquire metal resistance genes.

6.3.6. **Field Testing: Microbial Community Composition**

In all carbon treatments (Blank GAC, Cadmium GAC, and Chromate GAC) in the three respective longitudinal experiments, biofilm communities followed a trend of neutrophiles to acidophiles and high α-diversity to low α-diversity (often less than 50 taxa) (Figure 6.7). This trend matches community shifts observed on untreated concrete specimens in Chapter 5 of this thesis.

This community succession appears to occur more rapidly on chromate-treated samples than on untreated or cadmium-treated samples. The activated carbon used here presented a relatively high acid neutralization capacity as tested in the lab, so the blank carbon treatment had a buffering effect that likely slowed surface acidification. This may explain why the untreated carbon harbored neutrophiles longer than the chromate-treated carbon, as the chromate may have

been loaded onto surface sites that could otherwise be used to sorb H^+ ions and slow the pH drop.

The communities observed on all three types of GAC treatments were initially dominated by the bacterial family Halothiobacillaceae, a neutrophilic sulfur-oxidizing group that was observed in early-stage communities in Chapter 5 (Figure 6.7). On the blank and cadmium GAC treated specimens, *Brevundimonas* spp. sequences were detected during the intermediate corrosion stage in MH2. This genus includes heterotrophic opportunistic pathogen *Brevundimonas diminuta* (Ranganathan, 2000), and probably is involved in a neutrophilic, heterotrophic lifestyle using microbial by-products of sulfur-oxidizers as substrates.

After four months of exposure in MH1 or ten months of exposure in MH2, bacterial communities on both treated and untreated specimens contained over 80% *Acidithiobacillus* spp. sequences, as judged by V1V2 region Illumina sequencing. This taxa was also the dominant community members observed in late-stage corrosion in Chapter 5 and in severely corroded biofilms in Chapter 4. These microbes have been observed to thrive in metal-rich acid mine drainage environments (Toril-Gonzalez et al., 2003; Tyson et al., 2004), but cells present in the wastewater environment would not be expected to uptake or maintain heavy metals resistance genes, because municipal wastewater is regulated to very low levels of metals (parts per billion) (Choubert et al., 2011; Jenkins et al., 1994; USEPA, 1991).

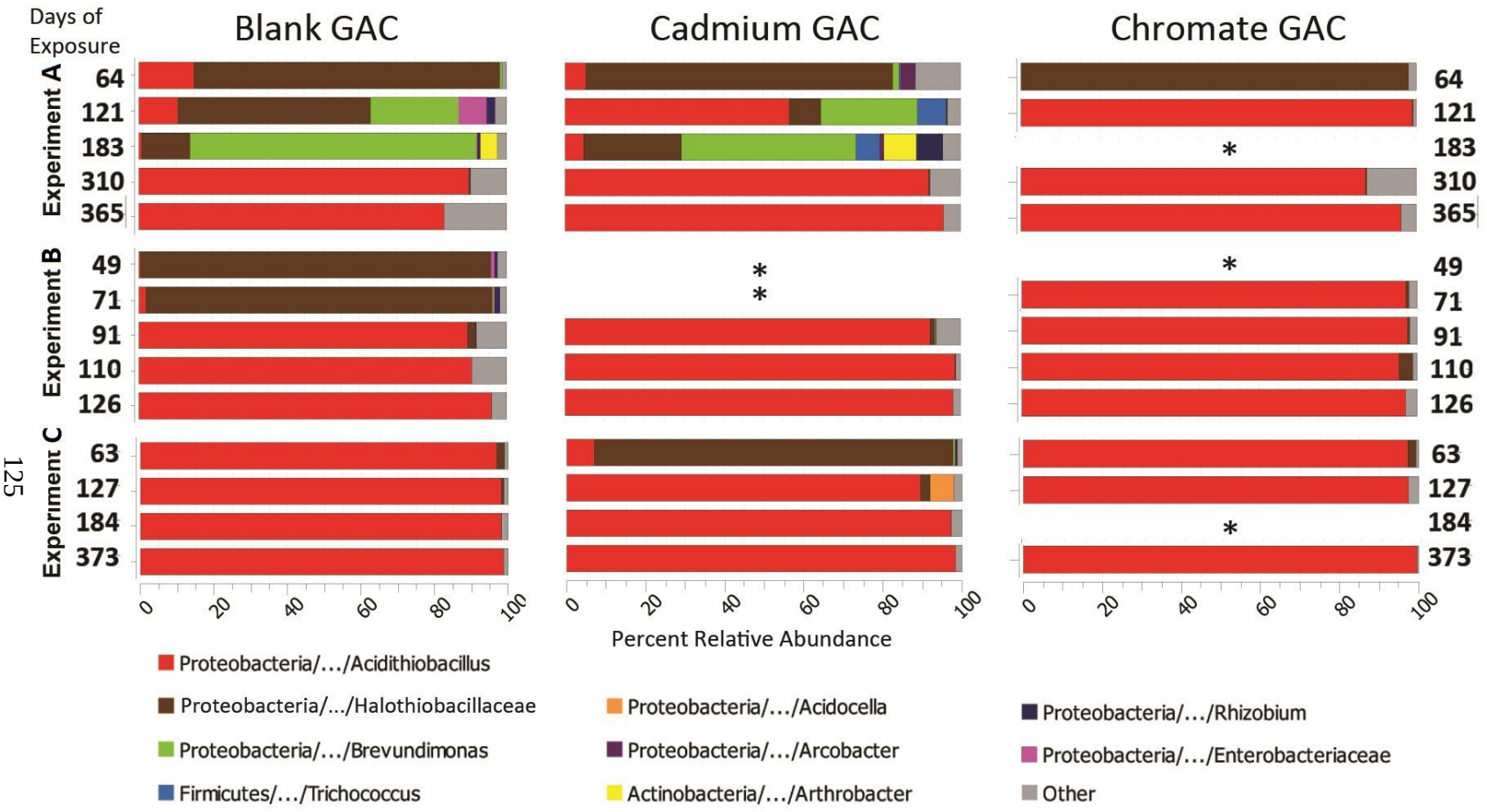

Figure 6.7: Bacterial community succession on otherwise identical specimens incorporating unloaded granular activated carbon (left) and granular activated carbon loaded with cadmium (center) and chromate (right) ions. Taxa definitions based on Illumina MiSeq sequencing of the V1V2 region of bacterial 16S rRNA genes and comparison to SILVA 115NR database. Bar widths indicate percent relative abundance of microbial taxa in sample libraries; bar colors indicate taxa identity. * indicates missing data due to low DNA recovery.

6.3.7. **Field Testing: Phospholipid Biomass Estimates**

Sample biomass was estimated by measuring lipid-associated phosphate as described in Section 3.1.7. As judged by phospholipids, the untreated samples and blank carbon-treated samples experienced similar trends of accumulating biomass (Figure 6.8). In the more severe MH1 (Experiments B and C), biomass increased on the untreated specimens more rapidly than on otherwise identical specimens with entrained metal-GAC formulation. Under more moderately corroding conditions (Experiment A in MH2), biomass appeared to decrease slightly between two months and eight months, and then increased at ten months. This may be due to a microbial selection response to pH as populations transition between neutrophilic and acidophilic regimes.

For the cadmium-treated carbon and chromate-treated carbon treated samples in MH1, biomass notably increased during the initial two months and stayed relatively for the duration of a year. Under highly corrosive conditions in MH1 (H_2S > 300 ppm), estimates of biomass accumulating on specimens which incorporated metal-GAC formulations were significantly lower than untreated concrete specimens (ANCOVA $p<0.01$), indicating that the treatment inhibited biofilm production. Under moderately corrosive conditions in MH2, metal-GAC treated specimens did not follow the same biomass accumulation trends. This may be because corrosion in this manhole did not progress to a phase where significant acidophilic populations developed in the observation period of one year.

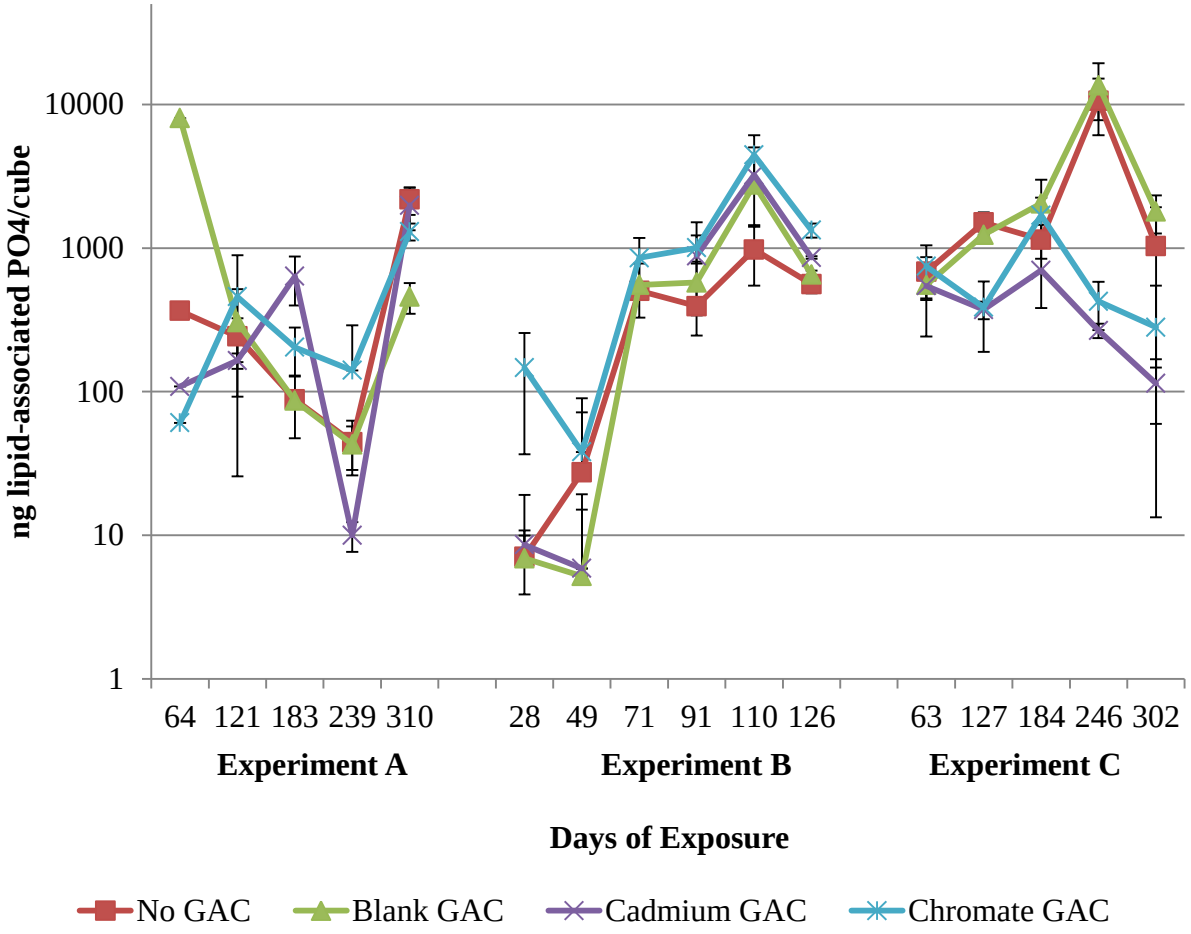

Figure 6.8: Lipid-associated phosphate per cube (indicator for biomass) for control concrete specimens (red and green) and concrete specimens treated with metal-carbon formulation (purple and blue) exposed for up to ten months in high H_2S sanitary manholes. (■) No GAC control; (Δ) GAC without metal; (×) GAC impregnated with cadmium cations; (⁎) GAC impregnated with chromate anions.

6.3.8. Field Testing: Electron Microscope Images of Corroding Concrete

Environmental scanning electron microscopy (ESEM) was used to characterize surface morphology of raw concrete that had not been exposed to a corrosive environment and the surfaces of untreated and metal-GAC treated samples that had been exposed to a high H_2S environment in MH1 for 110 days.

The raw (unexposed) concrete surface that was imaged was a cut face of the same type of concrete specimens that were exposed to corrosive environments in manholes. At a macro scale,

about 70% is cement binder and small aggregate, and about 30% is the cut face of large aggregate. On a small scale, the binder and small aggregate surface was characterized by smooth faces of aggregate and small cement binder crystals on the order of 1-5μm in size (Figure 6.9B). This is smaller than the 5-40μm calcium oxides crystals previously reported in Portland cement (Lawrence, 1998). The micrometer scale view of the cut aggregate surface showed smooth flat surfaces with angular breaks between them (Figure 6.9A). Elemental electron diffraction data indicates that this portion of the surface is composed of >90% silicon oxides. The surfaces with cement binder crystals is primarily composed of carbonates along with calcium, silicon, potassium, and aluminum, which is consistent with the composition of Portland cement (Lawrence, 1998).

The surface of exposed untreated concrete was typified by sharp blocky crystalline structures. About 40% of the surface had large crystals with greater than 10 μm long (Figure 6.9C), and the remaining surface had smaller crystals about 1-10 μm long (Figure 6.9D). The large crystals were comprised of only sulfur, while the smaller crystals also contained calcium and oxygen, indicating the possible presence of gypsum. This morphology is markedly different than that of unexposed concrete, and reflects the chemical changes associated with microbially induced corrosion and its byproducts.

The surface of exposed cadmium-treated concrete also had crystalline shapes, but the crystals were generally more rounded. The crystals were very tightly packed over about 30% of the surface (Figure 6.9E top left part). About 40% of the surface was characterized by a loosely-packed layer of these same crystals underlain by long, vertically-oriented crystals (Figure 6.9E bottom right part). Another 20% of the surface had rounded, pocked crystals 10-30 μm in diameter (Figure 6.9F), and 10% of the surface had round non-crystalline shapes 1-10 μm in

diameter (not shown). The surface morphology of the treated cube exposed to the high H_2S atmosphere is markedly different than that of the untreated, exposed sample. When considered in conjunction with the lower mass loss and surface area corrosion observed on treated specimens, this analysis indicate that the corrosion inhibition mechanism associated with the metal-carbon formulation affects the microscale crystal structure of the concrete surface.

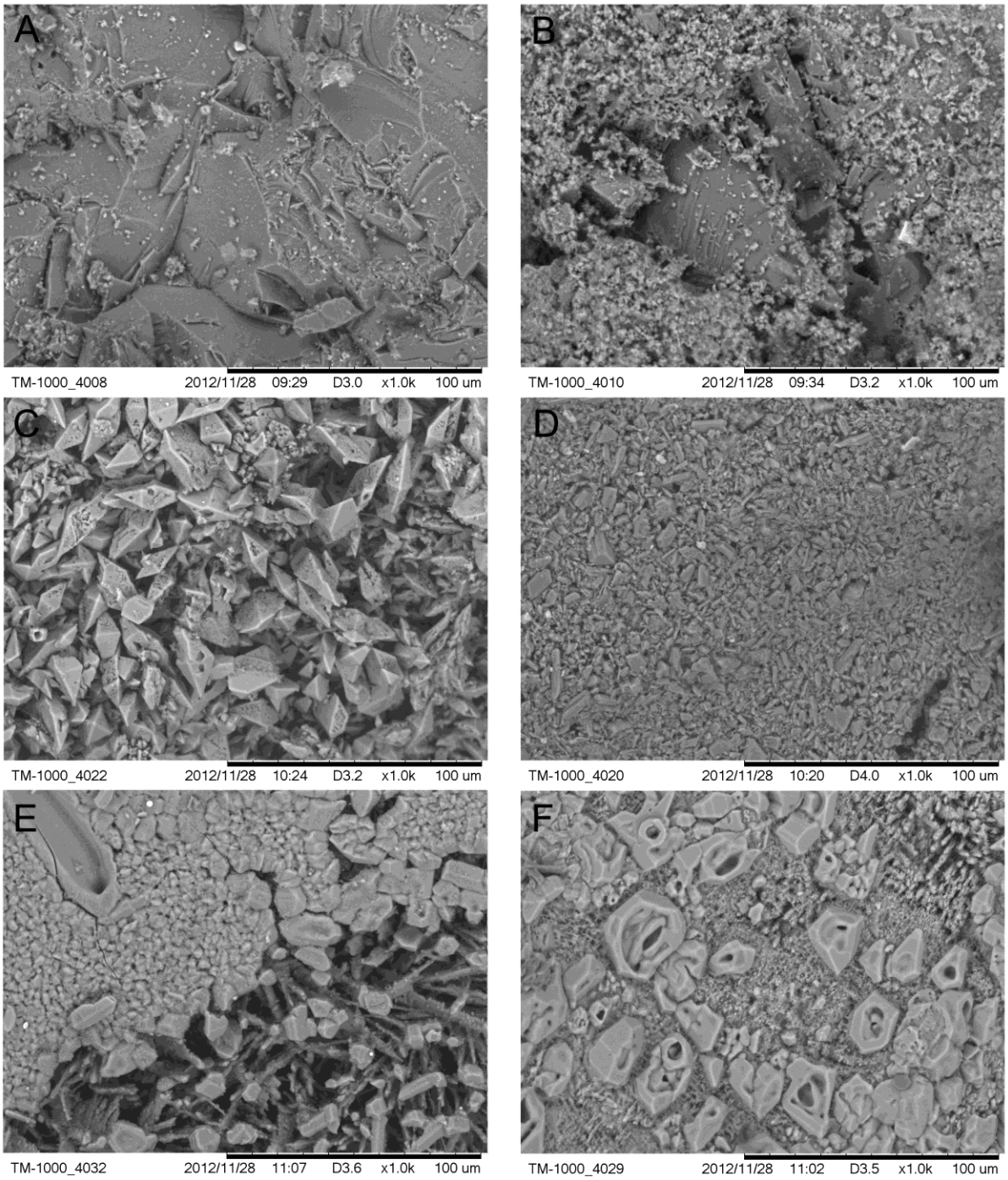

Figure 6.9: ESEM images of raw, control, and cadmium-treated concrete. A and B show raw concrete that has not been exposed to a corrosive environment, but is made with the same mix design as exposed samples. C and D show untreated corroded samples after 110 days of exposure. E and F show samples treated with cadmium-loaded activated carbon after 110 days of exposure. All images are at 1000x magnification.

6.4. Feasibility of Using Metal-Carbon Cement Formulation to Inhibit Corrosion

6.4.1. Technical Feasibility

Potential technical impediments to practical application of the formulation include the potential for biofilms to develop metals resistance and concern about the ultimate fate of released metals. The uptake of a "resistance gene" cassette has been observed to confer protection to relatively high (mM) concentrations of heavy metals under various environmental conditions (Cabrera et al., 2005; Tyson et al., 2004; Watkin et al., 2009). However, cells have energetic motivation to excise DNA that is not being used, so significant amounts of metal resistance genes are only expected in environments where (the targeted) metals exist under sustained conditions or have recently existed (Madigan et al., 2009; Oger et al., 2001; Sakamoto et al., 1989). While the use of surface-applied metal-carbon formulation may contribute to heavy metal selection pressure, the pH-dependent release of metal ions is expected to be intermittent in response to pH depression, and released metals will ultimately be removed from pore water to form precipitates with reduced sulfur species. As a result, the heavy metal selection pressure needed to acquire and maintain heavy metal resistance genes is likely to be absent or inconsistent at the pipe crown. In addition, the release of heavy metal from the activated carbon sorbent is expected to be localized on micrometer scales.

The only significant potential source of metals or metal resistance genes to the corroding concrete on unwetted sections of wastewater collection and treatment structures is the wastewater flow itself, which could reach the corrosion through splashing or aerosolization of bacterial cells. Because heavy metals are not able to enter a gaseous phase in sewers, they can only reach the corroding sections by aqueous transport. This may be a significant transport mechanism in wastewater collection systems with combined sewer overflows, as rain events may

cause pipes to flow full. However, in segregated wastewater collection systems, a full pipe is a poorly designed pipe, and the incidence of wastewater reaching the pipe crown is likely to be low. Based on average per capita residential discharge of cadmium and chromium to municipal wastewaters from a 1994 review (Jenkins et al., 1994), and using Boulder, Colorado's 20 MGD wastewater treatment facility serving 90,000 persons as an example, expected concentrations in municipal wastewater are on the order of 2 µg Cd/L (20 nM) and 9 µg Cr/L (180 nM). Another study in France (Choubert et al., 2011) found concentration to be less than 1 µg Cd/L and 5 µg Cr/L. These levels of cadmium and chromium in wastewater collection systems suggest that resistance to these metals should not be abundant. Further, the pH, alkalinity, and particle loads typical of raw sewage suggest that metals in these concentrations will be complexed, sorbed, or otherwise removed from the aqueous phase. In collection systems receiving large amounts of wastewater from metal-processing industries, these effluents exert a selection pressure that favors resistance and may contain transferrable heavy metals resistance genes (Madigan et al., 2009). However, the atmospheric barrier between the wastewater flow and the corroding pipe crown is likely to limit heavy metal selection pressure in corroding concrete, so resistance genes are unlikely to persist.

Another aspect of the tested metal-carbon formulation that concerns potential users is the ultimate fate of the heavy metals introduced to the wastewater collection system. However, the amounts of metal released by these metal-carbon formulations are relatively small and localized. For the treatment of one manhole, approximately 1 g of metal would be applied and released intermittently over a term of years in response to pH depression. Even if all of this metal is desorbed from the GAC and entered the wastewater flow in one day, a 20 MGD plant would see an increase of 50 ng/L metal in plant influent from a single manhole. Since typical levels of

metal in wastewater influents are 1-100 µg/L (Choubert et al., 2011; Jenkins et al., 1994), the metal released from the carbon would not significantly affect the plant's influent concentration. Also, the metal ions are strongly bound to the activated carbon and will only release in a localized corrosion front associated with low surface pH conditions in high H_2S headspaces. Any metal liberated would rapidly precipitate as a sulfide. These environments exist as a result of high sulfide concentrations in wastewater, so any metal entering the wastewater flow in these environments would form insoluble metal sulfides and be removed from the aqueous phase (USEPA, 1991). Regardless, as previously discussed, aqueous exchange between the corroding pipe crown and the wastewater flow is expected to be minimal, so the released metal ions are expected to ultimately precipitate as insoluble metal sulfides in the corrosion matrix.

6.4.2. **Economic Feasibility**

The metal-carbon formulations developed here can be manufactured at a low cost, because all of the required materials can obtained or produced from industrial or agricultural waste streams. Electroplating industries produce highly acidic wastewaters containing heavy metals of interest that is treated at high cost before being discharged to municipal sewers or waterways (USEPA, 1980, 1995). Metals from industrial plating waste streams contain large concentrations of metals, including cadmium, chromium, nickel and zinc. These waste streams are low pH and must be treated to stringent industrial waste standards before their disposal. These companies can redirect a portion of those wastes to activated carbon impregnation, creating a symbiotic relationship where they can spend less to manage metal wastes and the commercial sector can acquire metals for very low cost. Likewise, activated carbon for this application can be purchased at low cost from operations that produce it from agricultural by-products (Demiral et al., 2008; Fitzmorris et al., 2006; Kobya et al., 2005; Teker et al., 1998).

This makes the treatment both low-cost and sustainable. Preliminary cost estimates indicate that this formulation can be manufactured and sold at $25 per kilogram or per 10 cubic yards shotcrete, which is an order of magnitude less than the price of ConMicShield, a competing corrosion inhibition product.

6.5. Conclusions

This study demonstrated the effectiveness and feasibility of a corrosion-inhibiting, metal-carbon formulation that can be cost-effectively manufactured using recycled materials. Treated specimens in a severely corrosive environment experienced significantly less corrosion and presented different microscale surface morphology despite harboring similar microbial communities. Based on results from Chapter 4, which indicate that microbial communities associated with corrosion are similar on regional scales, similar corrosion-inhibition responses are expected regardless of locale. Additional results from Chapters 4 and 5 indicate that late-stage corrosion communities have very low α-diversity, which indicates that they are relatively susceptible to engineering controls, having the potential for less biological resilience than more diverse communities.

The potential for biofilms to develop heavy metal resistance and for these formulations to release metals to the wastewater flow are two potential flaws of this approach. However, the low concentrations of metals in municipal wastewater and the physical distance between the flow and the corrosion mean that heavy metals resistance genes are unlikely to be abundant or available to microbes in corroding concrete on sewer pipe crowns. In addition, the high solubility constants of metal sulfides mean that what metal might be released will not be bioavailable for activated sludge biofilms, and released metals will likely end up in wastewater biosolids at extremely low

concentrations. Any metals liberated in response to depressing pH in a corrosion front will likely be retained in the gypsum/ettringite corrosion matrix as insoluble metal sulfides.

Potential applications of the formulation include addition to concrete formulations, incorporation into non-cementitious concrete treatments, and addition to cementitious surficial treatments for the purpose of preventing corrosion in wastewater infrastructure, water infrastructure, petroleum infrastructure, hydraulic fracturing wells, and natural gas infrastructure—any environment where sulfur drives detrimental biofilm activity. In contrast to many widely used corrosion prevention strategies, this formulation directly targets the source of the problem—sulfur-oxidizing microbial metabolism. Whether applied proactively or retroactively to concrete in highly corrosive environments, this novel formulation has significant potential for enabling corrosion prevention around the world in a cost-effective manner.

7. Thesis Conclusions

7.1. Conclusions

The results presented here leveraged previous research and led to the following conclusions in the context of the research hypotheses tested.

AIM 1: GEOGRAPHIC SURVEY OF CONCRETE CORROSION CHARACTERISTICS.

a. Chemical, environmental, and hydraulic conditions are more strongly associated with corrosion severity and community structure than geography. Differences in community composition are influenced by gaseous concentrations of hydrogen sulfide, carbon dioxide, and methane.

b. Highly corroded sites as measured by concrete loss are characterized by low α-diversity, high moisture, high estimated biomass, and extremely low pH. Associated microbial communities will be dominated by sulfur-oxidizing genus *Acidithiobacillus*.

Conclusions: Two distinct community types observed coincided with moderate and severe corrosion, respectively. Highly corroded sites have very low α-diversity, typically less than five observed taxa, and are dominated by *Acidithiobacillus* spp., sometimes in conjunction with *Acidiphilium* spp. and *Mycobacterium* spp. These sites were characterized by high concentrations of both H_2S (>10 ppm) and CO_2 (>10,000 ppm), low pore water pH (<2), and high moisture content of corrosion products. In contrast, mild corrosion typically occurred in sites with lower levels of H_2S and CO_2 gas and supported a more diverse community that included heterotrophic and nitrogen-fixing genera. Methane concentrations were not observed to have an effect on either corrosion severity or microbial community composition. Based on

Sanger sequencing using universal primers, the community observed on an untreated specimen was markedly different than communities observed on specimens treated with commercial corrosion-prevention treatments. The untreated concrete hosted a community dominated by the archaeal genus *Ferroplasma*.

AIM 2: MICROBIAL COMMUNITY SUCCESSION

c. Corrosion associated communities follow a distinct succession of neutrophiles to acidophiles and decreasing α-diversity in response to decreasing pore water pH.

Conclusions: pH is the master environmental variable related to corrosion severity. Depressed pH occurs in response to biogenic sulfuric acid production associated with the metabolism of sulfur-oxidizing microbial communities. As corrosion progresses, the microbial community associated with a concrete surface changes from relatively diverse communities (α-diversity > 25 taxa) dominated by neutrophilic sulfur-oxidizing bacteria (primarily *Halothiobacillus* spp.) to low diversity communities (α-diversity < 5 taxa) dominated by acidophilic sulfur-oxidizing genus *Acidithiobacillus* spp. This trend was observed in two adjacent manhole environments with markedly different corrosion rates. In the first reported instance of archaea in a significant role in a corrosion environment, the iron-oxidizing archaea *Ferroplasma* spp. appear to dominate in some late-stage communities.

AIM 3: REMEDIATION STRATEGY DESIGN AND TESTING

d. Microbially induced concrete corrosion can be inhibited in the field by surface application of a metal-carbon formulation designed to release metal ions in response to

local-scale pH depression. Treated concrete coupons will experience less corrosion in the field than otherwise identical coupons as measured by mass loss, estimated biofilm biomass content, and pH drop.

e. The growth of both pure and enrichment sulfur-oxidizing cultures can be inhibited by selected metals liberated from activated carbon at low pH.

Conclusions: When alone in solution or entrained in cement, the metal-carbon formulation tested in this research releases metal ions in aqueous solutions when pH values drop below 5. These formulations are stable at neutral pH, where metals are strongly sorbed to carbon surfaces. When compared to otherwise identical untreated samples, concrete specimens treated with a surface application of metal- carbon modified cement experienced lower rates of surface corrosion and mass loss when exposed to corrosive field environments for up to a year. However, while treated concrete surfaces had lower estimated biomass than untreated surfaces, microbial community composition was similar between treated and untreated specimens. Preliminary laboratory culture work suggests that sulfur-oxidizing bacterial growth is inhibited by metal-carbon formulation, but extensive culture testing was unsuccessful.

7.2. Synthesis

The overarching purpose of this work was to contribute to knowledge regarding spatial and temporal variations in microbial communities responsible for concrete corrosion in wastewater collection and treatment systems. A significant contribution of this research is an improved model connecting the various environmental factors that are correlated to severe concrete corrosion. This includes, but is not limited to, the enrichment of H_2S and CO_2 in the headspaces of wastewater collection and treatment systems. Previous models generally do not consider CO_2 to be an accelerating factor. This environmental variable is likely a key consideration, since biogenic aced production in these environments is governed by autotrophic activity, which requires CO_2 as a carbon source.

The chemical, physical, and microbial properties of corroding concrete also change in response to environmental factors. Severe corrosion was found to result from a combination of several environmental factors, including H_2S and CO_2 concentrations and exposure time (i.e. age of the concrete pipe or manhole). These corrosion-inducing factors were correlated to severe corrosion in this thesis, as defined by pH, cement loss, moisture, and microbial community composition. Concrete dissolution presents failure risk, as the corrosion byproducts that replace cement binder are structurally unsupportive and can easily be removed from concrete surfaces through sloughing and erosion. "Exposure," as a conglomerate of time and gas concentrations, appeared to dictate corrosion rate and extent. Using this conglomerate exposure as the primary composite variable, Figure 7.1 summarizes the factors that promote corrosion juxtaposed with associated chemical, physical, and microbial parameters that drive the corrosion processes.

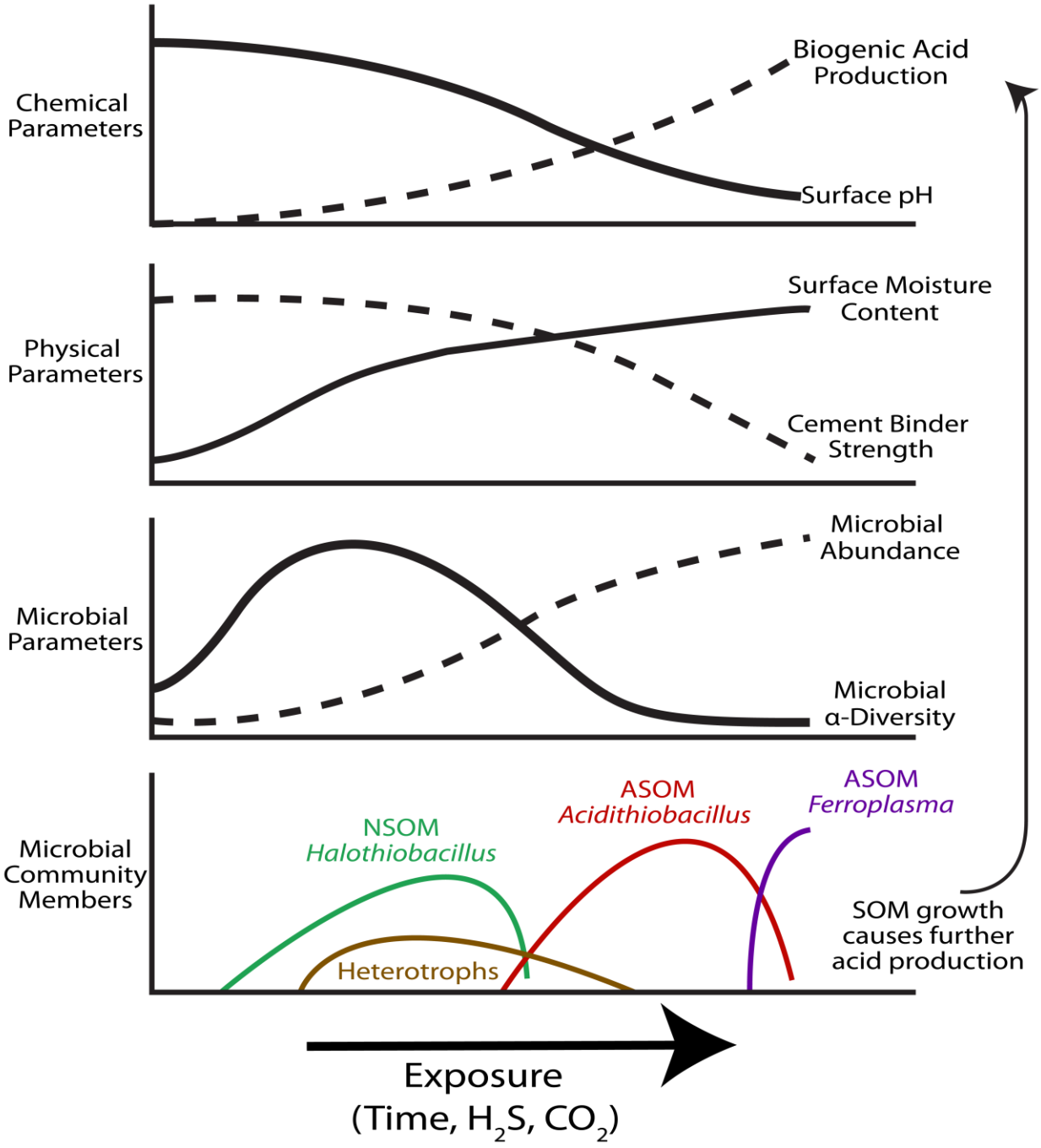

Figure 7.1: Juxtaposition of chemical, physical, and microbial changes associated with increased exposure (composite of time, H_2S, and CO_2) in microbially induced concrete corrosion

7.3. Applications to Engineering Practice

Culture-based models of the corrosion process have been generally accepted in the wastewater arena, but many inspectors and engineers remain unfamiliar with the role of microbes in exacerbating corrosion. This research outlines an improved model of corrosion processes through a better understanding of microbial communities driving them. The improved model could serve as a guide to corrosion processes to wastewater professionals.

The underlying corrosion mechanism suggested by these results is biogenic acid production by sulfur-oxidizing microbes. This acid then causes a series of chemical and physical changes that result in concrete deterioration. Treating massive amounts of wastewater to inhibit sulfide liberation in sewers is impractical and expensive, and surface treatments that do not inhibit acid generation are frequently ineffective. Design of corrosion prevention products can utilize the results of this thesis to focus on formulations that directly target the acidogenic microbial community. These low-diversity communities are expected to be especially susceptible to disruption by toxicity or environmental change.

The metal-carbon formulation tested here presents a low-cost corrosion inhibition approach with demonstrated success in corrosive field conditions. This formulation is expected to be several orders of magnitude cheaper than competing projects—about $25 to treat one cubic meter of cement. Similar formulations could be used in extremely corrosive environments in conjunction with an array of different concrete coatings to extend the life of pipe and other structures. Alternately, it could be applied on its own in mildly corrosive environments or on newly cured concrete pipe to provide low-cost corrosion prevention. A provisional United States patent that includes these innovations has been filed.

7.4. Future Recommendations

Microbially induced concrete corrosion is an expensive and widespread problem. The severity of this infrastructure epidemic continues to increase as wastewater collection systems around the world expand in age and size. Based on the findings of this thesis research, the following approaches are recommended for future study.

1.) As the chemical, physical, and biological drivers of corrosion continue to be studied in an academic context, open communication with the professional wastewater community and the corrosion protection industry should be maintained. This three-way dialogue will enable researchers to focus their work in areas of need and enable engineers and contractors to apply research findings to real corrosion prevention projects.

2.) From a scientific point of view, the concrete corrosion system studied here is a good model system for low-diversity environmental microbial communities and community succession in response to changing environmental conditions.

3.) Given the discrepancies observed between two different but widely accepted sequencing methodologies, a more thorough investigation of sequencing chemistry and data analysis should be conducted. The development of new sequencing platforms, reaction chemistry, and data analysis software may be outpacing the ability of scientists to understand the methods used to product their data. Most notably in this context, the role of archaea should be further investigated.

8. References

AEsoy, A., Osterhus, S. W., & Bentzen, G. (2002). Controlled treatment with nitrate in sewers to prevent corrosion. *Water Science and Technology: Water Supply, 2*(4), 137-144.

Allen, L. A. (1949). The effect of nitro-compounds and some other substances on production of hydrogen-sulphide by sulphate-reducting bacteria in sewage. *Proceedings of the Society of Applield Bacteriology, 2*, 26-38.

Amann, R., Krumholz, L., & Stahl, D. (1990). Fluorescent-oligonucleotide probing of whole cells for determinative, phylogenetic, and environmental studies in microbiology. *Journal of Bacteriology, 172*(2), 762-770.

ASCE. (2013). *2013 Report Card for America's Infrastructure*. <http://www.infrastructurereportcard.org/>: American Society of Civil Engineers.

Ayoub, G., Azar, N., Fadel, M., & Hamad, B. (2004). Assessment of hydrogen sulphide corrosion of cementitious sewer pipes: a case study. *Urban Water J., 1*(1), 39-53.

Babich, H., & Stotzky, G. (1980). Environmental factors that influence the toxicity of heavy metal and gaseous pollutants to microorganisms. *Critical Reviews in Microbiology, 8*(2), 99-145.

Baker, B. J., & Banfield, J. F. (2006). Microbial communities in acid mine drainage. *FEMS Microbiol. Ecol., 44*(2), 139-152.

Baker, G. C., Smith, J. J., & Cowan, D. A. (2003). Review and re-analysis of domain-specific 16S primers. *Journal of Microbiological Methods, 55*(3), 541-555.

Benner, S. G., Blowes, D. W., Ptacek, C. J., & Mayer, K. U. (2002). Rates of sulfate reduction and metal sulfide precipitation in a permeable reactive barrier. *Applied Geochemistry, 17*(3), 301-320.

Berndt, M. L. (2011). Evaluation of coatings, mortars and mix design for protection of concrete against sulphur oxidising bacteria. *Construction and Building Materials, 25*(10), 3893-3902.

Bhattacharyya, D., Jumawan, A. B., & Grieves, R. B. (1979). Separation of toxic heavy metals by sulfide precipitation. *Separation Science and Technology, 14*(5), 441-452.

Bielefeldt, A., Gutierrez-Padilla, M., Ovtchinnikov, S., Silverstein, J., & Hernandez, M. (2009). Bacterial kinetics of sulfur oxidizing bacteria and their biodeterioration rates of concrete sewer pipe samples. *J. Environ. Eng. , 136*(7), 731-738.

Bligh, E. G., & Dyer, W. J. (1959). A rapid method of total lipid extraction and purification. *Canadian Journal of Biochemistry and Physiology, 37*(8), 911-917.

Bond, P. L., Druschel, G. K., & Banfield, J. F. (2000). Comparison of Acid Mine Drainage Microbial Communities in Physically and Geochemically Distinct Ecosystems. *Applied and Environmental Microbiology, 66*(11), 4962-4971.

Bonnet, J. L., Bohatier, J., & Pépin, D. (1999). Effects of cadmium on the performance and microbiology of laboratory-scale lagoons treating domestic sewage. *Chemosphere, 38*(13), 3155-3168.

Borichewski, R. M. (1967). Keto acids as growth-limiting factors in autotrophic growth of *Thiobacillus thiooxidans*. *Journal of Bacteriology, 93*(2), 597-599.

Bowker, R. P. G., Smith, J. M., & Webster, N. A. (1989). *Odor and Corrosion Control in Sanitary Sewerage Systems and Treatment Plants*. Washington, DC: Hemisphere Publishing.

Braak, C. J. F. T. (1986). Canonical correspondence analysis: a new eigenvector technique for multivariate direct gradient analysis. *Ecology, 67*(5), 1167-1179.

Briones, A., & Raskin, L. (2003). Diversity and dynamics of microbial communities in engineered environments and their implications for process stability. *Current Opinion in Biotechnology, 14*(3), 270-276.

Cabrera, G., Gómez, J. M., & Cantero, D. (2005). Kinetic study of ferrous sulphate oxidation of Acidithiobacillus ferrooxidans in the presence of heavy metal ions. *Enzyme and Microbial Technology, 36*(2–3), 301-306.

Cadena, F., & Peters, R. W. (1988). Evaluation of chemical oxidizers for hydrogen sulfide control. *Journal of the Water Pollution Control Federation, 60*(7), 1259-1263.

Carpenter, R. (2009). 12th annual municipal survey. *Underground Constr., 64*(2).

Cayford, B., Dennis, P., Keller, J., Tyson, G., & Bond, P. (2012). High-throughput amplicon sequencing reveals distinct communities within a corroding concrete sewer system. *Appl. Env. Microbiol., 78*, 7160-7162.

Cayford, B. I. (2013). *Investigation of the microbial community and process responsible for the corrosion of concrete in sewer systems.* PhD Thesis, University of Queensland.

Cayford, B. I., Bond, P. L., Keller, J., & Tyson, G. W. (2010). *Microbial community composition of sulfide oxidising biofilms responsible for sewer corrosion*. Paper presented at the International Society for Microbial Ecology, Seattle, WA.

CBO. (2002). *Future investment in drinking water and wastewater infrastructure*. Congressional Budget Office <http://www.cbo.gov/sites/default/files/cbofiles/ftpdocs/39xx/doc3983/11-18-watersystems.pdf>.

Chang, Z.-T., Song, X.-J., Munn, R., & Marosszeky, M. (2005). Using limestone aggregates and different cements for enhancing resistance of concrete to sulphuric acid attack. *Cement Concrete Res., 35*(8), 1486-1494.

Chaussadent, T., Marceau, S., Lespinasse, F., & Tchetgnia-Ngassam, I. (2012). Physico-chemical properties and durability of polymer modified repair materials *Concrete Repair, Rehabilitation and Retrofitting III* (pp. 916-921). London, United Kingdom: CRC Press.

Cho, K. S., & Mori, T. (1995). A newly isolated fungus participates in the corrosion of concrete sewer pipes. *Water Science and Technology, 31*(7), 263-271.

Choubert, J. M., Pomies, M., Ruel, S. M., & Coquery, M. (2011). Influent concentrations and removal performances of metals through municipal wastewater treatment processes. *Water Science and Technology, 63*(9), 1967-1973.

Chow, G. C. (1960). Tests of equality between sets of coefficients in two linear regressions. *Econometrica, 28*(3), 591-605.

Churchill, P., & Elmer, D. (1999). Hydrogen sulfide odor control in wastewater collection systems. *NEWEA Journal, 33*(1), 57-63.

Coman, C., Drugă, B., Hegedus, A., Sicora, C., & Dragoş, N. (2013). Archaeal and bacterial diversity in two hot spring microbial mats from a geothermal region in Romania. *Extremophiles, 17*(3), 523-534.

Congress, n. U. S. Federal Water Pollution Control Act Amendments of 1972 (1972).

ConMicShield. (2011). Anti-microbial additive provides corrosion protection for concrete in Canadian wastewater systems. *Concrete Plant International, April 2, 2011*.

CSDLAC. (1988). *Internal Monthly Reports*. County Sanitation District of Los Angeles County.

Davis, J. L., Nica, D., Shields, K., & Roberts, D. J. (1998). Analysis of concrete from corroded sewer pipe. *Int. Biodeter. Biodeg., 42*(1), 75-84.

De Munyck, W., De Belie, N., & Verstraete, W. (2010). Antimicrobial mortar surfaces for the improvement of hygeine conditions. *Journal of Applied Microbiology, 108*(1), 62-72.

De Muynck, W., De Belie, N., & Verstraete, W. (2009). Effectiveness of admixtures, surface treatments and antimicrobial compounds against biogenic sulfuric acid corrosion of concrete. *Cement Concrete Comp., 31*(3), 163-170.

Demiral, H., Demiral, İ., Tümsek, F., & Karabacakoğlu, B. (2008). Adsorption of chromium(VI) from aqueous solution by activated carbon derived from olive bagasse and applicability of different adsorption models. *Chemical Engineering Journal, 144*(2), 188-196.

Dojka, M. A., Hugenholtz, P., Haack, S. K., & Pace, N. R. (1998). Microbial diversity in a hydrocarbon- and chlorinated-solvent-contaminated aquifer undergoing intrinsic bioremediation. *Appl. Env. Microbiol., 64*(10), 3869-3877.

Dopson, M., Baker-Austin, C., Hind, A., Bowman, J. P., & Bond, P. L. (2004). Characterization of *Ferroplasma* isolates and *Ferroplasma acidarmanus* sp. nov., extreme acidophiles from acid mine drainage and industrial bioleaching environments. *Applied and Environmental Microbiology, 70*(4), 2079-2088.

Dopson, M., Baker-Austin, C., Koppineedi, P. R., & Bond, P. L. (2003). Growth in sulfidic mineral environments: metal resistance mechanisms in acidophilic micro-organisms. *Microbiology, 149*, 1959-1970.

Edgar, R. C., Haas, B. J., Clemente, J. C., Quince, C., & Knight, R. (2011). UCHIME improves sensitivity and speed of chimera detection. *Bioinformatics, 27*(16), 2194-2200.

Edwards, M., Courtney, B., Heppler, P. S., & Hernandez, M. (1997). Beneficial discharge of iron coagulation sludge to sewers. *Journal of Environmental Engineering - ASCE, 123*(10), 1027-1032.

Ewing, B., & Green, P. (1998a). Base-calling of automated sequencer traces using phred. II. Error probabilities. *Genome Res., 8*(3), 186-194.

Ewing, B., Hillier, L., Wendl, M. C., & Green, P. (1998b). Base-calling of automated sequencer traces using phred. I. Accuracy assessment *Genome Research, 8*(3), 175-185.

Fang, H. H. P., Xu, L. C., & Chan, K. Y. (2002). Effects of toxic metals and chemicals on biofilm and biocorrosion. *Water Research, 36*(19), 4709-4716.

Farrell, R. F., Matthes, S. A., & Mackie, A. J. (1980). A simple low-cost method for the dissolution of metal and mineral samples in plastic pressure vessels. *Report of Investigations - Bureau of Mines, 8480*.

Feinstein, L. M., Sul, W. J., & Blackwood, C. B. (2009). Assessment of bias associated with incomplete extraction of microbial DNA from soil. *Applied and Environmental Microbiology, 75*(16), 5428-5433.

Ferrer, M., Golyshina, O. V., Beloqui, A., Golyshin, P. N., & Timmis, K. N. (2007). The cellular machinery of *Ferroplasma acidiphilum* is iron-protein-dominated. *Nature, 445*(7123), 91-94.

Fierer, N., & Lennon, J. T. (2011). The generation and maintenance of diversity in microbial communities. *American Journal of Botany, 98*(3), 439-448.

Findlay, R., King, G., & Watling, L. (1989). Efficacy of phospholipid analysis in determining microbial biomass in sediments. *Applied and Environmental Microbiology, 55*(11), 2888-2893.

Fitzmorris, K. B., Lima, I. M., Marshall, W. E., & Reimers, R. S. (2006). Anion or cation leaching or desorption from activated carbons from municipal sludge and poultry manure as affected by pH. *Water Environment Research, 78*(12), 2324-2329.

Frank, D. N. (2009). BARCRAWL and BARTAB: software tools for the design and implementation of barcoded primers for highly multiplexed DNA sequencing. *BMC Bioinformatics, 10*, 362.

Frank, D. N., Feazel, L. M., Bessesen, M. T., Price, C. S., Janoff, E. N., & Pace, N. R. (2010). The human nasal microbiota and *Staphylococcus aureus* carriage. *PLoS ONE, 5*(e10598).

Friedrich, C. G., Bardischewsky, F., Rother, D., Quentmeier, A., & Fischer, J. (2005). Prokaryotic sulfur oxidation. *Current Opinion in Microbiology, 8*(3), 253-259.

Gadd, G., & Griffiths, A. (1978). Microorganisms and heavy metal toxicity. *Microbial Ecology, 4*, 303-317.

Ganigue, R., Gutierrez, O., Rootsey, R., & Yuan, Z. (2011). Chemical dosing for sulfide control in Australia: An industry survey. *Water Research, 45*(19), 6564-6574.

García-Berthou, E. (2001). On the misuse of residuals in ecology: testing regression residuals vs. the analysis of covariance. *Journal of Animal Ecology, 70*(4), 708-711.

Gehrke, T., Hallmann, R., Kinzler, K., & Sand, W. (2001). The EPS of *Acidithiobacillus ferrooxidans*--a model for structure-function relationships of attached bacteria and their physiology. *Water Science and Technology, 43*(6), 159-167.

Gehrke, T., Telegdi, J., Thierry, D., & Sand, W. (1998). Importance of extracellular polymeric substances from *Thiobacillus ferrooxidans* for bioleaching. *Applied and Environmental Microbiology, 64*(7), 2743-2747.

Girvan, M. S., Campbell, C. D., Killham, K., Prosser, J. I., & Glover, L. A. (2005). Bacterial diversity promotes community stability and functional resilience after perturbation. *Environmental Microbiology, 7*(3), 301-313.

Gomez-Alvarez, V., Revetta, R. P., & Santo Domingo, J. W. (2012). Metagenome analyses of corroded concrete wastewater pipe biofilms reveal a complex microbial system. *BMC Microbiol., 12*, 122-136.

González, D., Lara, R., Alvarado, K., Valdez-Pérez, D., Navarro-Contreras, H., Cruz, R., & García-Meza, J. (2012). Evolution of biofilms during the colonization process of pyrite by *Acidithiobacillus thiooxidans*. *Applied Microbiology and Biotechnology, 93*(2), 763-775.

Gordon, D., Abajian, C., & Green, P. (1998). Consed: a graphical tool for sequence finishing. *Genome Res., 8*(3), 195-202.

Gu, J. D., Ford, T. E., Berke, N. S., & Mitchell, R. (1998). Biodeterioration of concrete by the fungus *Fusarium*. *International Biodeterioration and Biodegradation, 41*(2), 101-109.

Guisasola, A., De Haas, D., Keller, J., & Yuan, Z. G. (2008). Methane formation in sewer systems. *Water Res., 42*(6-7), 1421-1430.

Gustafsson, J. P. (2011). Visual MINTEQ Version 3.0. <http://www.minteq.com>

Gutierrez, O., Mohanakrishnan, J., Sharma, K. R., Meyer, R. L., Keller, J., & Yuan, Z. (2008). Evaluation of oxygen injection as a means of controlling sulfide production in a sewer system. *Water Research, 42*(17), 4549-4561.

Haile, T., & Nakhla, G. (2008). A Novel Zeolite Coating for Protection of Concrete Sewers from Biological Sulfuric Acid Attack. *Geomicrobiology Journal, 25*(6), 322-331.

Haile, T., & Nakhla, G. (2010). The inhibitory effect of antimicrobial zeolite on the biofilm of Acidithiobacillus thiooxidans. *Biodegradation, 21*(1), 123-134.

Hamady, M., Walker, J., Harris, J., Gold, N., & Knight, R. (2008). Error-correcting barcoded primers for pyrosequencing hundreds of samples in multiplex. *Nature Methods, 5*(3), 235-237.

Hamdaoui, O., Djeribi, R., & Naffrechoux, E. (2005). Desorption of metal ions from activated carbon in the presence of ultrasound. *Industrial and Engineering Chemistry Research, 44*, 4737-4744.

Hara, N., Alkanani, A. K., Ir, D., Robertson, C. E., Wagner, B. D., Frank, D. N., & Zipris, D. (2012). Prevention of Virus-Induced Type 1 Diabetes with Antibiotic Therapy. *Journal of Immunology, 189*(8), 3805-3814.

Harrison, A. P. (1984). The acidophilic thiobacilli and other acidophilic bacteria that share their habitat. *Annu. Rev. Microbiol., 38*(1), 265-292.

Hewayde, E. H., Nakhla, G. F., Allouche, E. N., & Mohan, P. K. (2007a). Beneficial impact of coatings on biological generation of sulfide in concrete sewer pipes. *Structure and Infrastructure Engineering, 3*(3), 267-277.

Hewayde, E. H., Nehdi, M., Allouche, E. N., & Nakhla, G. F. (2007b). Effect of mixture design parameters and wetting-drying cycles on resistance of concrete to sulfuric acid attack. *J. Mater. Civil Eng., 19*(2), 155-163.

Holt, S. (2008). Thiobacillus and microbial induced corrosion. *CoatingsPro Magazine*.

Hu, Z., Lei, L., Li, Y., & Ni, Y. (2003). Chromium adsorption on high-performance activated carbons from aqueous solution. *Separation and Purification Technology, 31*(1), 13-18.

Huang, X., Chen, Y., & Chenker, M. (2007). Solid phosphorus phase in aluminum- and iron-treated biosolids. *Journal of Environmental Quality, 36*(2), 549-556.

Hudon, E., Mizra, S., & Frigon, D. (2011). Biodeterioration of concrete sewer pipes: state of the art research needs. *J. Pipeline Syst. Eng. Practice, 2*(2), 42-52.

Hughes, J., Hellmann, J., Ricketts, T., & Bohannan, B. (2001). Counting the uncountable: statistical approaches to estimating microbial diversity. *Appl. Env. Microbiol., 67*(10), 4399-4406.

Hvitved-Jacobsen, T. (2002). *Sewer Processes: Microbial and Chemical Process Engineering of Sewer Networks*. Boca Raton, FL: CRC Press.

Islander, R., Devinny, J., Mansfeld, F., Postyn, A., & Hong, S. (1991). Microbial ecology of crown corrosion in sewers. *J. Environ. Eng. , 117*(6), 751-770.

Ismail, N., Nonaka, T., Noda, S., & Mori, T. (1993). Effect of carbonation on microbial corrosion of concretes. *J. Constr. Eng. M., 474*(20), 133-138.

Jenkins, D., & Russell, L. L. (1994). Heavy metals contribution of household washing products to municipal wastewater. *Water Environment Research, 66*(6), 805-813.

Jensen, H. S., Nielsen, A. H., Hvitved-Jacobsen, T., & Vollertsen, J. (2008). Survival of hydrogen sulfide oxidizing bacteria on corroded concrete surfaces of sewer systems. *Water Science and Technology, 57*(11), 1721-1726.

Jensen, H. S., Nielsen, A. H., Hvitved-Jacobsen, T., & Vollertsen, J. (2009). Modeling of hydrogen sulfide oxidation in concrete corrosion products from sewer pipes. *Water Environment Research, 81*(4), 365-373.

Jia, Y. F., & Thomas, K. M. (1999). Adsorption of cadmium ions on oxygen surface sites in activated carbon. *Langmuir, 16*(3), 1114-1122.

Jiang, G., Gutierrez, O., & Yuan, Z. (2011). The strong biocidal effect of free nitrous acid on anaerobic sewer biofilms. *Water Research, 45*(12), 3735-3743.

Joseph, A. P., Keller, J., Bustamante, H., & Bond, P. L. (2012). Surface neutralization and H_2S oxidation at early states of sewer corrosion: influence of temperature, relative humidity and H_2S concentration. *Water Res., 46*(13), 4235-4245.

Kadirvelu, K., & Namasivayam, C. (2003). Activated carbon from coconut coirpith as metal adsorbent: adsorption of Cd(II) from aqueous solution. *Advances in Environmental Research, 7*(2), 471-478.

Keller, M., & Zengler, K. (2004). Tapping into microbial diversity. *Nature Reviews Microbiology, 2*(2), 141-150.

Kelly, D. P. (1982). Biochemistry of the chemolithotrophic oxidation of inorganic sulphur. *Philos. T. R. Soc. B, 298*(1093), 499-528.

Kelly, D. P., Shergill, J. K., Lu, W. P., & Wood, A. P. (1997). Oxidative metabolism of inorganic sulfur compounds by bacteria. *Antonie van Leeuwenhoek, 71*(1-2), 95-107.

Kelly, D. P., & Wood, A. P. (2000). Reclassification of some species of *Thiobacillus* to the newly designated genera *Acidithiobacillus* gen. nov., *Halothiobacillus* gen. nov., and *Thermithiobacillus* gen. nov. *International Journal of Systematic and Evolutionary Microbiology, 50*, 511-516.

Kelly, R., & Smolik, J. (2011). Restoring a corroded sewer. *Pipe Rehabilitation*.

Kirchman, D., Sigda, J., Kapuscinski, R., & Mitchell, R. (1982). Statistical analysis of the direct count method for enumerating bacteria. *Applied and Environmental Microbiology, 44*(2), 376-382.

Kobya, M., Demirbas, E., Senturk, E., & Ince, M. (2005). Adsorption of heavy metal ions from aqueous solution by activated carbon prepared from apricot stone. *Bioresource Technology, 96*, 1518-1521.

Koch, G., Brongers, M., Thompson, N., Virmani, Y., & Payer, C. (2002). *Corrosion costs and prevention strategies in the United States*. (FHWA-RD-01-156). Washington, DC: Federal Highway Administration. <http://events.nace.org/publicaffairs/images_cocorr/ccsupp.pdf>.

Kreader, C. A. (1996). Relief of amplification inhibition in PCR with bovine serum albumin or T4 gene 32 protein. *Appl. Env. Microbiol., 62*(3), 1102-1106.

Kuang, J. L., Huang, L. N., Chen, L. X., Hua, Z. S., Li, S. J., Hu, M., Li, J. T., & Shu, W. S. (2013). Contemporary environmental variation determines microbial diversity patterns in acid mine drainage. *ISME Journal, 7*(5), 1038-1050.

Kusumi, A., Li, X. S., & Katayama, Y. (2011). Mycobacteria isolated from Angkor monument sandstones grow chemolithoautotrephically by oxidizing elemental sulfur. *Front. Microbiol., 2*, 104.

Lawrence, C. D. (1998). The constitution and specification of portland cements. In P. C. Hewlett (Ed.), *Lea's Chemistry of Cement and Concrete*. New York, NY: Wiley and Sons.

Legendre, P., & Legendre, L. (1998). *Numerical Ecology* (2nd ed.). Amsterdam, The Netherlands: Elsevier Science.

Lemos, L. N., Fulthorpe, R. R., & Roesch, L. F. (2012). Low sequencing efforts bias analyses of shared taxa in microbial communities. *Folia Microbiol., 57*(5), 409-413.

Lemos, L. N., Fulthorpe, R. R., Triplett, E. W., & Roesch, L. F. (2011). Rethinking microbial diversity analysis in the high throughput sequencing era. *J. Microbiol. Meth., 86*(1), 42-51.

Ley, R. E., Harris, J. K., Wilcox, J., Spear, J. R., Miller, S. R., Bebout, B. M., Maresca, J. A., Bryant, D. A., Sogin, M. L., & Pace, N. R. (2006a). Unexpected diversity and complexity of the Guerrero Negro hypersaline microbial mat. *Appl. Env. Microbiol., 72*(5), 3685-3695.

Ley, R. E., Turnbaugh, P. J., Klein, S., & Gordon, J. I. (2006b). Microbial ecology: human gut microbes associated with obesity. *Nature, 444*(7122), 1022-1023.

Leyva-Ramos, R., Rangel-Mendez, J. R., Mendoza-Barron, J., Fuentes-Rubio, L., & Guerrero-Coronado, R. M. (1997). Adsorption of cadmium(II) from aqueous solution onto activated carbon. *Water Science and Technology, 35*(7), 205-211.

Little, B. J., Ray, R. I., & Pope, R. K. (2000). Relationship between corrosion and the biological sulfur cycle: a review. *Corrosion, 56*(4), 433-443.

Ludwig, W., Strunk, O., Westram, R., Richter, L., Meier, H., Yadhukumar, Buchner, A., Lai, T., Steppi, S., Jobb, G., Forster, W., Brettske, I., Gerber, S., Ginhart, A., Gross, O., Grumann, S., Hermann, S., Jost, R., Konig, A., Liss, T., Lussmann, R., May, M., Nonhoff, B., Reichel, B., Strehlow, R., Stamatakis, A., Stuckmann, N., Vilbig, A., Lenke, M., Ludwig, T., Bode, A., & Schleifer, K. (2004). ARB: a software environment for sequence data. *Nucleic Acids Res., 32*(4), 1363-1371.

Madigan, M. T., Martinko, J. M., Dunlap, P. V., & Clark, D. P. (2009). *Brock Biology of Microorganisms* (12th Ed. ed.). San Francisco, CA: Pearson Education.

Magurran, A. E. (2004). *Measuring Biological Diversity*. Malden, MA: Blackwell Publishing Company.

Maier, J. (2013). [Personal Convertsation with Jeff Maier of Colorado Trenchless Technologies, LLC].

Markle, J. G., Frank, D. N., Mortin-Toth, S., Robertson, C. E., Feazel, L. M., Rolle-Kampczyk, U., von Bergen, M., McCoy, K. D., Macpherson, A. J., & Danska, J. S. (2013). Sex differences in the gut microbiome drive hormone-dependent regulation of autoimmunity. *Science, 339*(6123), 1084-1088.

Martin-Laurent, F., Philippot, L., Hallet, S., Chaussod, R., Germon, J. C., Soulas, G., & Catroux, G. (2001). DNA extraction from soils: old bias for new microbial diversity analysis methods. *Applied and Environmental Microbiology, 67*(5), 2354-2359.

Marzal, P., Seco, A., & Gabaldon, C. (1996). Cadmium and zinc adsorption onto activated carbon: influence of temperature, pH, and metal/carbon ratio. *Journal of Chemical Technology and Biotechnology, 66*, 279-285.

Mazierski, J. (1995). Effect of chromium (CrVI) on the growth rate of activated sludge bacteria. *Water Research, 29*(6), 1479-1482.

Miller, D. N., Bryant, J. E., Madsen, E. L., & Ghiorse, W. C. (1999). Evaluation and optimization of DNA extraction and purification procedures for soil and sediment samples. *Appl. Env. Microbiol., 65*(11), 4715-4724.

Milonjic, S. K., & Ruvarac, A. L. (1975). The heat of immersion of natural magnetite in aquatic solutions. *Thermochimica Acta, 11*, 261-266.

Monser, L., & Adhoum, N. (2002). Modified activated carbon for the removal of copper, zinc, chromium and cyanide from wastewater. *Separation and Purification Technology, 26*(2–3), 137-146.

Monteny, J., De Belie, N., Vincke, E., Verstraete, W., & Taerwe, L. (2001). Chemical and microbiological tests to simulate sulfuric acid corrosion of polymer-modified concrete. *Cement and Concrete Research, 31*(9), 1359-1365.

Monteny, J., Vincke, E., Beeldens, A., De Belie, N., Taerwe, L., Van Gemert, D., & Verstraete, W. (2000). Chemical, microbiological, and in situ test methods for biogenic sulfuric acid corrosion of concrete. *Cement and Concrete Research, 30*(4), 623-634.

Mori, T., Nonaka, T., Tazaki, K., Koga, M., Hikosaka, Y., & Noda, S. (1992). Interactions of nutrients, moisture, and pH on microbial corrosion of concrete sewer pipes. *Water Res., 26*(1), 29-37.

Morton, R. L., Yanko, W. A., Grahom, D. W., & Arnold, R. G. (1991). Relationship between metal concentrations and crown corrosion in Los Angeles County sewers. *Research Journal of the Water Pollution Control Federation, 63*, 789-798.

Nevostrueva, S. (2009). *Enhancing the metal removal capacity of activated carbon in acidic environments via oxidation and impregnation with benzotriazole derivatives.* PhD Thesis, University of Colorado.

Nica, D., Davis, J., Kirby, L., Zuo, G., & Roberts, D. (2000). Isolation and characterization of microorganisms involved in the biodeterioration of concrete in sewers. *International Biodeterioration and Biodegradation, 46*(1), 61-68.

Nielsen, A. H., Lens, P., Vollertsen, J., & Hvitved-Jacobsen, T. (2005). Sulfide-iron interactions in domestic wastewater from a gravity sewer. *Water Res., 39*(12), 2747-2755.

Nielsen, A. H., Vollertsen, J., Jensen, H. S., Madsen, H. I., & Hvitved-Jacobsen, T. (2008). Aerobic and anaerobic transformations of sulfide in a sewer system--field study and model simulations. *Water Environ. Res., 80*(1), 16-25.

Nies, D. (1999). Microbial heavy-metal resistance. *Applied Microbiology and Biotechnology, 51*, 730-750.

O'Connell, M., McNally, C., & Richardson, M. (2010). Biochemical attack on concrete in wastewater applications: a state of the art review. *Cement Concrete Comp., 32*(7), 479-485.

Oger, C., Berthe, T., Quillet, L., Barray, S., Chiffoleau, J.-F., & Petit, F. (2001). Estimation of the abundance of the cadmium resistance gene cadA in microbial communities in polluted estuary water. *Research in Microbiology, 152*(7), 671-678.

Okabe, S., Ito, T., Sugita, K., & Satoh, H. (2005). Succession of internal sulfur cycles and sulfur-oxidizing bacterial communities in microaerophilic wastewater biofilms. *Applied and Environmental Microbiology, 71*(5), 2520-2529.

Okabe, S., Odagiri, M., Ito, T., & Satoh, H. (2007). Succession of sulfur-oxidizing bacteria in the microbial community on corroding concrete in sewer systems. *Appl. Env. Microbiol., 73*(3), 971-980.

Oksanen, J., Blanchet, F. G., Kindt, R., Legendre, P., Minchin, P. R., O'Hara, R. B., Simpson, G. L., Solymos, P., Stevens, M. H. H., & Wagner, H. (2013). Vegan: community ecology package *R package version 2.0-7*. http://CRAN.R-project.org/package=vegan.

Olmstead, W. M., & Hamlin, H. (1900). Converting portions of the Los Angeles outfall sewer into a septic tank. *Engineering News, 44*, 317-318.

Opel, K. L., Chung, D., & McCord, B. R. (2010). A study of PCR inhibition mechanisms using real time PCR. *J. Forensic Sci., 55*(1), 25-33.

Padival, N. A., Kimbell, W. A., & Redner, J. A. (1995). Use of iron salts to control dissolved sulfide in trunk sewers. *Journal of Environmental Engineering - ASCE, 121*, 824-829.

Parker, C. D. (1945). The corrosion of concrete: 1. The isolation of a species of bacterius associated with the corrosion of concrete exposed to atmospheres containing hydrogen sulphide. *Aust. J. Exp. Biol. Med., 23*, 81-90.

Parker, C. D. (1947). Species of sulphur bacteria associated with the corrosion of concrete. *Nature, 159*, 439-440.

Periasamy, K., & Namasivayam, C. (1994). Process development for removal and recovery of cadmium from wastewater by a low-cost adsorbent: adsorption rates and equilibrium studies. *Industrial & Engineering Chemistry Research, 33*(2), 317-320.

Polz, M. F., & Cavanaugh, C. M. (1998). Bias in template-to-product ratios in multitemplate PCR. *Applied and Environmental Microbiology, 64*(10), 3724-3730.

Porter, K. G., & Feig, Y. S. (1980). The use of DAPI for identifying and counting aquatic microflora. *Limnology and Oceanography, 25*(5), 943-948.

Pruesse, E., Peplies, J., & Glöckner, F. O. (2012). SINA: accurate high throughput multiple sequence alignment of ribosomal RNA genes. *Bioinformatics, 28*(14), 1823-1829.

Quast, C., Pruesse, E., Yilmaz, P., Gerken, J., Schweer, T., Yarza, P., Peplies, J., & Glöckner, F. O. (2013). The SILVA ribosomal RNA gene database project: improved data processing and web-based tools. *Nucleic Acids Res., 41*(D590).

Quatrini, R., Appia-Ayme, C., Denis, Y., Jedlicki, E., Holmes, D. S., & Bonnefoy, V. (2009). Extending the models ofr iron and sulfur oxidation in the extreme acidophile *Acidithiobacillus ferrooxidans*. *BMC Genomics, 10*(394).

Ranganathan, K. (2000). Chromium removal by activated carbons prepared from Casurina equisetifolia leaves. *Bioresource Technology, 73*(2), 99-103.

Rao, M. M., Ramesh, A., Rao, G. P. C., & Seshaiah, K. (2006). Removal of copper and cadmium from the aqueous solutions by activated carbon derived from Ceiba pentandra hulls. *Journal of Hazardous Materials, 129*(1–3), 123-129.

RCoreTeam. (2013). R: a language and environment for statistical computing. R Foundation for Statistical Computing. http://www.r-project.org/.

Reed, B. E., Arunachalam, S., & Thomas, B. (1994). Removal of lead and cadmium from aqueous waste streams using granular activated carbon (GAC) columns. *Environmental Progress, 13*(1), 60-64.

Reed, B. E., & Matsumoto, M. R. (1993). Modeling cadmium adsorption by activated carbon using the Langmuir and Freundlich isotherm. *Sparation Science and Technology, 28*(13-14), 2179-2195.

Roberts, D., Nica, D., Zuo, G., & Davis, J. (2002). Quantifying microbially induced deterioration of concrete: initial studies. *Int. Biodeter. Biodeg., 49*(4), 227-234.

Robertson, C. E., Harris, J. K., Wagner, B. D., Granger, D., Browne, K., Tatem, B., Feazel, L. M., Park, K., Pace, N. R., & Frank, D. N. (2013). Explicet: Graphical user interface software for metadata-driven management, analysis, and visualization of microbiome data. *Bioinformatics, doi: 10.1093/bioinformatics/btt526*.

Rodríguez-Gómez, L. E., Delgado, S., Álvarez, M., & Elmaleh, S. (2005). Inhibition of sulfide generation in a reclaimed wastewater pipe by nitrate dosage and denitrification kinetics. *Water Environment Research, 77*(2), 193-198.

Rohwerder, T., & Sand, W. (2007). Oxidation of inorganic sulfur compounds in acidophilic prokaryotes. *Engineering in Life Sciences, 7*(4), 301-309.

Rootsey, R., & Yuan, Z. G. (2010). *New insights into sewer odour and corrosion*. Paper presented at the 6th Intornational Conference on Sewer Processes and Networks, Surfers Paradise, Australia.

Ross, M. G., Russ, C., Costello, M., Hollinger, A., Lennon, N. J., Hegarty, R., Nusbaum, C., & Jaffe, D. B. (2013). Characterizing and measuring bias in sequence data. *Genome Biology, 14*, R51.

Sakamoto, K., Yagasaki, M., Kirimura, K., & Usami, S. (1989). Resistance acquisition of Thiobacillus thiooxidans upon cadmium and zinc ion addition and formation of cadmium

ion-binding and zinc ion-binding proteins exhibiting metallothionein-like properties. *Journal of Fermentation and Bioengineering, 67*(4), 266-273.

Sand, W. (1987). Importance of hydrogen sulfide, thiosulfate, and methylmercaptan for growth of thiobacilli during simulation of concrete corrosion. *Applied and Environmental Microbiology, 53*(7), 1645-1648.

Sand, W., & Bock, E. (1984). Concrete corrosion in the Hamburg sewer system. *Environ. Technol. Lett., 5*(12), 517-528.

Santo Domingo, J. W., Revetta, R. P., Iker, B., Gomez-Alvarez, V., Garcia, J., Sullivan, J., & Weast, J. (2011). Molecular survey of concrete sewer biofilm microbial communities. *Biofouling, 27*(9), 993-1001.

Satoh, H., Odagiri, M., Ito, T., & Okabe, S. (2009). Microbial community structures and in situ sulfate-reducing and sulfur-oxidizing activities in biofilms developed on mortar specimens in a corroded sewer system. *Water Res., 43*(18), 4729-4739.

Schloss, P. D., Gevers, D., & Westcott, S. L. (2011a). Reducing the effects of PCR amplification and sequencing artifacts on 16S rRNA-based studies. *PLoS ONE, 6*(12), e27310.

Schloss, P. D., & Westcott, S. L. (2011b). Assessing and improving methods used in operational taxonomic unit-based approaches for 16S rRNA gene sequence analysis. *Applied and Environmental Microbiology, 77*(10), 3219-3226.

Schrenk, M. O., Edwards, K. J., Goodman, R. M., Hamers, R. J., & Banfield, J. F. (1998). Distribution of *Thiobacillus ferrooxidans* and *Leptospirillum ferrooxidans*: Implications for generation of acid mine drainage. *Science, 279*(5356), 1519-1522.

Scrivener, K. L., & Capmas, A. (1998). Calcuim aluminate cements. In P. C. Hewlett (Ed.), *Lea's Chemstry of Cement and Concrete*. New York, NY: Wiley and Sons.

Scrivener, K. L., & De Belie, N. (2013). Bacteriogenic sulfuric acid attack of cemintitious materials in sewage systems. In M. G. Alexander, A. Bertron & N. De Belie (Eds.), *Performance of Cement-based Materials in Aggressive Aqueous Environments*. Dortrecht, Netherlands: Springer.

Selvi, K., Pattabhi, S., & Kadirvelu, K. (2001). Removal of Cr(VI) from aqueous solution by adsorption onto activated carbon. *Bioresource Technology, 80*, 87-89.

Snoeyink, V. L., & Weber, W. J. (1967). The surface chemistry of active carbon; a discussion of structure and surface functional groups. *Environ. Sci. Technol., 1*(3), 228-234.

Stahl, J. S., Redner, J., & Caballero, R. (1989). *Sulfide corrosion in the sewer system of Los Angeles County*. Paper presented at the ASCE Conference on Sulfide Control in Wastewater Collection and Treatment Systems, Tucson, AZ.

Starosvetsky, J., Zukerman, U., & Armon, R. H. (2013). A simple medium modification for isolation, growth and enumeration of *Acidithiobacillus thiooxidans* (syn. *Thiobacillus thiooxidans*) from water samples. *Journal of Microbiological Methods, 92*(2), 178-182.

Stumm, W., & Morgan, J. J. (1996). *Aquatic Chemistry: Chemical Equilibria and Rates in Natural Waters* (3rd ed.). New York, NY: Wiley-Interscience.

Suzuki, I. (1999). Oxidation of inorganic sulfur compounds: chemical and enzymatic reactions. *Canadian Journal of Microbiology, 45*(2), 97-105.

Takeno, N. (2005). *Atlas of Eh-pH diagrams*. Geological Survey of Japan. National Institute of Advanced Industrial Science and Technology of Japan. <http://www.fssm.ucam.ac.ma/biblioadmin/opac_css/chimie/Atlas_Eh-pH_diagrams.pdf>.

Tchobanoglous, G., Burton, F. L., & Stensel, H. D. (2002). *Wastewater Engineering: Treatment and Reuse* (4th ed.). New York, NY: McGraw-Hill.

Teker, M., Imamoglu, M., & Saltabas, O. (1998). Adsorption of copper and cadmium ions by activated carbon from rice hulls. *Turkish Journal of Chemistry, 23*, 185-191.

Toril-Gonzalez, E., Llobet-Brossa, E., Casamayor, E. O., Amman, R., & Amils, R. (2003). Microbial ecology of an extreme acidic environment, the Tinto River. *Appl. Env. Microbiol., 69*(8), 4853-4865.

Trevors, J. T., Oddie, K. M., & B.H., B. (1985). Metal resistance in bacteria. *FEMS Microbiology Letters, 32*(1), 39-54.

Trudinger, P. A. (1979). The biological sulfur cycle. In P. A. Trudinger & D. J. Swaine (Eds.), *Biogeochemical Cycling of Mineral-Forming Elements*. New York, NY: Elsevier.

Tsai, Y.-P., You, S.-J., Pai, T.-Y., & Chen, K.-W. (2005). Effect of cadmium on composition and diversity of bacterial communities in activated sludges. *International Biodeterioration & Biodegradation, 55*(4), 285-291.

Turenne, C. Y., Cook, V. J., Burdz, T. V., Pauls, R. J., Thibert, L., Wolfe, J. N., & Kabani, A. (2004). Mycobacterium parascrofulaceum sp. nov., novel slowly growing, scotochromogenic clinical isolates related to Mycobacterium simiae. *International Journal of Systematic and Evolutionary Microbiology, 54*(5), 1543-1551.

Tyson, G., Chapman, J., Hugenholtz, P., Allen, E., Ram, R., Richardson, P., Solovyev, V., Rubin, E., Rokhsar, D., & Banfield, J. (2004). Community structure and metabolism through reconstruction of microbial genomes from the environment. *Nature, 428*, 37-43.

USEPA. (1974). *Process design manual for sulfide control in sanitary sewerage systems*. Environmental Protection Agency.

USEPA. (1980). *Control and treatment technology for the metal finishing industry: sulfide precipitation*. (EPA 625/8-80-003). Environmental Protection Agency.

USEPA. (1985). *Odor and corrosion control in sanitary sewerage systems and treatment plants*. (EPA 625-1-85-O18). Environmental Protection Agency.

USEPA. (1991). *Hydrogen sulfide corrosion in wastewater collection and treatment systems: technical report to Congress* (EPA 430/09-91-010). Environmental Protection Agency.

USEPA. (1995). *Profile of the fabricated metal products industry*. (EPA 310-R-95-007). Environmental Protection Agency.

USEPA. (2009). *Rehabilitation of wastewater collection and water distribution systems*. (EPA/600/R-09/048). Environmental Protection Agency.

USEPA. (2010). *State of technology for rehabilitation of wastewater collection systems*. (EPA/600/R-10/078). Environmental Protection Agency.

Utgikar, V. P., Tabak, H. H., Haines, J. R., & Govind, R. (2003). Quantification of toxic and inhibitory impact of copper and zinc on mixed cultures of sulfate-reducing bacteria. *Biotechnology and Bioengineering, 82*(3), 306-312.

Vadiya, S., Montes, C., & Allouche, E. N. (2007). *Use of nanomaterials concrete pipe protection*. Paper presented at the Pipelines 2007, Boston, MA.

Valix, M., & Bustamante, H. (2010a). *Sulfuric acid permeation in epoxy mortar coatings*. Paper presented at the 6th International Conference on Sewer Processes and Networks, Surfers Paradise, Australia.

Valix, M., Zamri, D., Mineyama, H., Cheung, W. H., Shi, J., & Bustamante, H. (2010b). *Successive growth of micro-organisms in corrosion of concrete and protective coatings in gravity sewers*. Paper presented at the 6th Internation Conference on Sewer Processes and Networks, Surfers Paradise, Australia.

Vincke, E., Boon, N., & Verstraete, W. (2001). Analysis of the microbial communities on corroded concrete sewer pipes - a case study. *Appl. Microbiol. Biot., 57*(5-6), 776-785.

Vollertsen, J., Nielsen, A. H., Jensen, H. S., Wium-Andersen, T., & Huitued-Jacobsen, T. (2008). Corrosion of concrete sewers - The kinetics of hydrogen sulfide oxidation. *Science of the Total Environment, 394*(1), 162-170.

Wagner, B. D., Robertson, C. E., & Harris, J. K. (2011). Application of two-part statistics for comparison of sequence variant counts. *PLoS ONE, 6*(5), e20296.

Waksman, S. A. (1922). Microorganisms concerned in the oxidation of sulfur in the soil: a solid medium for the isolation and cultivation of Thiobacillus thiooxidans. *Journal of Bacteriology, 7*(6), 605-608.

Walker, J. J., Spear, J. R., & Pace, N. R. (2005). Geobiology of a microbial endolithic community in the Yellowstone geothermal environment. *Nature, 434*, 1011-1014.

Wang, J. Z., & Summers, R. S. (1995). Biofiltration performance 1: relationship to biomass. *Journal American Water Works Association, 87*(12), 55-63.

Watkin, E. L. J., Keeling, S. E., Perrot, F. A., Shiers, D. W., Palmer, M. L., & Walting, H. R. (2009). Metals tolerance in moderately thermophilic isolates from a spent copper sulfide heap, closely related to *Acidithiobacillus caldus*, *Acidimicrobium ferrooxidans* and *Sulfobacillus thermosulfidooxidans*. *Journal of Industrial Microbiology and Biotechnology, 36*(3), 461-465.

WERF. (2007). *Minimization of odors and corrosion in collection systems*. (04-CTS-1). Water Environment Research Foundation.

Wilczak, A., & Keinath, T. M. (1993). Kinetics of sorption and desorption of copper(II) and lead(II) on activated carbon. *Water Environment Research, 65*(3), 238-244.

Wolda, H. (1981). Similarity indices, sample size and diversity. *Oecologia, 50*(3), 296-302.

Zhang, L., De Gusseme, B., De Schryver, P., Mendoza, L., Marzorati, M., & Verstraete, W. (2009). Decreasing sulfide generation in sewage by dosing formaldehyde and its derivatives under anaerobic conditions. *Water Science and Technology, 59*(6), 1248-1254.

Zhang, L., De Schryver, P., De Gusseme, B., De Muynck, W., Boon, N., & Verstraete, W. (2008). Chemical and biological technologies for hydrogen sulfide emission control in sewer systems: A review. *Water Research, 42*(1-2), 1-12.

Ziegler, S., Waidner, B., Itoh, T., Schumann, P., Spring, S., & Gescher, J. (2012). *Metallibacterium scheffleri* gen. nov., sp. nov., an alkalinizing gammaproteobacterium isolated from an acidic biofilm. *International Journal of Systematic and Evolutionary Microbiology, 63*(4), 1499-1504.